

REGION 3

Pampanga River Basin:

DREAM Flood Forecasting
and Flood Hazard Mapping



TRAINING CENTER FOR APPLIED GEODESY AND PHOTOGRAMMETRY

2015





© University of the Philippines and the Department of Science and Technology 2015

Published by the UP Training Center for Applied Geodesy and Photogrammetry (TCAGP)
College of Engineering
University of the Philippines Diliman
Quezon City
1101 PHILIPPINES

This research work is supported by the Department of Science and Technology (DOST) Grants-in-Aid Program and is to be cited as:

UP TCAGP (2015), Flood Forecasting and Flood Hazard Mapping for Pampanga River Basin, Disaster Risk Exposure and Assessment for Mitigation (DREAM), DOST Grants-in-Aid Program, 99 pp.

The text of this information may be copied and distributed for research and educational purposes with proper acknowledgement. While every care is taken to ensure the accuracy of this publication, the UP TCAGP disclaims all responsibility and all liability (including without limitation, liability in negligence) and costs which might incur as a result of the materials in this publication being inaccurate or incomplete in any way and for any reason.

For questions/queries regarding this report, contact:

Alfredo Mahar Francisco A. Lagmay, PhD.

Project Leader, Flood Modeling Component, DREAM Program
University of the Philippines Diliman
Quezon City, Philippines 1101
Email: amfal2@yahoo.com

Enrico C. Paringit, Dr. Eng.

Program Leader, DREAM Program
University of the Philippines Diliman
Quezon City, Philippines 1101
E-mail: paringit@gmail.com

National Library of the Philippines
ISBN: 978-621-95189-1-8



Table of Contents

INTRODUCTION	1
1.1 About the DREAM Program	2
1.2 Objectives and Target Outputs	2
1.3 General Methodological Framework	3
1.4 Scope of Work of the Flood Modeling Component	4
1.5 Limitations	4
1.6 Operational Framework	4
THE PAMPANGA RIVER BASIN	5
METHODOLOGY	9
3.1 Pre-processing and Data Used	10
3.1.1 Elevation Data	10
3.1.1.1 Hydro-corrected SRTM DEM	10
3.1.1.2 LiDAR DEM	10
3.1.2 Land Cover and Soil Type	12
3.1.3 Hydrometry and Rainfall Data	12
3.1.3.1 Hydrometry for Different Discharge Points	12
3.1.3.1.1 Cong Dado Dam, Pampanga	13
3.1.3.1.3 Alejo Santos Bridge, Bulacan	14
3.1.3.1.4 Ilog Baliwag, Nueva Ecija	14
3.1.3.1.5 Sto. Niño Bridge, Bulacan	15
3.1.3.2 Rainfall Intensity Duration Frequency (RIDF)	15
3.1.4 Rating Curves	18
3.1.4.1 Cong Dado Dam, Pampanga Rating Curve	19
3.1.4.2 Alejo Bridge, Bulacan Rating Curve	19
3.1.4.3 Ilog Baliwag, Nueva Ecija Rating Curve	19
3.1.4.4 Sto. Niño Bridge, Bulacan Rating Curve	20
3.2 Rainfall-Runoff Hydrologic Model Development	21
3.2.1 Watershed Delineation and Basin Model Pre-processing	21
3.2.2 Basin Model Calibration	23
3.3 HEC-HMS Hydrologic Simulations for Discharge Computations using PAGASA RIDF Curves	24
3.3.1 Discharge Computation using Rainfall-Runoff Hydrologic Model	
3.3.2 Discharge Computation using Dr. Horritt's Recommended Hydrologic Method	24
3.3.2.1 Determination of Catchment Properties	24
3.3.2.2 HEC-HMS Implementation	25
3.3.2.3 Discharge validation against other estimates	27
3.4 Hazard and Flow Depth Mapping using FLO-2D	28
3.4.1 Floodplain Delineation	29
3.4.2 Flood Model Generation	29
3.4.3 Flow Depth and Hazard Map Simulation	29
3.4.4 Hazard Map and Flow Depth Map Creation	33
RESULTS AND DISCUSSION	35
4.1 Efficiency of HEC-HMS Rainfall-Runoff Models Calibrated Based on Field Survey and Gauges Data	37
4.1.1 Cong Dado Dam, Pampanga HMS Calibration Results	38
4.1.2 Abad Santos Bridge, Pampanga HMS model Pampanga Calibration Results	39



Table of Contents

4.1.3 Alejo Santos Bridge, Bulacan HMS Model Calibration Results	40
4.1.4 Ilog Baliwag Bridge, Nueva Ecija HMS Calibration Results	41
4.1.5 Sto. Niño Bridge, Bulacan HMS Calibration Results	42
4.2 Calculated Outflow Hydrographs and Discharge Values for Different Rainfall Return Periods	43
4.2.1 Hydrograph Using the Rainfall-Runoff Model	43
4.2.1.1 Cong Dado Dam, Pampanga	43
4.2.1.2 Abad Santos Bridge, Pangasinan	47
4.2.1.3 Alejo Santos Bridge, Bulacan	49
4.2.1.4 Ilog Baliwag Bridge, Nueva Ecija	53
4.2.1.5 Sto. Niño Bridge, Bulacan	56
4.2.2 Discharge Data Using Dr. Horritt's Recommended Hydrological Method	60
4.3 Flood Hazard and Flow Depth Maps	61
BIBLIOGRAPHY	68
APPENDICES	69
Appendix A. Cong Dado Dam Model Basin Parameters	70
Appendix B. Abad Santos Bridge Model Basin Parameters	78
Appendix C. Alejo Santos Model Basin Parameters	80
Appendix D. Ilog Baliwag Model basin Parameters	81
Appendix E. Sto Nino Model Basin Parameters	83
Appendix F. Cong Dado Dam Model Reach Parameters	90
Appendix G. Abad Santos Bridge Model Reach Parameters	92
Appendix H. Alejo Santos Model Reach Parameters	93
Appendix I. Sto. Nino Model Reach Parameters	94
Appendix J. Pampanga River Discharge HEC-HMS Computation	96



List of Figures

Figure 1.	The general methodological framework of the program	3
Figure 2.	The operational framework and specific work flow of the Flood Modeling Component	4
Figure 3.	The Pampanga River Basin Location Map	6
Figure 4.	Pampanga River Basin Soil Map	7
Figure 5.	Pampanga River Basin Land Cover Map	7
Figure 6.	Summary of data needed for the purpose of flood modeling	10
Figure 7.	Digital Elevation Model (DEM) of the Pampanga River Basin using Light Detection and Ranging (LiDAR) technology	11
Figure 8.	The 1-meter resolution LiDAR data resampled to a 10-meter raster grid in GIS software to ensure that values are properly adjusted	11
Figure 9.	Stitched Quickbird images for the Pampanga floodplain	12
Figure 10.	Cong Dado Dam Rainfall and outflow data used for modeling	13
Figure 11.	Abad Santos Bridge Rainfall and outflow data used for modeling	13
Figure 12.	Alejo Santos Bridge Rainfall and outflow data used for modeling	14
Figure 13.	Ilog Baliwag Rainfall and outflow data used for modeling	14
Figure 14.	Sto. Niño Bridge Rainfall and outflow data used for modeling	15
Figure 15.	Thiessen Polygon of Rainfall Intensity Duration Frequency (RIDF) Stations for the whole Philippines	16
Figure 16.	Cabanatuan Rainfall Intensity Duration Frequency (RIDF) curves	17
Figure 17.	Science Garden Rainfall Intensity Duration Frequency (RIDF) curves	17
Figure 18.	Water level vs. Discharge Curve for Cong Dado Dam	18
Figure 19.	Rating Curve for Alejo Santos Bridge	19
Figure 20.	Water level vs. Discharge Curve for Ilog Baliwag Bridge	19
Figure 21.	Water level vs. Discharge Curve for Sto. Niño Bridge	20
Figure 22.	The Rainfall-Runoff Basin Model Development Scheme	21
Figure 23.	Pampanga HEC-HMS Model domain generated by WMS	22
Figure 24.	Map showing the location of the rain gauges within the Pampanga River Basin	23
Figure 25.	Different data needed as input for HEC-HMS discharge simulation using Dr. Horritt's recommended hydrology method	25
Figure 26.	Delineation upper watershed for Pampanga floodplain discharge computation	26
Figure 27.	HEC-HMS simulation discharge results using Dr. Horritt's Method	28
Figure 28.	Screenshot showing how boundary grid elements are defined by line	29
Figure 29.	Screenshots of PTS files when loaded into the FLO-2D program	29
Figure 30.	Areal image of Pampanga floodplain	30
Figure 31.	Screenshot of Manning's n-value rendering	32
Figure 32.	Flo-2D Mapper Pro General Procedure	33
Figure 33.	Pampanga Floodplain Generated Hazard Maps using FLO-2D Mapper	34
Figure 34.	Pampanga floodplain generated flow depth map using FLO-2D Mapper	34
Figure 35.	Basic Layout and Elements of the Hazard Maps	35
Figure 36.	Cong Dado Dam Outflow Hydrograph produced by the HEC-HMS model compared with observed outflow	38
Figure 37.	Abad Santos Outflow Hydrograph produced by the HEC-HMS model compared with observed outflow	39
Figure 38.	Alejo Santos Bridge Outflow Hydrograph produced by the HEC-HMS model compared with observed outflow	40



List of Figures

Figure 39.	Ilog Baliwag Outflow Hydrograph produced by the HEC-HMS model compared with observed outflow	41
Figure 40.	Sto. Niño Outflow Hydrograph produced by the HEC-HMS model compared with observed outflow	42
Figure 41.	Sample DREAM Water Level Forecast	43
Figure 42.	Cong Dado Dam outflow hydrograph generated using the Cabanatuan 5-Year RIDF inputted in WMS and HEC-HMS Basin Model	44
Figure 43.	Cong Dado Dam outflow hydrograph generated using the Cabanatuan 10-Year RIDF inputted in WMS and HEC-HMS Basin Model	45
Figure 44.	Cong Dado Dam outflow hydrograph generated using the Cabanatuan 25-Year RIDF inputted in WMS and HEC-HMS Basin Model	45
Figure 45.	Cong Dado Dam outflow hydrograph generated using the Cabanatuan 50-Year RIDF inputted in WMS and HEC-HMS Basin Model	46
Figure 46.	Cong Dado Dam outflow hydrograph generated using the Cabanatuan 100-Year RIDF inputted in WMS and HEC-HMS Basin Model	47
Figure 47.	Abad Santos Bridge outflow hydrograph generated using the Cabanatuan 5-Year RIDF inputted in WMS and HEC-HMS Basin Model	47
Figure 48.	Abad Santos Bridge outflow hydrograph generated using the Cabanatuan 10-Year RIDF inputted in WMS and HEC-HMS Basin Model	48
Figure 49.	Abad Santos Bridge outflow hydrograph generated using the Cabanatuan 25-Year RIDF inputted in WMS and HEC-HMS Basin Model	48
Figure 50.	Abad Santos Bridge outflow hydrograph generated using the Cabanatuan 50-Year RIDF inputted in WMS and HEC-HMS Basin Model	49
Figure 51.	Abad Santos Bridge outflow hydrograph generated using the Cabanatuan 100-Year RIDF inputted in WMS and HEC-HMS Basin Model	50
Figure 52.	Alejo Santos Bridge outflow hydrograph generated using the Cabanatuan 5-Year RIDF inputted in WMS and HEC-HMS Basin Model	50
Figure 53.	Alejo Santos Bridge outflow hydrograph generated using the Cabanatuan 10-Year RIDF inputted in WMS and HEC-HMS Basin Model	51
Figure 54.	Alejo Santos Bridge outflow hydrograph generated using the Cabanatuan 25-Year RIDF inputted in WMS and HEC-HMS Basin Model	51
Figure 55.	Alejo Santos Bridge outflow hydrograph generated using the Cabanatuan 50-Year RIDF inputted in WMS and HEC-HMS Basin Model	52
Figure 56.	Alejo Santos Bridge outflow hydrograph generated using the Cabanatuan 100-Year RIDF inputted in WMS and HEC-HMS Basin Model	53
Figure 57.	Ilog Baliwag Bridge outflow hydrograph generated using the Cabanatuan 5-Year RIDF inputted in WMS and HEC-HMS Basin Model	54
Figure 58.	Ilog Baliwag Bridge outflow hydrograph generated using the Cabanatuan 10-Year RIDF inputted in WMS and HEC-HMS Basin Model	54
Figure 59.	Ilog Baliwag Bridge outflow hydrograph generated using the Cabanatuan 25-Year RIDF inputted in WMS and HEC-HMS Basin Model	55
Figure 60.	Ilog Baliwag Bridge outflow hydrograph generated using the Cabanatuan 50-Year RIDF inputted in WMS and HEC-HMS Basin Model	55
Figure 61.	Ilog Baliwag Bridge outflow hydrograph generated using the Cabanatuan 100-Year RIDF inputted in WMS and HEC-HMS Basin Model	56
Figure 62.	Sto. Niño Bridge Outflow hydrograph generated using the Cabanatuan 5-Year RIDF inputted in HEC-HMS	56



List of Figures

Figure 63.	Sto. Niño Bridge Outflow hydrograph generated using the Cabanatuan 10-Year RIDF inputted in HEC-HMS	57
Figure 64.	Sto. Niño Bridge Outflow hydrograph generated using the Cabanatuan 25-Year RIDF inputted in HEC-HMS	57
Figure 65.	Sto. Niño Bridge Outflow hydrograph generated using the Cabanatuan 50-Year RIDF inputted in HEC-HMS	57
Figure 66.	Sto. Niño Bridge Outflow hydrograph generated using the Cabanatuan 100-Year RIDF inputted in HEC-HMS	58
Figure 67.	Outflow hydrograph generated for Pampanga using the Science Garden, Iba, and Cabanatuan stations' 5-, 25-, 100-Year Rainfall Intensity Duration Frequency in HEC-HMS	60
Figure 68.	100-year Flood Hazard Map for Pampanga River Basin	62
Figure 69.	100-year Flow Depth Map for Pampanga River Basin	63
Figure 70.	25-year Flood Hazard Map for Pampanga River Basin	64
Figure 71.	25-year Flow Depth Map for Pampanga River Basin	65
Figure 72.	5-year Flood Hazard Map for Pampanga River Basin	66
Figure 73.	5-year Flow Depth Map for Pampanga River Basin	67



List of Tables

Table 1.	Methods used for the different calculation types for the hydrologic elements	23
Table 2.	Summary of Gamu outflow using Cabanatuan Station Rainfall Intensity Duration Frequency (RIDF)	46
Table 3.	Summary of Abad Santos outflow using Cabanatuan Station Rainfall Intensity Duration Frequency (RIDF)	49
Table 4.	Summary of Alejo Santos outflow using Cabanatuan Station Rainfall Intensity Duration Frequency (RIDF)	52
Table 5.	Summary of Baliwag outflow using Cabanatuan Station Rainfall Intensity Duration Frequency (RIDF)	56
Table 6.	Summary of Sto. Niño outflow using Cabanatuan Station Rainfall Intensity Duration Frequency (RIDF)	59
Table 7.	Summary of Pampanga river discharge using the recommended hydrological method by Dr. Horritt	60
Table 8.	Validation of river discharge estimate using the bankful method	61



List of Equations

Equation 1.	Rating Curve	18
Equation 2.	Determination of maximum potential retention using the average curve number of the catchment	27
Equation 3.	Lag Time Equation Calibrated for Philippine Setting	27
Equation 4.	Ratio of river discharge of a 5-year rain return to a 2-year rain return scenario from measured discharge data	28
Equation 5.	Discharge validation equation using bankful method	28
Equation 6.	Bankful discharge equation using measurable channel parameters	29



List of Abbreviations

ACDP	Acoustic Doppler Current Profiler
AOI	Area of Interest
ARG	Automated Rain Gauge
AWLS	Automated Water Level Sensor
DAC	Data Acquisition Component
DEM	Digital Elevation Model
DOST	Department of Science and Technology
DPC	Data Processing Component
DREAM	Disaster Risk Exposure and Assessment for Mitigation
DTM	Digital Terrain Model
DVC	Data Validation Component
FMC	Flood Modelling Component
GDS	Grid Developer System
HEC-HMS	Hydrologic Engineering Center – Hydrologic Modeling System
LiDAR	Light Detecting and Ranging
PAGASA	Philippine Atmospheric, Geophysical and Astronomical Services Administration
RIDF	Rainfall Intensity Duration Frequency
SCS	Soil Conservation Service
SRTM	Shuttle Radar Topography Mission
UP-TCAGP	UP Training Center for Applied Geodesy and Photogrammetry







Introduction

Introduction

1.1 About the DREAM Program

The UP Training Center for Applied Geodesy and Photogrammetry (UP TCAGP) conducts a research program entitled “Nationwide Disaster Risk and Exposure Assessment for Mitigation (DREAM) Program” funded by the Department of Science and Technology (DOST) Grants-in-Aid Program. The DREAM Program aims to produce detailed, up-to-date, national elevation dataset for 3D flood and hazard mapping to address disaster risk reduction and mitigation in the country.

The DREAM Program consists of four components that operationalize the various stages of implementation. The Data Acquisition Component (DAC) conducts aerial surveys to collect Light Detecting and Ranging (LiDAR) data and aerial images in major river basins and priority areas. The Data Validation Component (DVC) implements ground surveys to validate acquired LiDAR data, along with bathymetric measurements to gather river discharge data. The Data Processing Component (DPC) processes and compiles all data generated by the DAC and DVC. Finally, the Flood Modeling Component (FMC) utilizes compiled data for flood modeling and simulation.

Overall, the target output is a national elevation dataset suitable for 1:5000 scale mapping, with 50 centimeter horizontal and vertical accuracies. These accuracies are achieved through the use of state-of-the-art airborne Light Detection and Ranging (LiDAR) technology and appended with Synthetic-aperture radar (SAR) in some areas. It collects point cloud data at a rate of 100,000 to 500,000 points per second, and is capable of collecting elevation data at a rate of 300 to 400 square kilometers per day, per sensor

1.2 Objectives and Target Outputs

The program aims to achieve the following objectives:

- a) To acquire a national elevation and resource dataset at sufficient resolution to produce information necessary to support the different phases of disaster management,
- b) To operationalize the development of flood hazard models that would produce updated and detailed flood hazard maps for the major river systems in the country,
- c) To develop the capacity to process, produce and analyze various proven and potential thematic map layers from the 3D data useful for government agencies,
- d) To transfer product development technologies to government agencies with geospatial information requirements, and,
- e) To generate the following outputs
 - 1) flood hazard map
 - 2) digital surface model
 - 3) digital terrain model and
 - 4) orthophotograph.



Introduction

1.3 General Methodological Framework

The methodology to accomplish the program's expected outputs are subdivided into four (4) major components, as shown in Figure 1. Each component is described in detail in the following section.

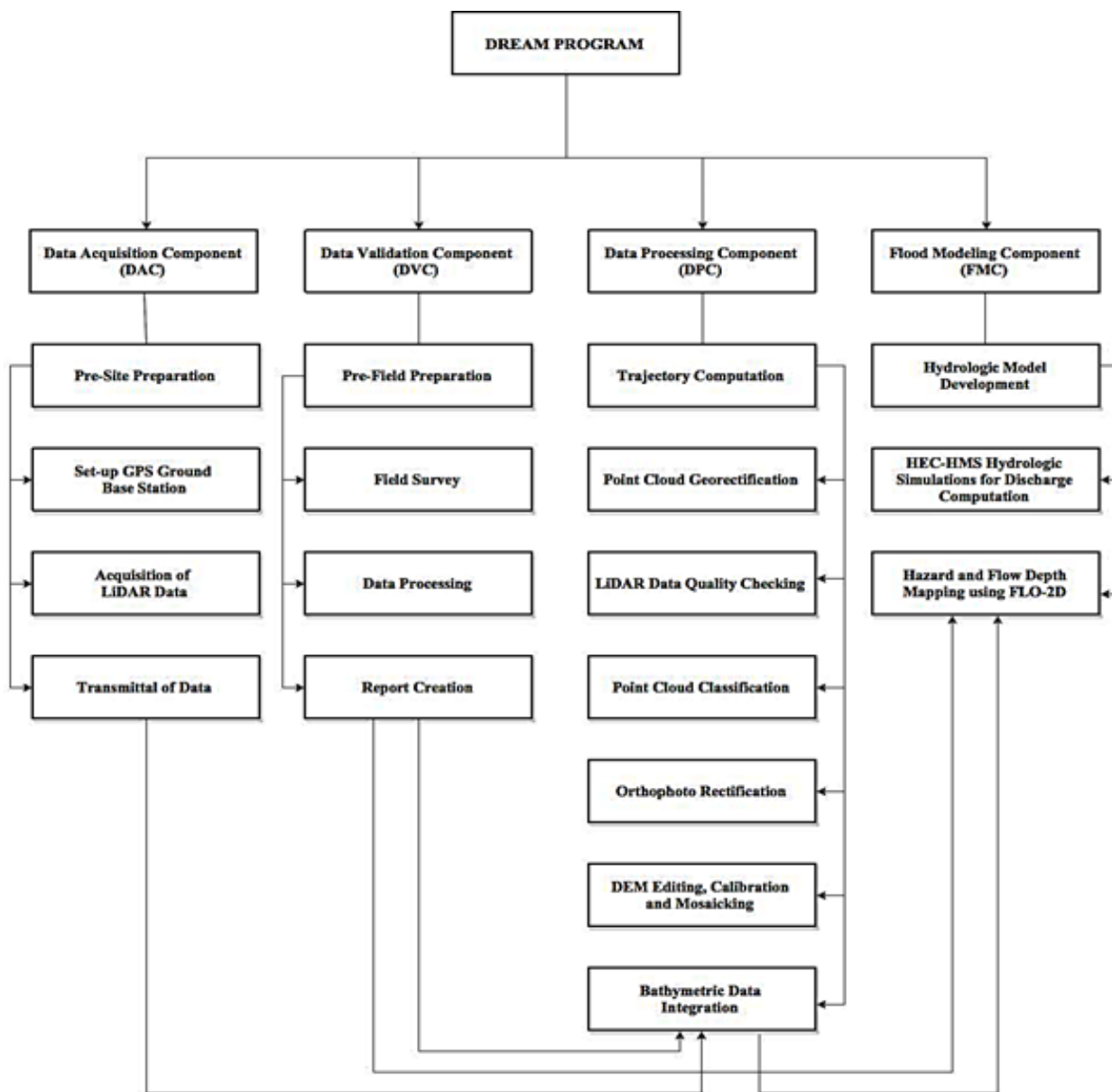


Figure 1. The general methodological framework of the program

Introduction

1.4 Scope of Work of the Flood Modeling Component

The scope of work of the Flood Modeling Component is listed as the following:

- a) To develop the watershed hydrologic model of the Pampanga River Basin;
- b) To compute the discharge values quantifying the amount of water entering the floodplain using HEC-HMS;
- c) To create flood simulations using hydrologic models of the Pampanga floodplain using FLO-2D GDS Pro; and
- d) To prepare the static flood hazard and flow depth maps for the Pampanga river basin.

1.5 Limitations

This research is limited to the usage of the available data, such as the following:

1. Digital Elevation Models (DEM) surveyed by the Data Acquisition Component (DAC) and processed by the Data Processing Component (DPC)
2. Outflow data surveyed by the Data Validation and Bathymetric Component (DVC)
3. Observed Rainfall from ASTI sensors

While the findings of this research could be further used in related-studies, the accuracy of such is dependent on the accuracy of the available data. Also, this research adapts the limitations of the software used: ArcGIS 10.2, HEC-GeoHMS 10.2 extension, WMS 9.1, HEC-HMS 3.5 and FLO-2D GDS Pro.

1.6 Operational Framework

The flow for the operational framework of the Flood Modeling Component is shown in Figure 2.

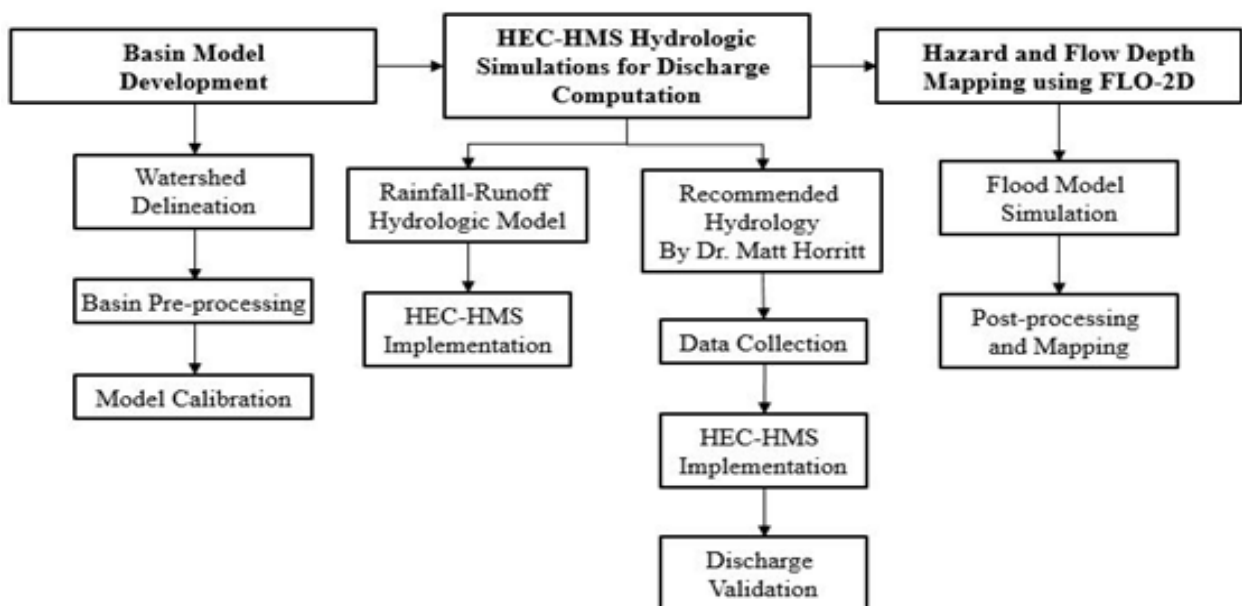
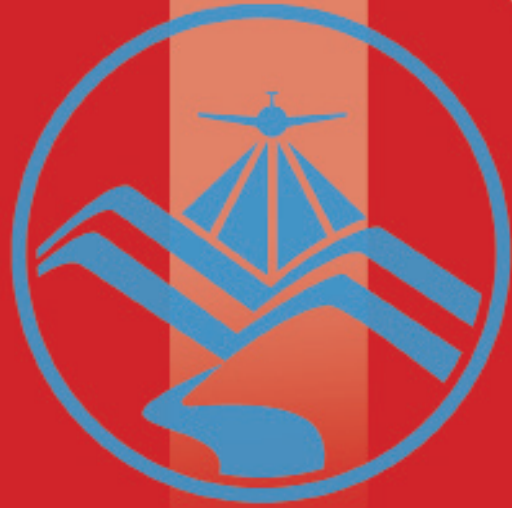


Figure 2. The operational framework and specific work flow of the Flood Modeling Component



The Pampanga River Basin

The Pampanga River Basin

The Pampanga River Basin is located in the Central Luzon Region. The Pampanga River Basin is considered as the fourth largest river basin in the Philippines. It is also considered as the second largest of Luzon's catchments, next to Cagayan River. It has an estimated basin area of 9,759 square kilometers. The location of Pampanga River Basin is as shown in Figure 3.

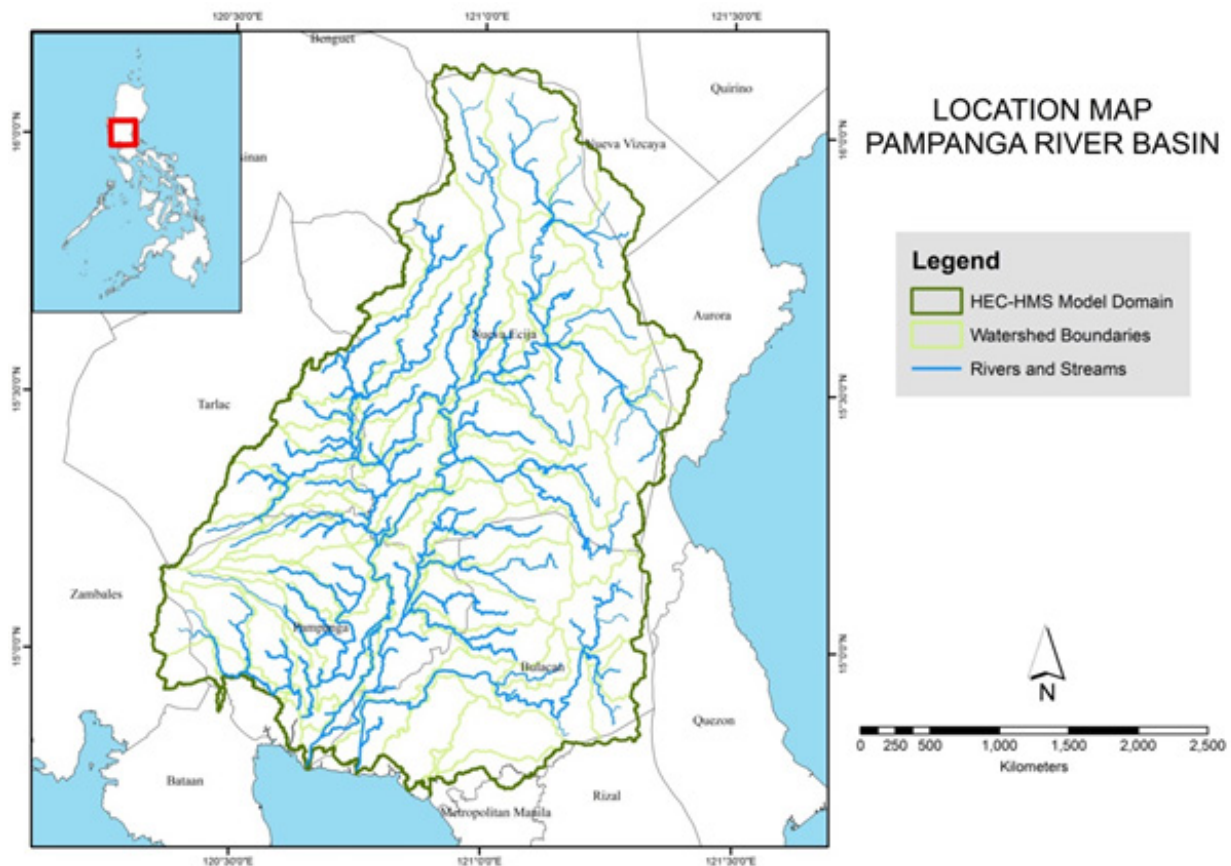


Figure 3. The Pampanga River Basin Location Map

It traverses from the southern slopes of Caraballo Mountains, range of Sierra Madre, Central Plain of the Luzon Island to its mouth in Manila Bay via the Lanbangan Channel. It is supported by four tributaries namely: Penaranda River, Coronel-Santor River, Rio Chico River and Bagbag River. The river basin encompasses parts of the following provinces: Aurora, Bataan, Bulacan, Nueva Ecija, Nueva Vizcaya, Pampanga, Pangasinan, Rizal and some parts of the national capital region including Valenzuela, Caloocan, and Quezon City. The Pampanga River Basin serves as a source of water supply for the irrigation of Nueva Ecija.

The land and soil characteristics are important parameters used in assigning the roughness coefficient for different areas within the river basin. The roughness coefficient, also called Manning's coefficient, represents the variable flow of water in different land covers (i.e. rougher, restricted flow within vegetated areas, smoother flow within channels and fluvial environments).

The shape files of the soil and land cover were taken from the Bureau of Soils, which is under the Department of Environment and Natural Resources Management, and National Mapping and Resource Information Authority (NAMRIA). The soil and land cover of the Pampanga River Basin are shown in Figures 4 and 5, respectively.

The Pampanga River Basin

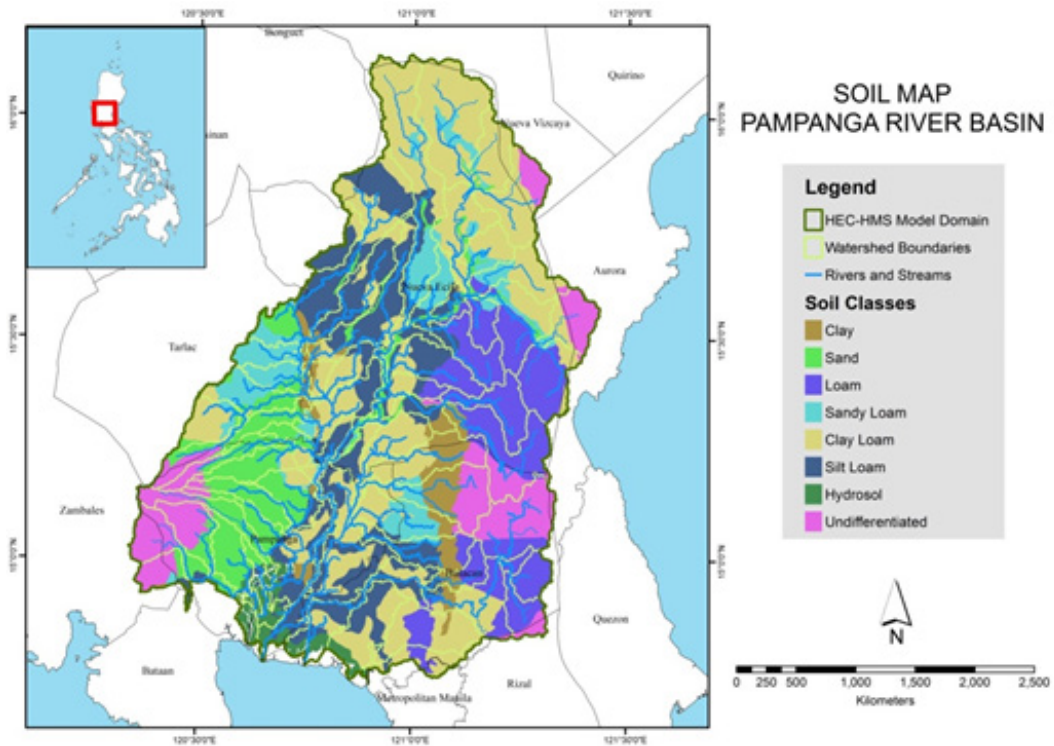


Figure 4. Pampanga River Basin Soil Map

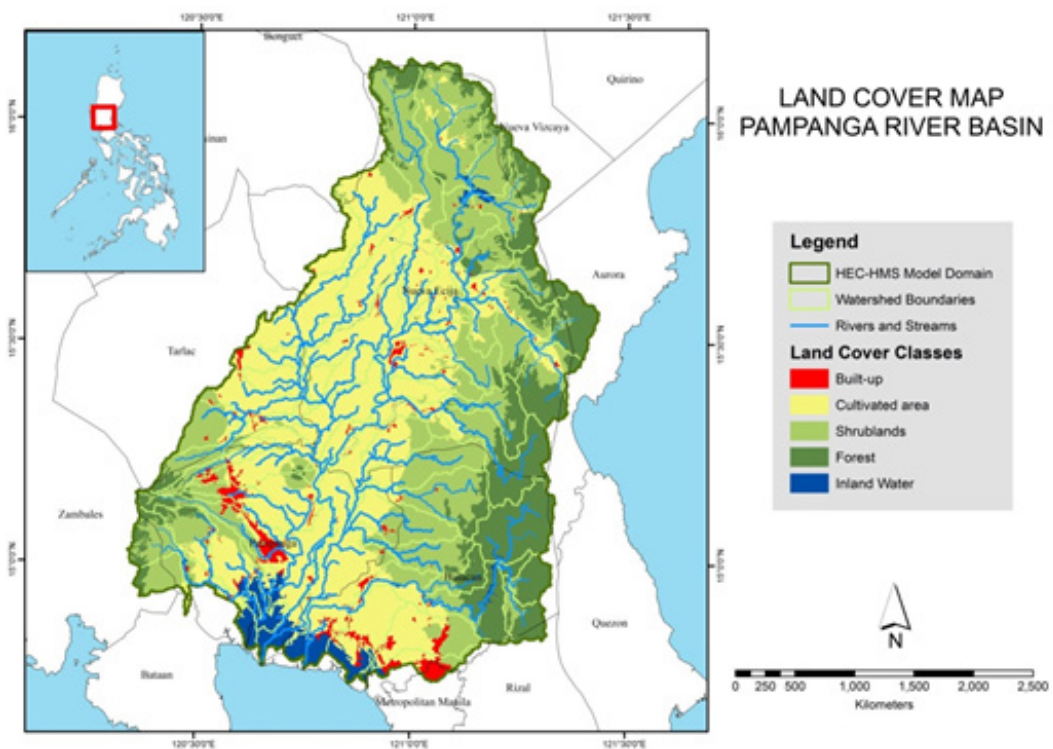


Figure 5. Pampanga River Basin Land Cover Map





Methodology

3.1 Pre-processing and Data Used

Flood modeling involved several data and parameters to achieve realistic simulations and outputs. Figure 6 shows a summary of the data needed to for the research.

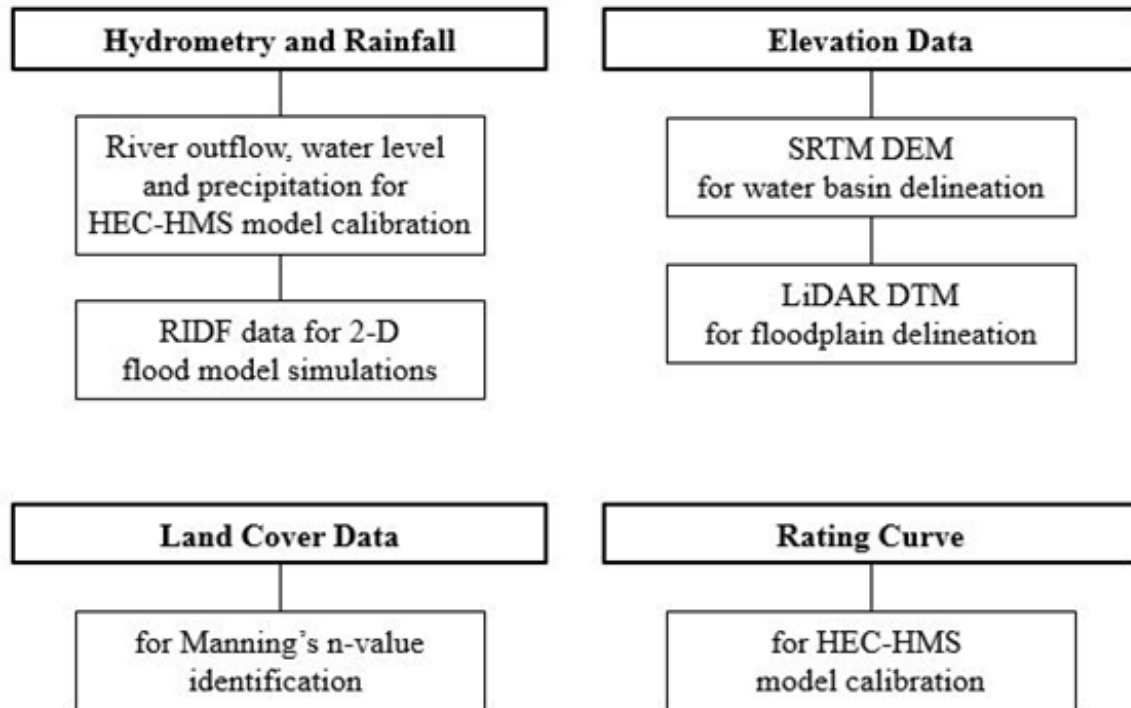


Figure 6. Summary of data needed for the purpose of flood modeling

3.1.1 Elevation Data

3.1.1.1 Hydro Corrected SRTM DEM

With the Shuttle Radar Topography Mission Digital Elevation Model (SRTM DEM) data as an input in determining the extent of the delineated water basin, the model was set-up. The Digital Elevation Model (DEM) is a set of elevation values for a range of points within a designated area. SRTM DEM has a 90 meter spatial mosaic of the entire country. Survey data of cross sections and profile points were integrated to the SRTM DEM for the hydro-correction.

3.1.1.2 LiDAR DEM

LiDAR was used to generate the Digital Elevation Model (DEM) of the different floodplains. DEMs used for flood modeling were already converted to digital terrain models (DTMs) which only show topography, and are thus cleared of land features such as trees and buildings. These terrain features would allow water to flow realistically in the models.

Figure 7 shows an image of the DEM generated through LiDAR.

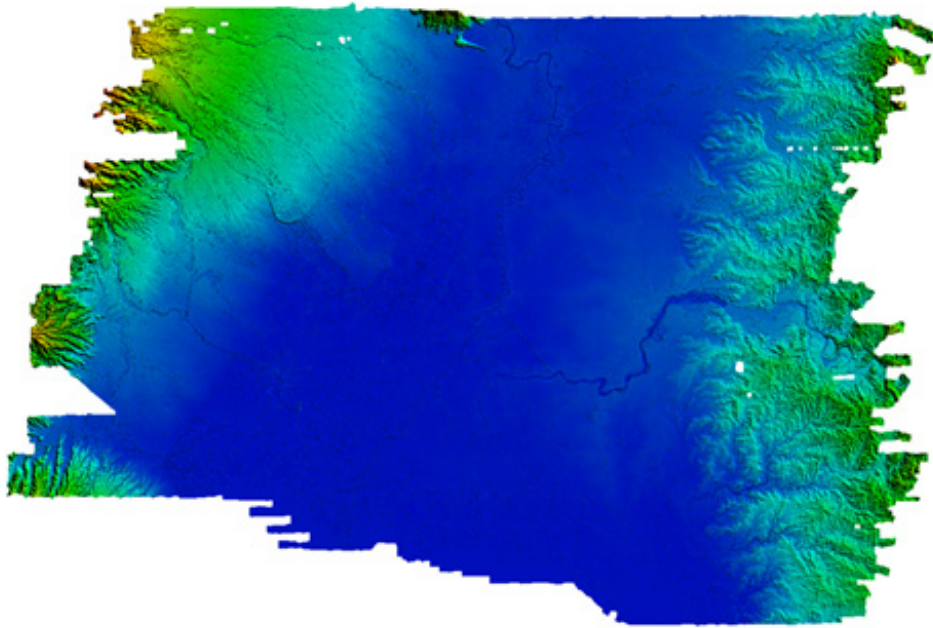


Figure 7. Digital Elevation Model (DEM) of the Pampanga River Basin using Light Detection and Ranging (LiDAR) technology

Elevation points were created from LiDAR DTMs. Since DTMs were provided as 1-meter spatial resolution rasters (while flood models for Pampanga were created using a 10-meter grid), the DTM raster had to be resampled to a raster grid with a 10-meter cell size using

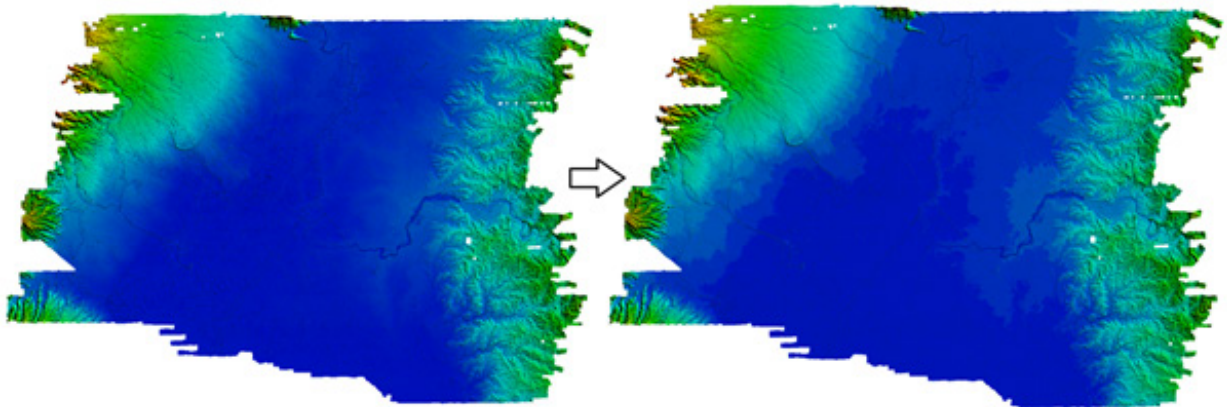


Figure 8. The 1-meter resolution LiDAR data resampled to a 10-meter raster grid in GIS software to ensure that values are properly adjusted.

Methodology

3.1.2 Land Cover and Soil Type

The land and soil characteristics are important parameters used in assigning the roughness coefficient for different areas within the river basin. The roughness coefficient, also called Manning's coefficient, represents the variable flow of water in different land covers (i.e. rougher, restricted flow within vegetated areas, smoother flow within channels and fluvial environments).

A general approach was done for the Pampanga floodplain. Streams were identified against built-up areas and rice fields. Identification was done visually using stitched Quickbird images from Google Earth. Areas with different land covers are shown on Figure 9. Different Manning n-values are assigned to each grid element coinciding with these main classifications during the modeling phase.



Figure 9. Stitched Quickbird images for the Pampanga floodplain.

3.1.3 Hydrometry and Rainfall Data

3.1.3.1 Hydrometry for different discharge points

3.1.3.1.1 Cong Dado Dam, Pampanga

River outflow from the Data Validation Component was used to calibrate the HEC-HMS model. This was taken from Cong Dado Dam, Apalit, Pampanga ($15^{\circ}11'18.34''$ N, $120^{\circ}46'33.76''$ E). This was recorded during October 27, 2012. Peak discharge is 1704.7 at 7:50 PM and is shown in Figure 10.

Methodology

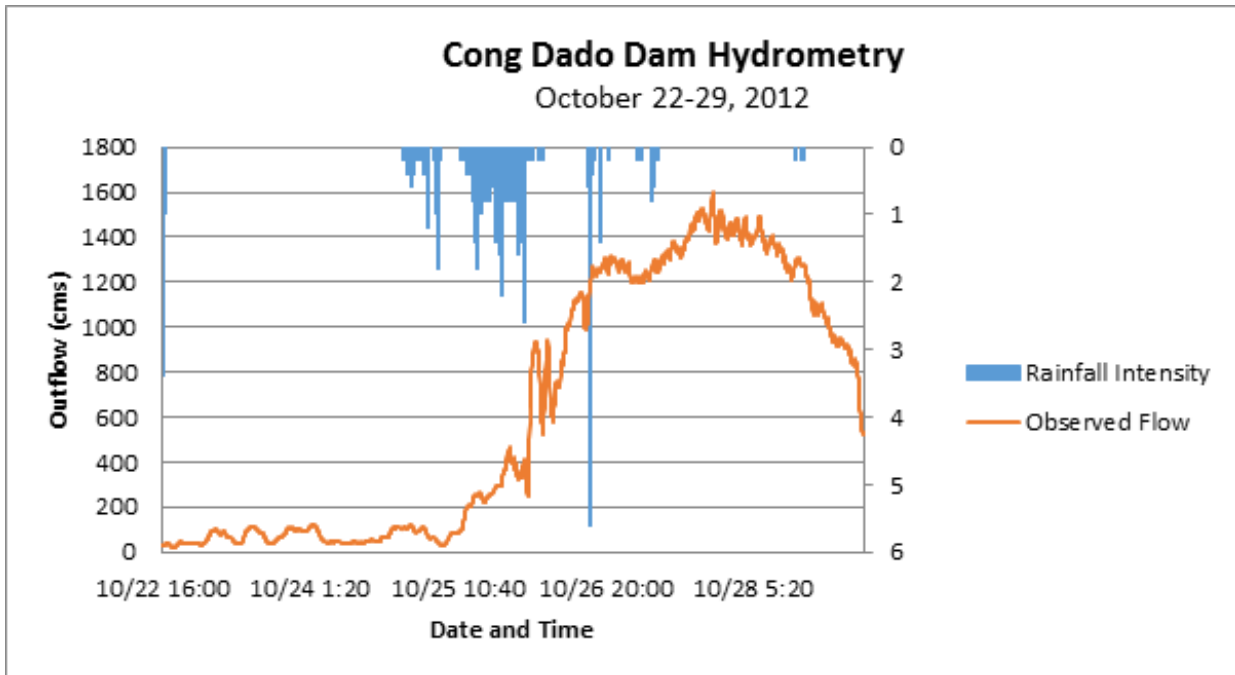


Figure 10. Cong Dado Dam Rainfall and outflow data used for modeling

3.1.3.1.2 Abad Santos Bridge, Pampanga

River outflow from the Department of Public Works and Highways' Bureau of Research and Standards (DPWH BRS) was used to calibrate the Abad Santos Bridge HEC-HMS model. This was taken from Jose Abad Santos Bridge, Lubao, Pampanga (14°54'56.69"N, 120°34'14.65"E). This was recorded during the month of October 1985. Peak discharge is 145.7 m³/s at Oct 21, 1985 and is shown in Figure 11. The BRS data contains only river discharge. Hence, no HQ- Curve can be generated.

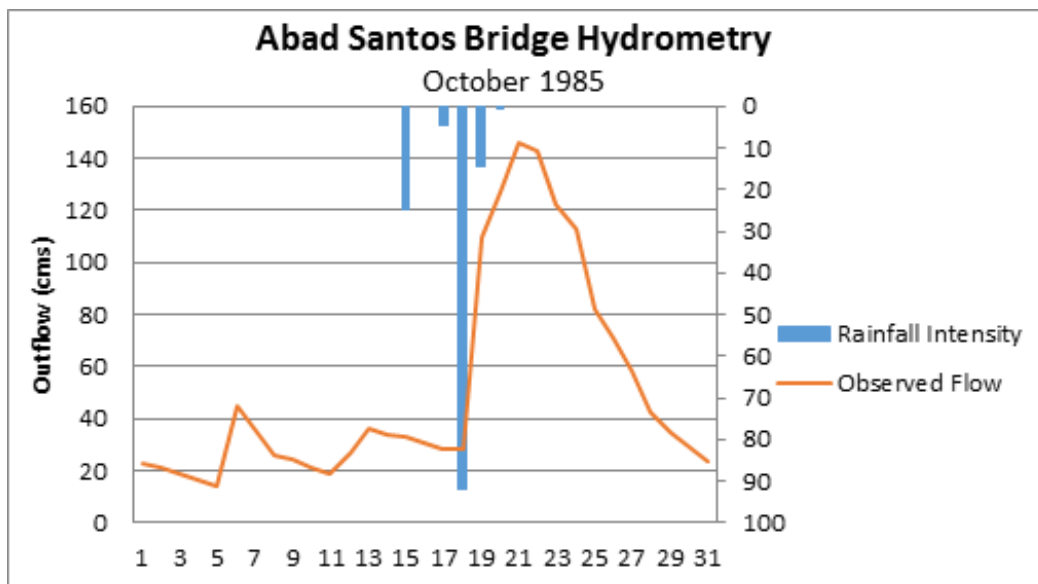


Figure 11. Abad Santos Bridge Rainfall and outflow data used for modeling

3.1.3.1.3 Alejo Santos Bridge, Bulacan

The river outflow was computed using the derived rating curve equation. This discharge was used to calibrate the HEC-HMS model. It was taken from Alejo Santos Bridge, Bulacan (14°57'23.32"N, 120°54'26.48"E). The recorded peak discharge is 39.02 cms at 9:55 PM, July 22, 2012 and is shown in Figure 12.

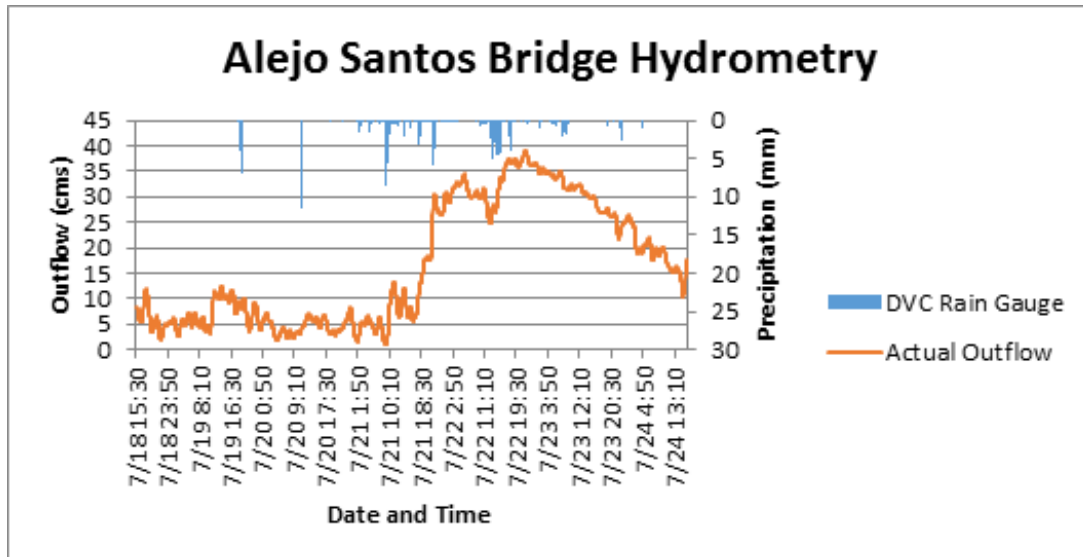


Figure 12. Alejo Santos Bridge Rainfall and outflow data used for modeling

3.1.3.1.4 Ilog Baliwag, Nueva Ecija

The river outflow was computed using the derived rating curve equation. This discharge was used to calibrate the HEC-HMS model. It was taken from Ilog Baliwag Bridge, Nueva Ecija (15°39'59.97" N, 120°51'14.46" E). The recorded peak discharge is 3.60 cms at 06:30 PM, October 1, 2013 and is shown in Figure 13.

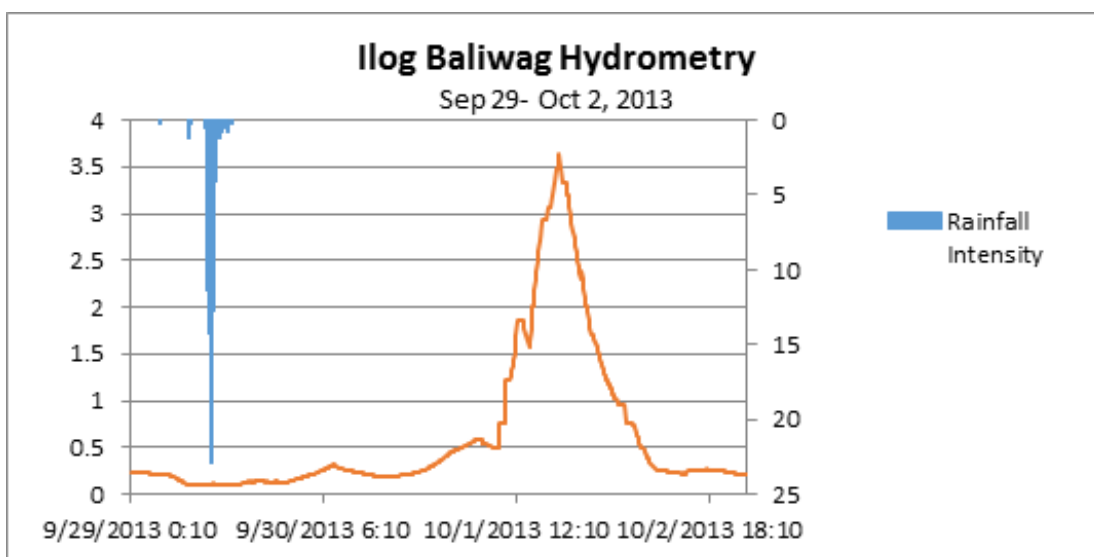


Figure 13. Ilog Baliwag Rainfall and outflow data used for modeling



Results and Discussion

3.1.3.1.5 Sto. Niño Bridge, Bulacan

The river outflow was computed using the derived rating curve equation. This discharge was used to calibrate the HEC-HMS model. It was taken from Sto. Nino Bridge, Bulacan (14°54'17.09"N, 120°46'32.19"E). The recorded peak discharge is 38.40 cms at 11:56 AM, October 12, 2013 and is shown in Figure 14.

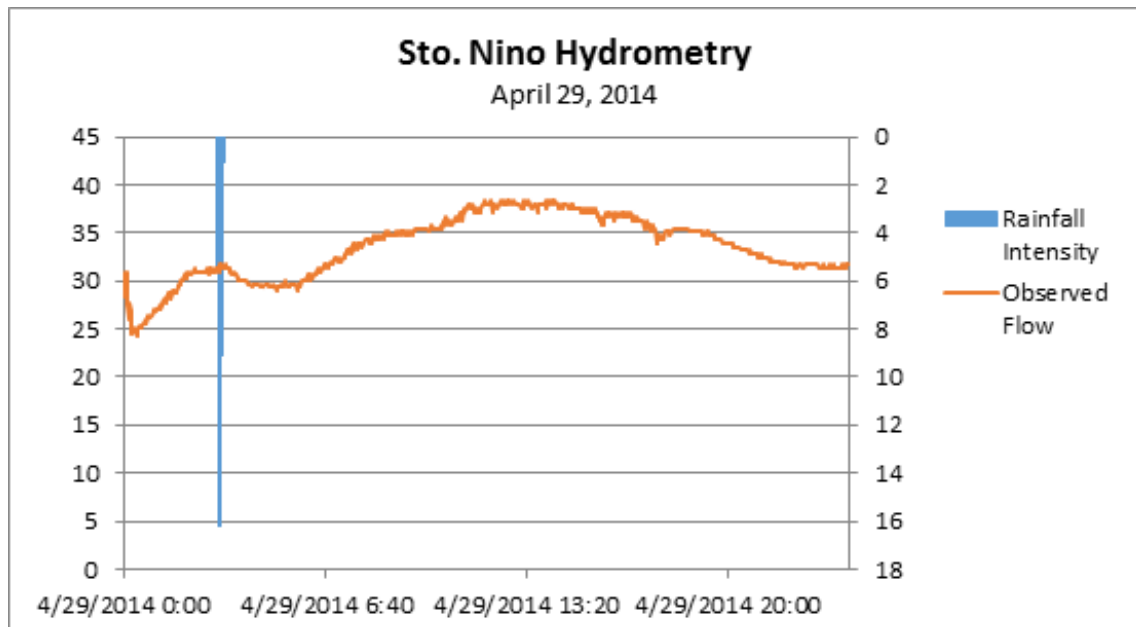


Figure 14. Sto. Niño Bridge Rainfall and outflow data used for modeling

3.1.3.2 Rainfall Intensity Duration Frequency (RIDF)

The Philippines Atmospheric Geophysical and Astronomical Services Administration (PAGASA) computed Rainfall Intensity Duration Frequency (RIDF) values for the Cabanatuan Rain Gauge. This station was chosen based on its proximity to the Pampanga watershed. The extreme values for this watershed were computed based on a 57-year record.

Five return periods were used, namely, 5-, 10-, 25-, 50-, and 100-year RIDFs. All return periods are 24 hours long and peaks after 12 hours.

Methodology

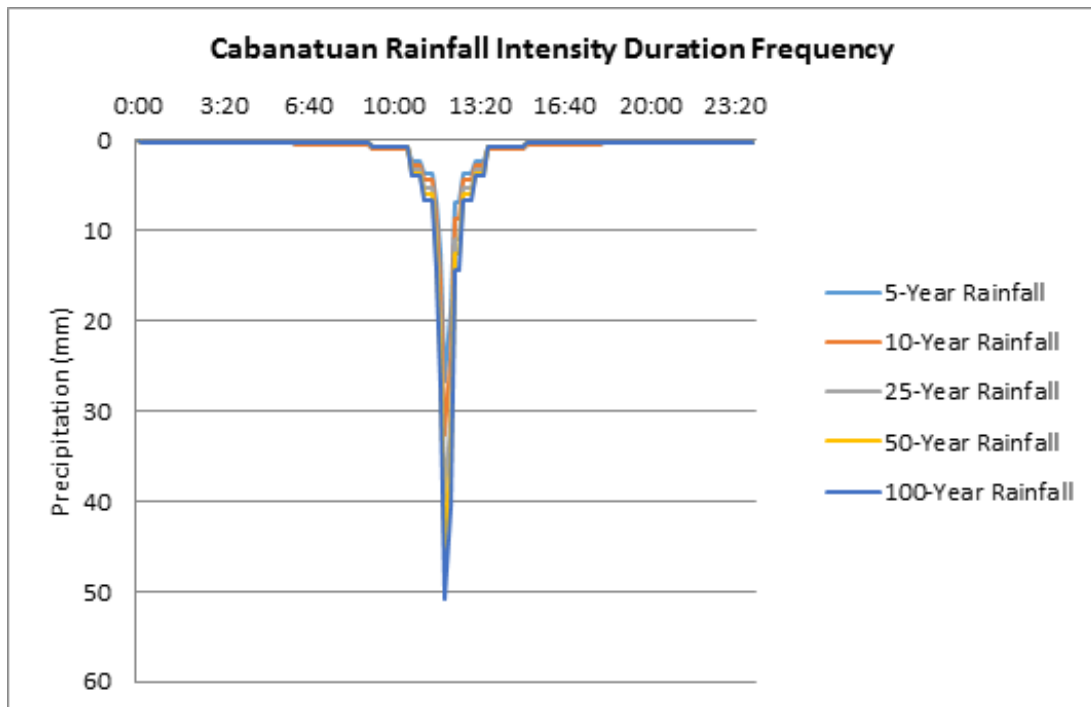


Figure 16. Cabanatuan Rainfall Intensity Duration Frequency (RIDF) curves.

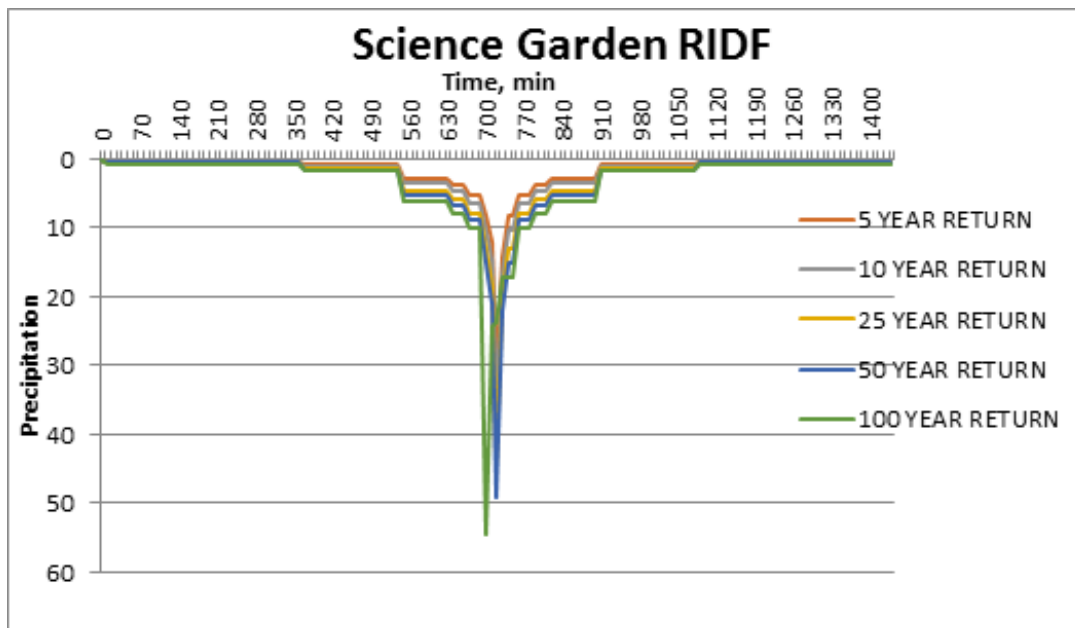


Figure 17. Science Garden Rainfall Intensity Duration Frequency (RIDF) curves.

The outflow values at the discharge points in the Pampanga river basin were computed for the five return periods, namely, 5-, 10-, 25-, 50-, and 100-year RIDFs using Cabanatuan Station. Science garden was used for the flood hazard mapping.

Methodology

3.1.4 Rating Curves

Rating curves were provided by DVC. This curve gives the relationship between the observed water levels from the AWLS used and outflow watershed at the said locations.

Rating curves are expressed in the form of Equation 1 with the discharge (Q) as a function of the gauge height (h) readings from AWLS and constants (a and n).

$$Q = a^{nh}$$

Equation 1. Rating Curve

3.1.4.1 Cong Dado Dam, Pampanga Rating Curve

For Cong Dado Dam, the rating curve is expressed as $Q = 166.8x - 694.13$ as shown in Figure 18.

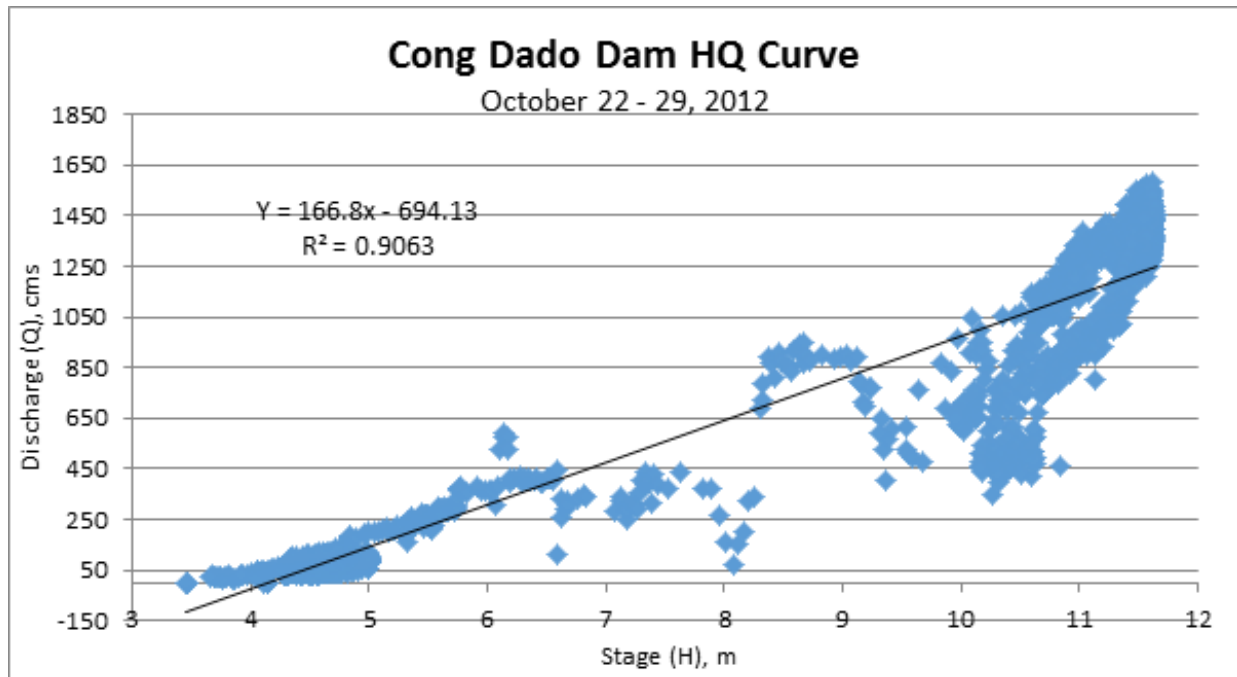


Figure 18. Water level vs. Discharge Curve for Cong Dado Dam

3.1.4.2 Alejo Bridge, Bulacan Rating Curve

For Alejo Santos Bridge, the rating curve is expressed as $Q = 0.0647e^{1.7277h}$ as shown in Figure 19.



Methodology

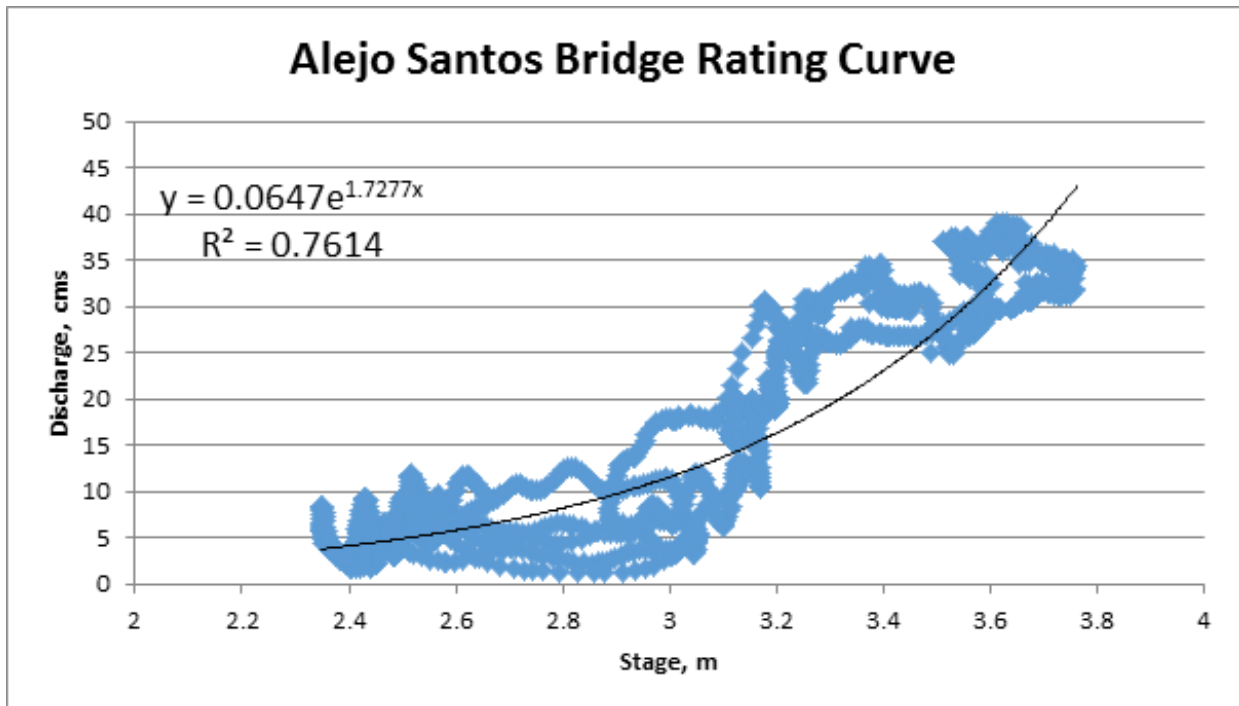


Figure 19. Rating Curve for Alejo Santos Bridge

3.1.4.3 Ilog Baliwag, Nueva Ecija Rating Curve

For Ilog Baliwag Bridge, the rating curve is expressed as $Q = 0.0949e^{4.1879x}$ as shown in Figure 20.

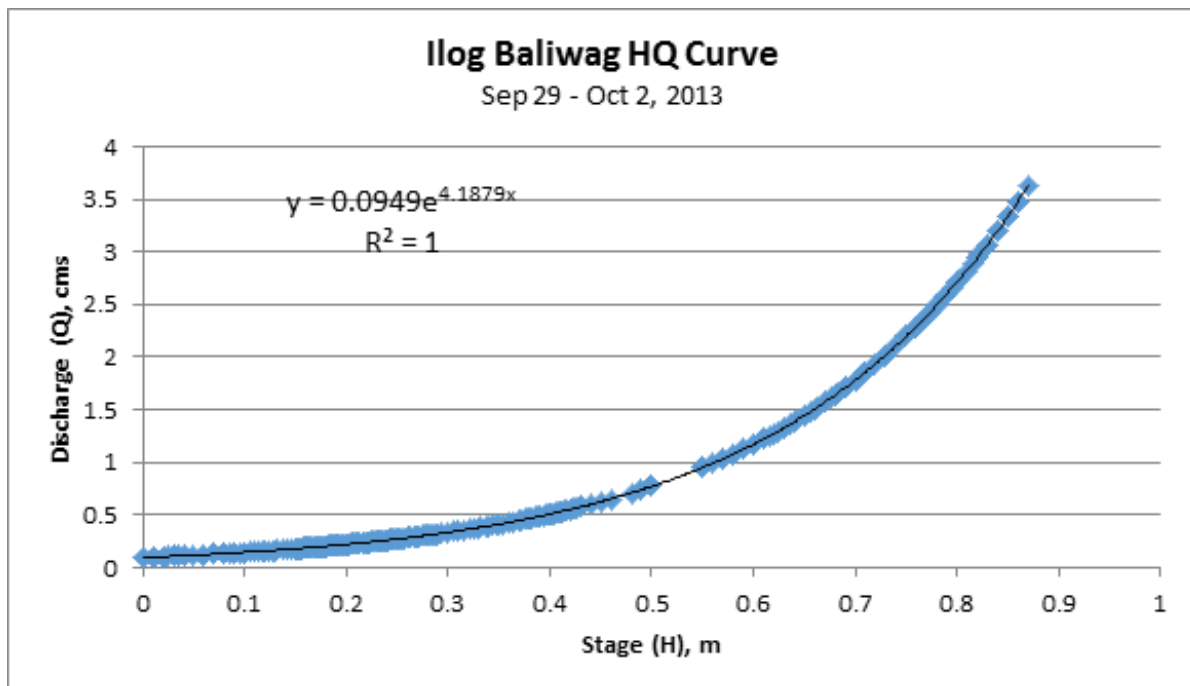


Figure 20. Water level vs. Discharge Curve for Ilog Baliwag Bridge

Methodology

3.1.4.4 Sto. Niño Bridge, Bulacan Rating Curve

For Sto. Nino Bridge, the rating curve is expressed as $Q = 0.0003e^{1.122x}$ as shown in Figure 21.

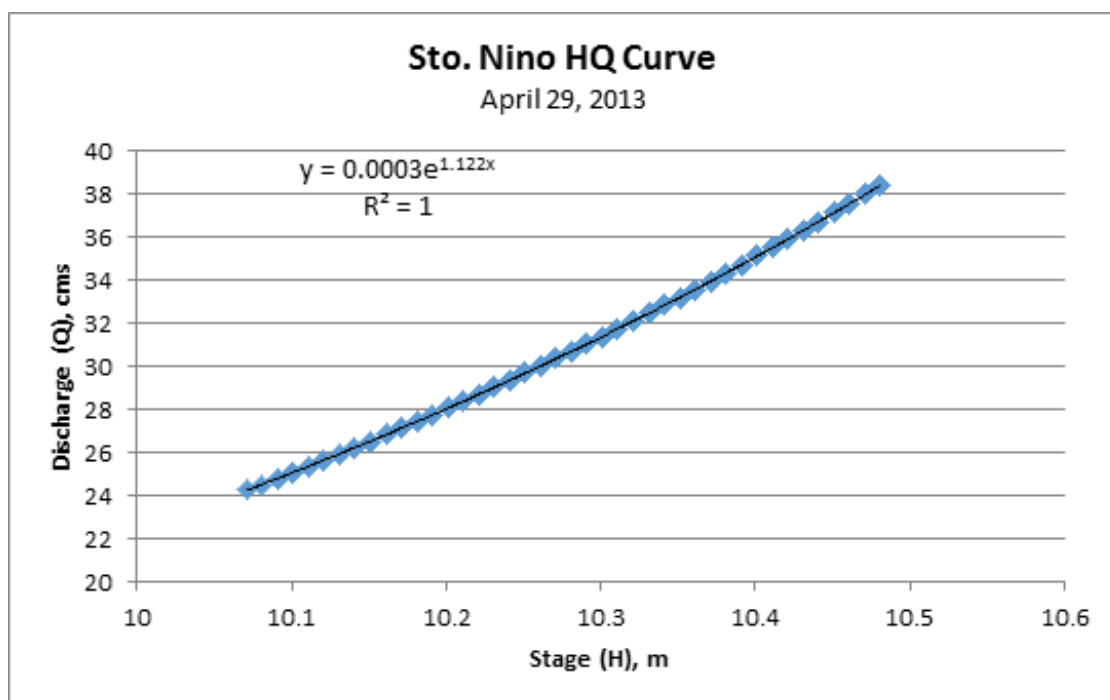


Figure 21. Water level vs. Discharge Curve for Sto. Niño Bridge



Methodology

3.2 Rainfall-Runoff Hydrologic Model Development

3.2.1 Watershed Delineation and Basin Model Pre-processing

The hydrologic model of Pampanga River Basin was developed using Watershed Modeling System (WMS) version 9.1. The software was developed by Aquaveo, a water resources engineering consulting firm in United States. WMS is a program capable of various watershed computations and hydrologic simulations. The hydrologic model development follows the scheme shown in Figure 22.

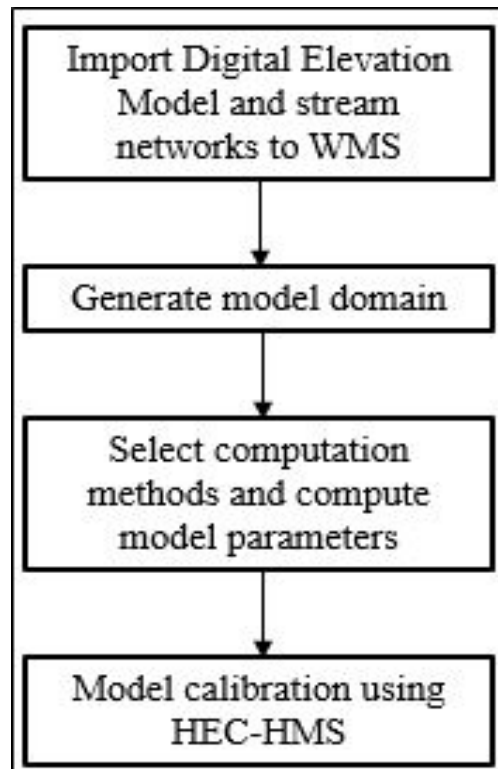


Figure 22. The Rainfall-Runoff Basin Model Development Scheme

Hydro-corrected SRTM DEM was used as the terrain for the basin model. The watershed delineation and its hydrologic elements, namely the subbasins, junctions and reaches, were generated using WMS after importing the elevation data and stream networks.

The Pampanga basin model consists of 96 sub basins, 80 reaches, and 84 junctions. The main outlet is 107C. This basin model is illustrated in Figure 23. The basins were identified based on soil and land cover characteristics of the area. Precipitation from the 22-29 October, 2012 was taken from Data Validation rain gauges. Finally, it was calibrated using data from the Data Validation Component using Acoustic Doppler Current Profiler (ADCP).

Methodology

Table 1. Methods used for the different Calculation types for the hydrologic elements

Hydrologic Element	Calculation Type	Method
Subbasin	Loss Rate	SCS Curve Number
	Transform	Clark's unit hydrograph
	Baseflow	Bounded recession
Reach	Routing	Muskingum-Cunge

3.2.2 Basin Model Calibration

The basin model made using WMS was exported to Hydrologic Modeling System (HEC-HMS) version 3.5, a software made by the Hydrologic Engineering Center of the US Army Corps of Engineers, to create the final rainfall-runoff model. The developers described HEC-HMS as a program designed to simulate the hydrologic processes of a dendritic watershed systems. In this study, the rainfall-runoff model was developed to calculate inflow from the watershed to the floodplain.

Precipitation data was taken from the rain gauge installed by the Data Validation Component (DVC). But there are fourteen automatic rain gauges (ARGs) installed by the Department of Science and Technology – Advanced Science and Technology Institute (DOST-ASTI). The location of the rain gauges is seen in Figure 25.

For Abad Santos Bridge River, the precipitation was taken from the PAGASA rain gauge in Cabanatuan.

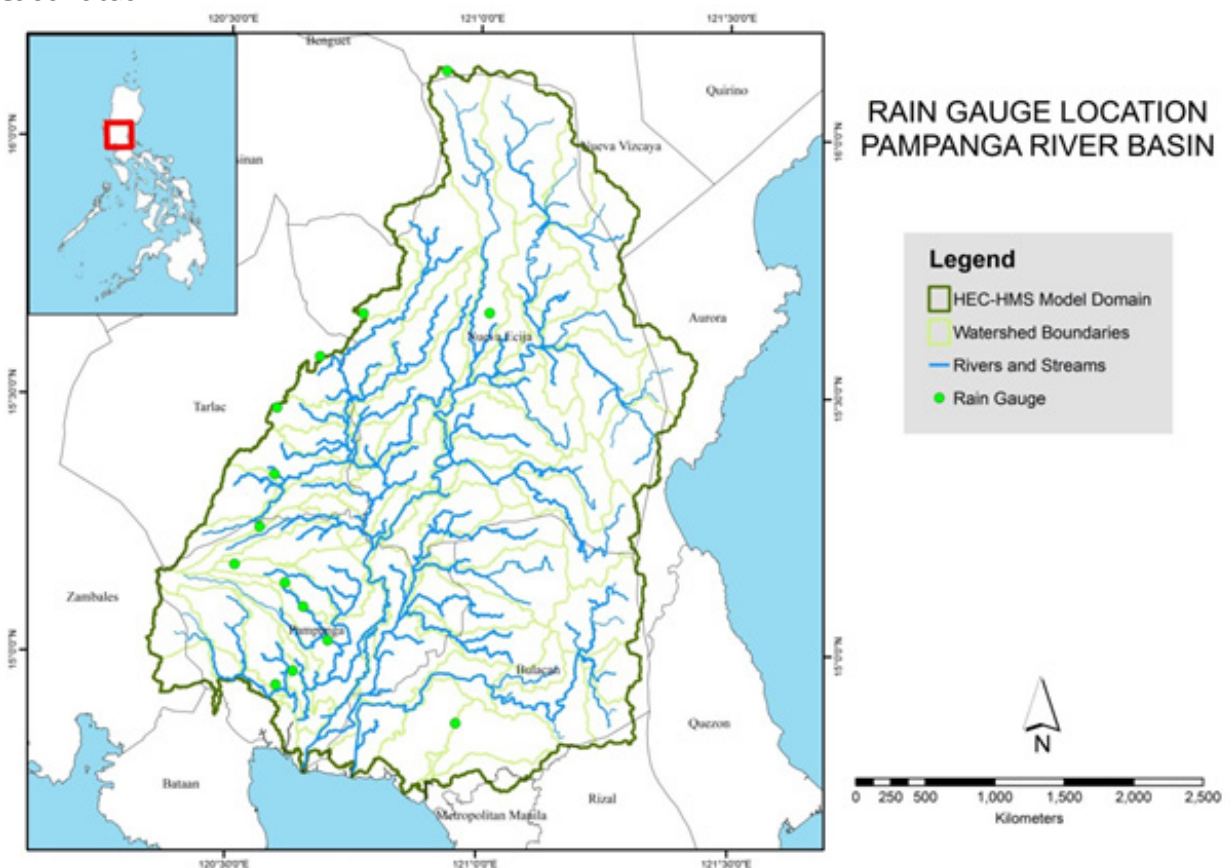


Figure 24. Map showing the location of the rain gauges within the Pampanga River Basin

Methodology

The outflow hydrograph for the downstream-most discharge point with field data was also encoded to the model as a basis for the calibration. Using the said data, HEC-HMS could perform rainfall-runoff simulation and the resulting outflow hydrograph was compared with the observed hydrograph. The values of the parameters were adjusted and optimized in order for the calculated outflow hydrograph to appear like the observed hydrograph. Acceptable values of the subbasin and reach parameters from the manual and past literatures were considered in the calibration.

After the calibration of the downstream-most discharge point, model calibration of the discharge points along the major tributaries of the main river/s were also performed (see Applications).

3.3 HEC-HMS Hydrologic Simulations for Discharge Computations using PAGASA RIDF Curves

3.3.1 Discharge Computation using Rainfall-Runoff Hydrologic Model

The calibrated rainfall-Runoff Hydrologic Model for the Pampanga River Basin using WMS and HEC-HMS was used to simulate the flow for for the five return periods, namely, 5-, 10-, 25-, 50-, and 100-year RIDFs. Time-series data of the precipitation data using the Cabanatuan RIDF curves were encoded to HEC-HMS for the aforementioned return periods, wherein each return period corresponds to a scenario. This process was performed for all discharge points – Cong Dado Dam, Abad Santos Bridge, Alejo Bridge, Ilog Baliwag bridge and Sto. Niño Bridge. The output for each simulation was an outflow hydrograph from that result, the total inflow to the floodplain and time difference between the peak outflow and peak precipitation could be determined.

3.3.2 Discharge Computation using Dr. Horritt’s Recommended Hydrological Method

The required data to be accumulated for the implementation of Dr. Horrit’s method is shown on Figure 25.

Methodology

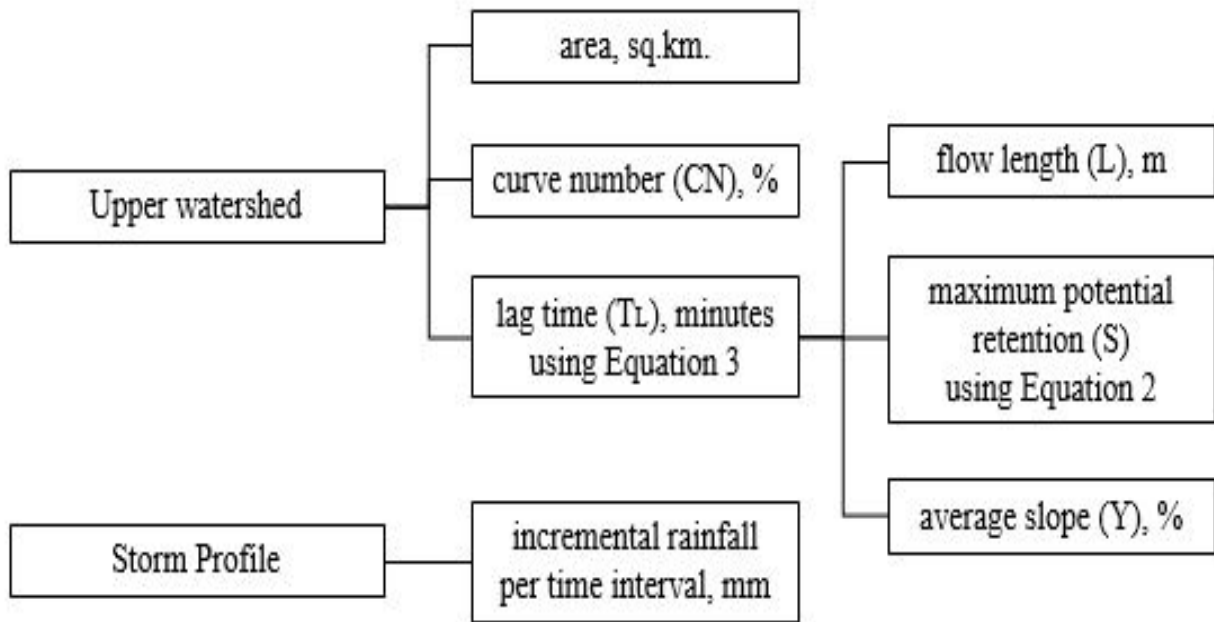


Figure 25. Different data needed as input for HEC-HMS discharge simulation using Dr. Horritt's recommended hydrology method.

Flows from streams were computed using the hydrology method developed by the flood modeling component with Dr. Matt Horritt, a British hydrologist that specializes in flood research. The methodology was based on an approach developed by CH2M Hill and Horritt Consulting for Taiwan which has been successfully validated in a region with meteorology and hydrology similar to the Philippines. It utilizes the SCS curve number and unit hydrograph method to have an accurate approximation of river discharge data from measurable catchment parameters.

3.3.2.1 Determination of Catchment Properties

RADARSAT DTM data for the different areas of the Philippines were compiled with the aid of ArcMap. RADARSAT satellites provide advance geospatial information and these were processed in the forms of shapefiles and layers that are readable and can be analyzed by ArcMap. These shapefiles are digital vectors that store geometric locations.

The watershed flow length is defined as the longest drainage path within the catchment, measured from the top of the watershed to the point of the outlet. With the tools provided by the ArcMap program and the data from RADARSAT DTM, the longest stream was selected and its geometric property, flow length, was then calculated in the program.

The area of the watershed is determined with the longest stream as the guide. The compiled RADARSAT data has a shapefile with defined small catchments based on mean elevation. These parameters were used in determining which catchments, along with the area, belong in the upper watershed. A sample image of the floodplain and upper watershed is shown in Figure 26.



Figure 26. Delineation upper watershed for Pampanga floodplain discharge computation

Methodology

The value of the curve number was obtained using the RADARSAT data that contains information of the Philippine national curve number map. An ArcMap tool was used to determine the average curve number of the area bounded by the upper watershed shapefile. The same method was implemented in determining the average slope using RADARSAT with slope data for the whole country.

After determining the curve number (CN), the maximum potential retention (S) was determined by Equation 2.

$$S = \frac{1000}{CN} - 10$$

Equation 2. Determination of maximum potential retention using the average curve number of the catchment

The watershed length (L), average slope (Y) and maximum potential retention (S) are used to estimate the lag time of the upper watershed as illustrated in Equation 3.

$$T_L = \frac{L^{0.8}(S + 1)^{0.7}}{560Y^{0.5}}$$

Equation 3. Lag Time Equation Calibrated for Philippine Setting

Finally, the final parameter that will be derived is the storm profile. The synoptic station which covers the majority of the upper watershed was identified. Using the RIDF data, the incremental values of rainfall in millimeter per 0.1 hour was used as the storm profile.

3.3.2.2 HEC-HMS Implementation

With all the parameters available, HEC-HMS was then utilized. Obtained values from the previous section were used as input and a brief simulation would result in the tabulation of discharge results per time interval. The maximum discharge and time-to-peak for the whole simulation as well as the river discharge hydrograph were used for the flood simulation process. The time series results (discharge per time interval) were stored as HYD files for input in FLO-2D GDS Pro.

Methodology

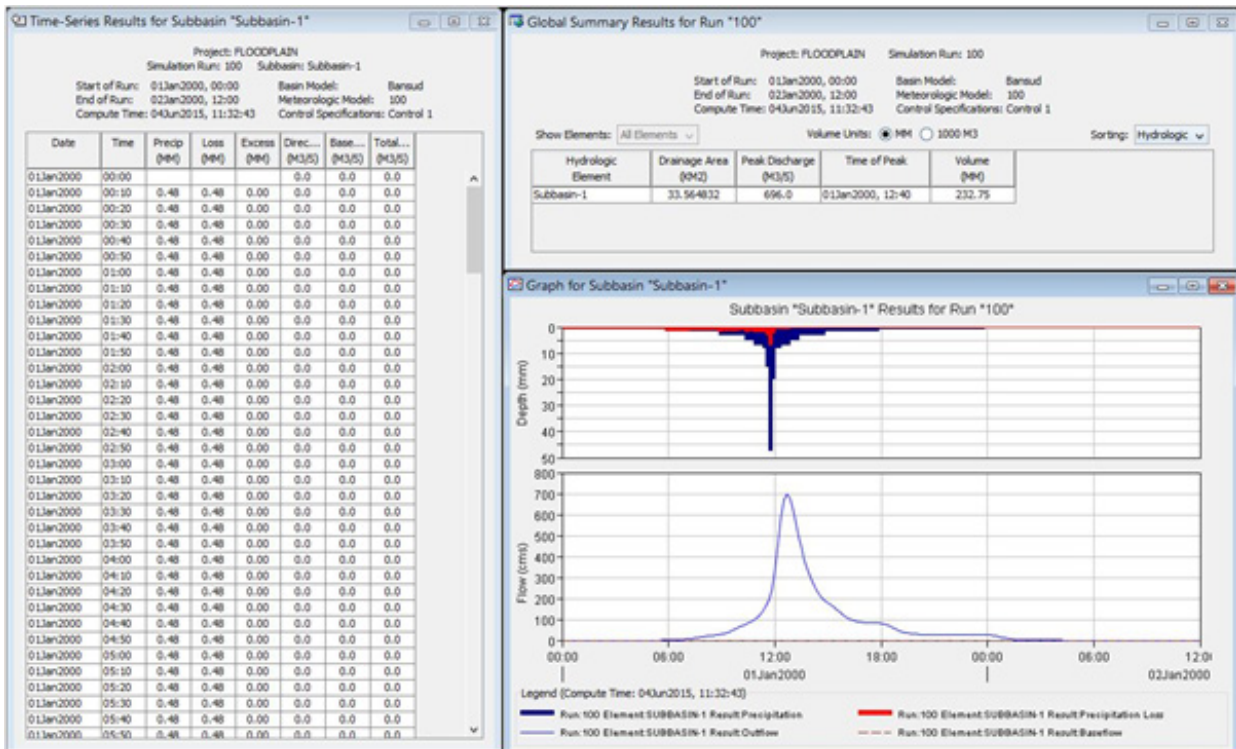


Figure 27. HEC-HMS simulation discharge results using Dr. Horritt’s Method

3.3.2.3 Discharge validation against other estimates

As a general rule, the river discharge of a 2-year rain return, Q_{MED} , should approximately be equal to the bankful discharge, $Q_{bankful}$, of the river. This assumes that the river is in equilibrium, with its deposition being balanced by erosion. Since the simulations of the river discharge are done for 5-, 25-, and 100-year rainfall return scenarios, a simple ratio for the 2-year and 5-year return was computed with samples from actual discharge data of different rivers. It was found out to have a constant of 0.88. This constant, however, should still be continuously checked and calibrated when necessary.

$$Q_{MED} = 0.88Q_{5yr}$$

Equation 4. Ratio of river discharge of a 5-year rain return to a 2-year rain return scenario from measured discharge data

For the discharge calculation to pass the validation using the bankful method, Equation 5 must be satisfied.

$$50\% Q_{bankful} \leq Q_{MED} \leq 150\% Q_{bankful}$$

Equation 5. Discharge validation equation using bankful method

The bankful discharge was estimated using channel width (w), channel depth (h), bed slope (S) and Manning’s constant (n). Derived from the Manning’s Equation, the equation for the bankful discharge is by Equation 6.



$$Q_{bankful} = \frac{(wh)^{\frac{5}{3}} S^{\frac{1}{2}}}{n(w + 2h)^{\frac{2}{3}}}$$

Equation 6. Bankful discharge equation using measurable channel parameters

3.4 Hazard and Flow Depth Mapping using FLO-2D

3.4.1 Floodplain Delineation

The boundaries of subbasins within the floodplain were delineated based on elevation values given by the DEM. Each subbasin is marked by ridges dividing catchment areas. These catchments were delineated using a set of ArcMap tools compiled by Al Duncan, a UK Geomatics Specialist, into a single processing model. The tool allows ArcMap to compute for the flow direction and acceleration based on the elevations provided by the DEM.

Running the tool creates features representing large, medium-sized, and small streams, as well as large, medium-sized, and small catchments. For the purpose of this particular model, the large, medium-sized, and small streams were set to have an area threshold of 100,000sqm, 50,000sqm, and 10,000sqm respectively. These thresholds define the values where the algorithm refers to in delineating a trough in the DEM as a stream feature, i.e. a large stream feature should drain a catchment area totalling 100,000 sqm to be considered as such. These values differ from the standard values used (10,000sqm, 1,000 sqm and 100sqm) to limit the detail of the project, as well as the file sizes, allowing the software to process the data faster.

The tool also shows the direction in which the water is going to flow across the catchment area. This information was used as the basis for delineating the floodplain. The entire area of the floodplain was subdivided into several zones in such a way that it can be processed properly. This was done by grouping the catchments together, taking special account of the inflows and outflows of water across the entire area. To be able to simulate actual conditions, all the catchments comprising a particular computational domain were set to have outflows that merged towards a single point. The area of each subdivision was limited to 250,000 grids or less to allow for an optimal simulation in FLO-2D GDS Pro. Larger models tend to run longer, while smaller models may not be as accurate as a large one.

3.4.2 Flood Model Generation

The software used to run the simulation is FLO-2D GDS Pro. It is a GIS integrated software tool that creates an integrated river and floodplain model by simulating the flow of the water over a system of square grid elements.

After loading the shapefile of the subcatchment onto FLO-2D, 10 meter by 10 meter grids that encompassed the entire area of interest were created.

The boundary for the area was set by defining the boundary grid elements. This can either be

Methodology

done by defining each element individually, or by drawing a line that traces the boundaries of the subcatchment. The grid elements inside of the defined boundary were considered as the computational area in which the simulation will be run.

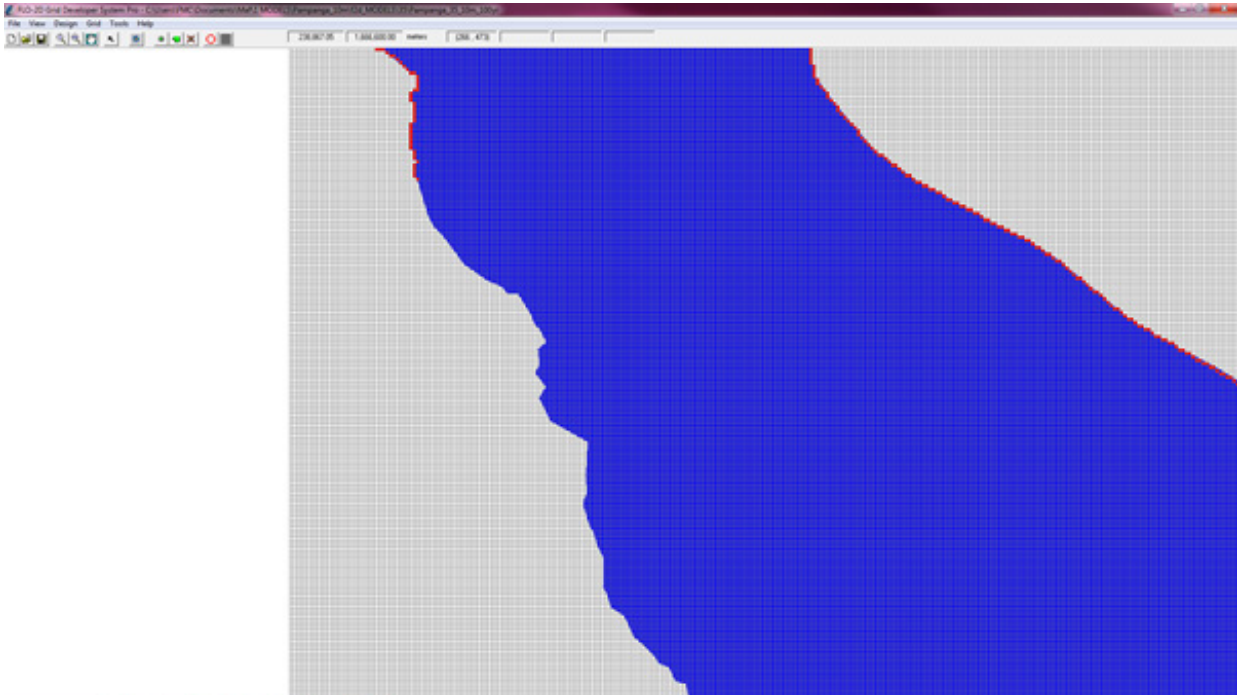


Figure 28. Screenshot showing how boundary grid elements are defined by line
Elevation data was imported in the form of the DEM gathered through LiDAR. These elevation points in PTS format were extrapolated into the model, providing an elevation value for each grid element.

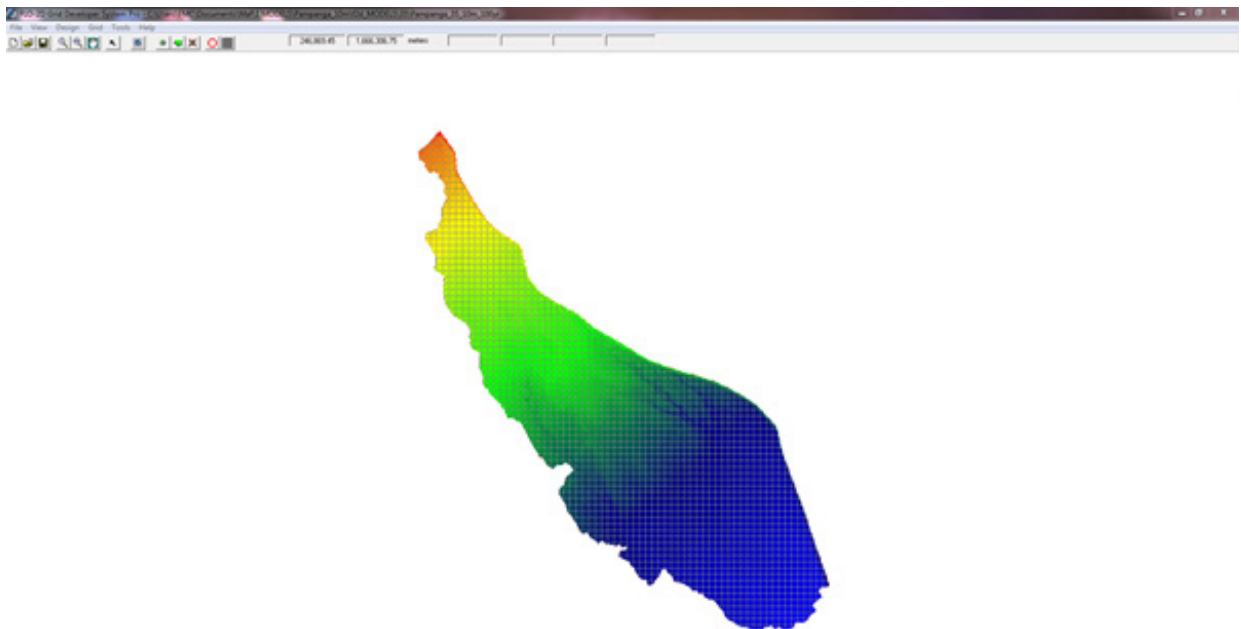


Figure 29. Screenshots of PTS files when loaded into the FLO-2D program

Methodology

The floodplain is predominantly composed of rice fields, which have a Manning coefficient of 0.15. All the inner grid elements were selected and the Manning coefficient of 0.15 was assigned. To differentiate the streams from the rest of the floodplain, a shapefile containing all the streams and rivers in the area were imported into the software. The shapefile was generated using Al Duncan's catchment tool for ArcMap. The streams were then traced onto their corresponding grid elements.

These grid elements were all selected and assigned a Manning coefficient of 0.03. The DEM and aerial imagery were also used as bases for tracing the streams and rivers.

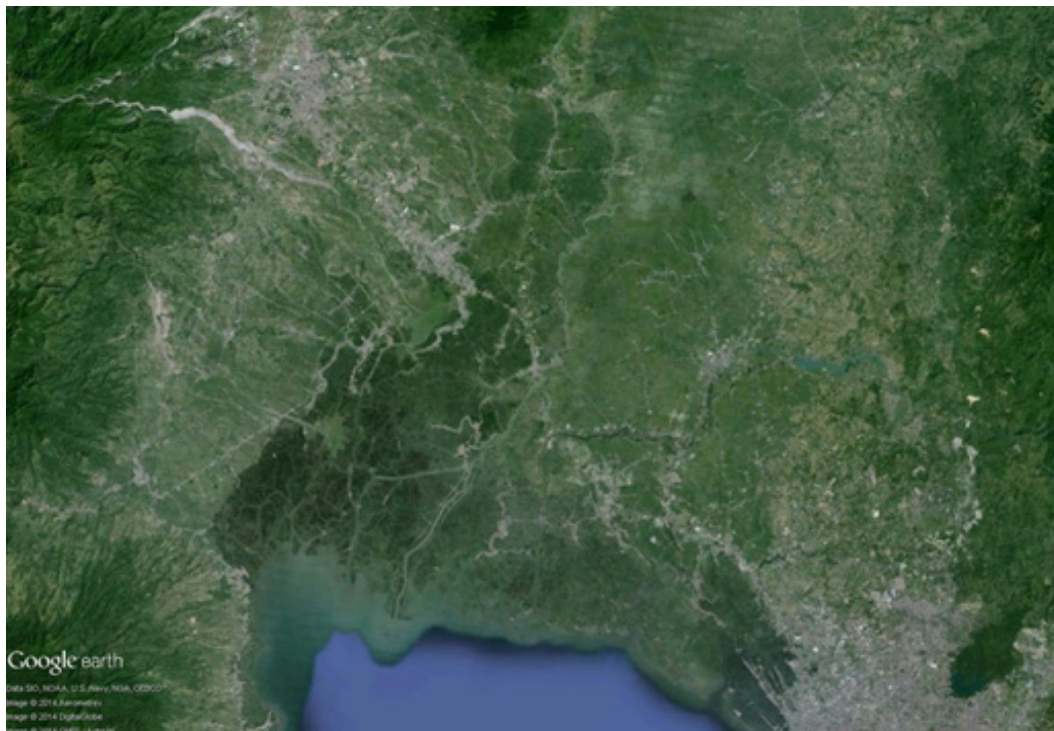


Figure 30. Aerial Image of the Pampanga floodplain

Methodology

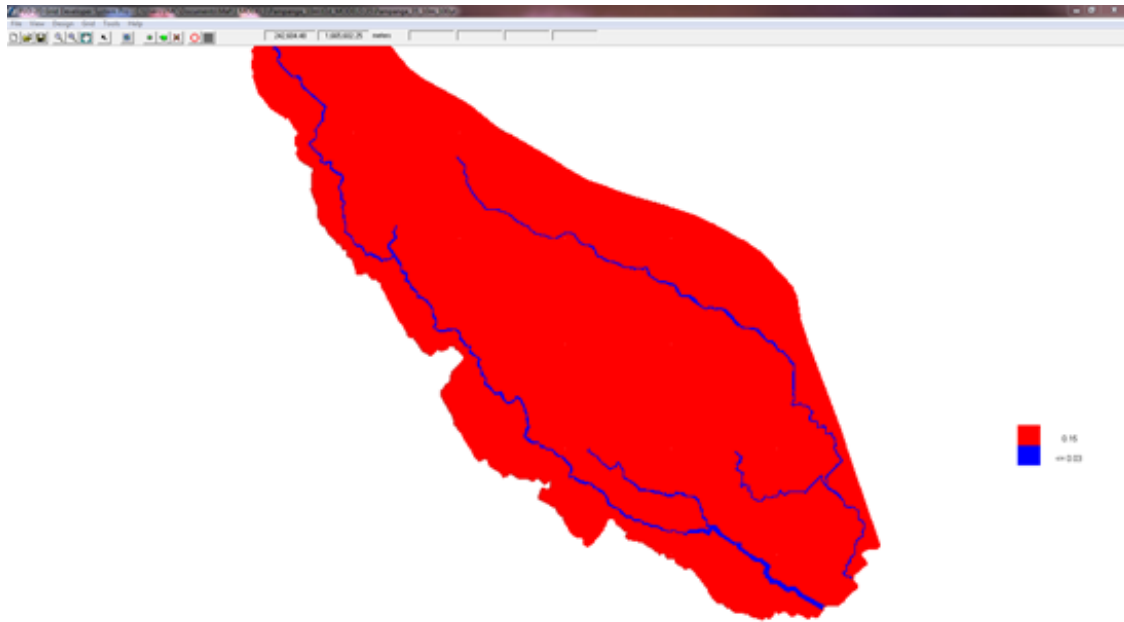


Figure 23. Screenshot of Manning's n-value rendering

After assigning Manning coefficients for each grid, the infiltration parameters were identified. Green-Ampt infiltration method by W. Heber Green and G.S Ampt were used for all the models. The initial saturations applied to the model were 0.99, 0.8, and 0.7 for 100-year, 25-year, and 5-year rain return periods respectively. These initial saturations were used in the computation of the infiltration value.

The Green-Ampt infiltration method by W. Heber Green and G.S Ampt method is based on a simple physical model in which the equation parameter can be related to physical properties of the soil. Physically, Green and Ampt assumed that the soil was saturated behind the wetting front and that one could define some “effective” matric potential at the wetting front (Kirkham, 2005). Basically, the system is assumed to consist of a uniformly wetted near-saturated transmission zone above a sharply defined wetting front of constant pressure head (Diamond & Shanley, 2003).

The next step was to allocate inflow nodes based on the locations of the outlets of the streams from the upper watershed. The inflow values came from the computed discharges that were input as hyd files.

Outflow nodes were allocated for the model. These outflow nodes show the locations where the water received by the watershed is discharged. The water that will remain in the watershed will result to flooding on low lying areas.

For the models to be able to simulate actual conditions, the inflow and outflow of each computational domain should be indicated properly. In situations wherein water flows from one subcatchment to the other, the corresponding models are processed one after the other. The outflow generated by the source subcatchment was used as inflow for the subcatchment area that it flows into.

Methodology

The standard simulation time used to run each model is the time-to-peak (TP) plus an additional 12 hours. This gives enough time for the water to flow into and out of the model area, illustrating the complete process from entry to exit as shown in the hydrograph. The additional 12 hours allows enough time for the water to drain fully into the next subcatchment. After all the parameters were set, the model was run through FLO-2D GDS Pro.

3.4.3 Flow Depth and Hazard Map Simulation

After running the flood map simulation in FLO-2D GDS Pro, FLO-2D Mapper Pro was used to read the resulting hazard and flow depth maps. The standard input values for reading the simulation results are shown on Figure 24.

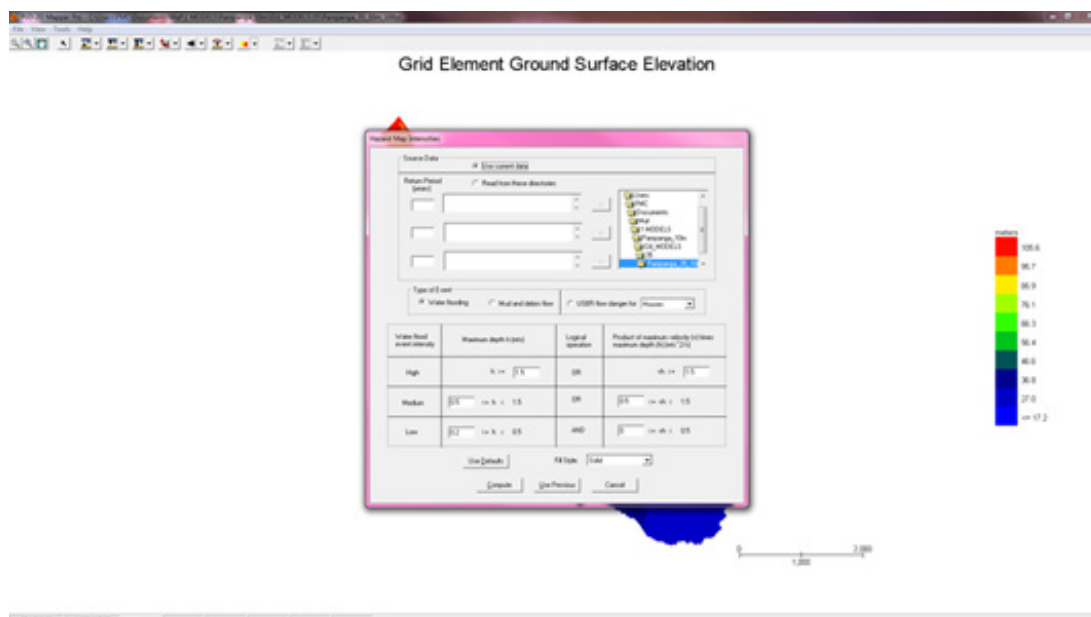


Figure 32. Flo-2D Mapper Pro General Procedure

In order to produce the hazard maps, set input for low maximum depth as 0.2 m, and vh , product of maximum velocity and maximum depth (m^2/s), as greater than or equal to zero. The program will then compute for the flood inundation and will generate shapefiles for the hazard and flow depth scenario.

Methodology

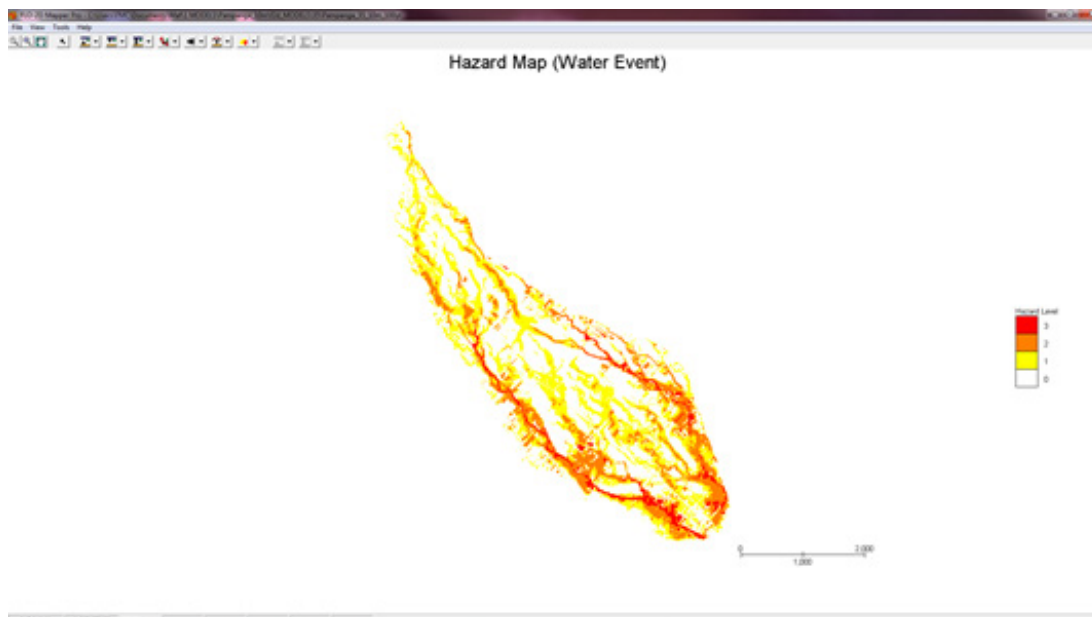


Figure 33. Pampanga Floodplain Generated Hazard Maps using Flo-2D Mapper

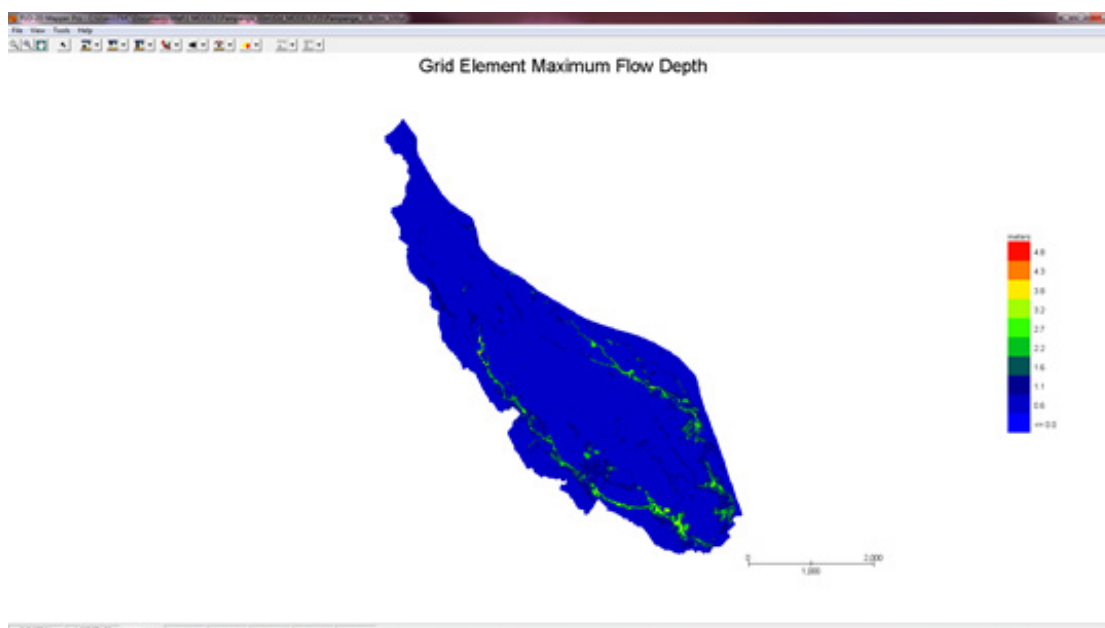
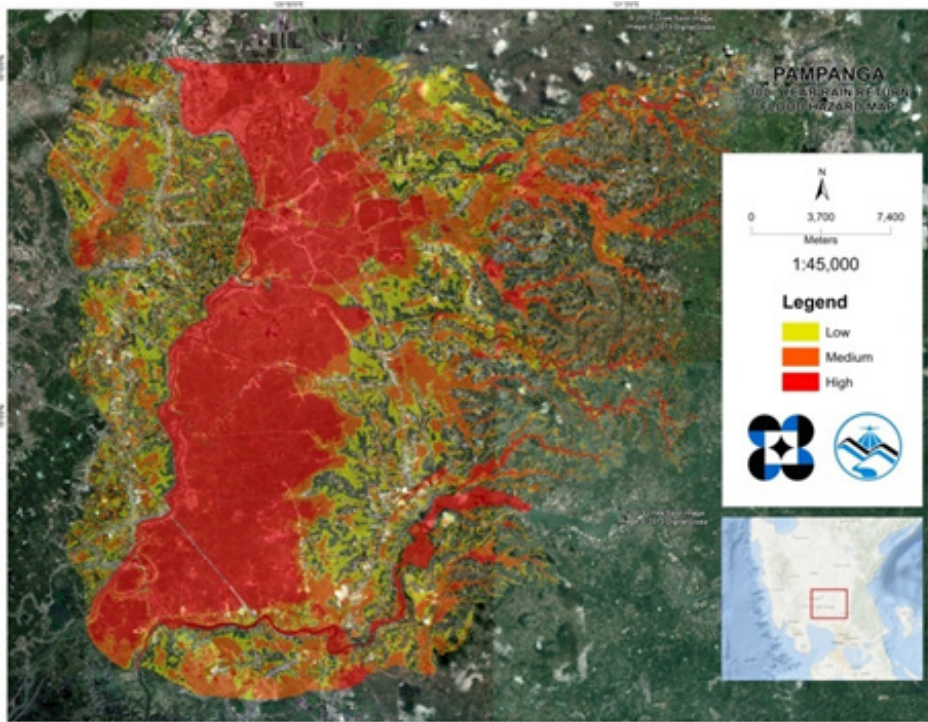


Figure 34. Pampanga floodplain generated flow depth map using Flo-2D Mapper

Methodology

3.4.4 Hazard Map and Flow Depth Map Creation

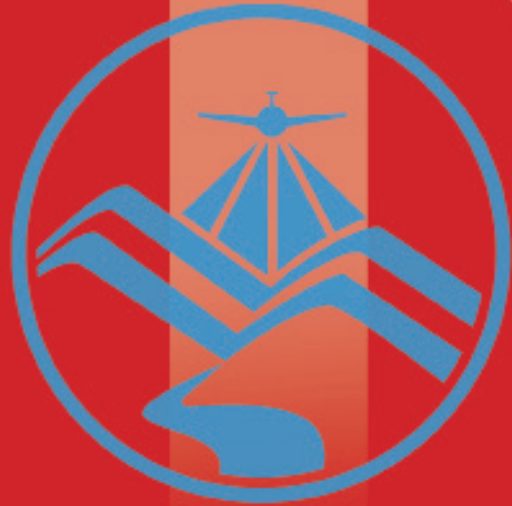
The final procedure in creating the maps is to prepare them with the aid of ArcMap. The generated shapefiles from FLO-2D Mapper Pro were opened in ArcMap. The basic layout of a hazard map is shown in Figure 35. The same map elements are also found in a flow depth map.



ELEMENTS:

1. River Basin Name
2. Hazard/Flow Depth Shapefile
3. Provincial Inset
4. Philippine Inset
5. Hi-Res image of the area
6. North Arrow
7. Scale Text and Bar

Figure 35. Basic Layout and Elements of the Hazard Maps



Results and Discussion

Results and Discussion

4.1 Efficiency of HEC-HMS Rainfall-Runoff Models calibrated based on field survey and gauges data

4.1.1 Cong Dado Dam, Pampanga HMS Calibration Results

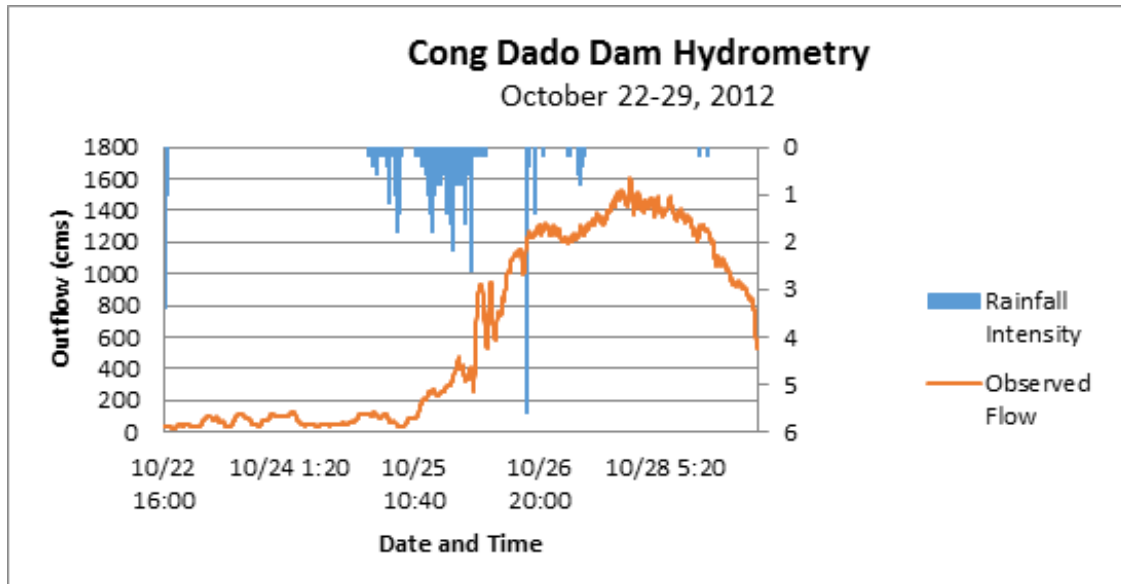


Figure 36. Cong Dado Dam Outflow Hydrograph produced by the HEC-HMS model compared with observed outflow

After calibrating the Cong Dado Dam HEC-HMS river basin model, its accuracy was measured against the observed values. Figure 36 shows the comparison between the two discharge data.

The Root Mean Square Error (RMSE) method aggregates the individual differences of these two measurements. It was identified at 115.4 m³/s.

The Pearson correlation coefficient (r^2) assesses the strength of the linear relationship between the observations and the model. This value being close to 1 corresponds to an almost perfect match of the observed discharge and the resulting discharge from the HEC HMS model. Here, it measured 0.996437753.

The Nash-Sutcliffe (E) method was also used to assess the predictive power of the model. Here the optimal value is 1. The model attained an efficiency coefficient of 0.91.

A positive Percent Bias (PBIAS) indicates a model's propensity towards under-prediction. Negative values indicate bias towards over-prediction. Again, the optimal value is 0. In the model, the PBIAS is -4.40

The Observation Standard Deviation Ratio, RSR, is an error index. A perfect model attains a value of 0. The model has an RSR value of 0.29.



Results and Discussion

4.1.2 Abad Santos Bridge, Pampanga HMS model Pampanga Calibration Results

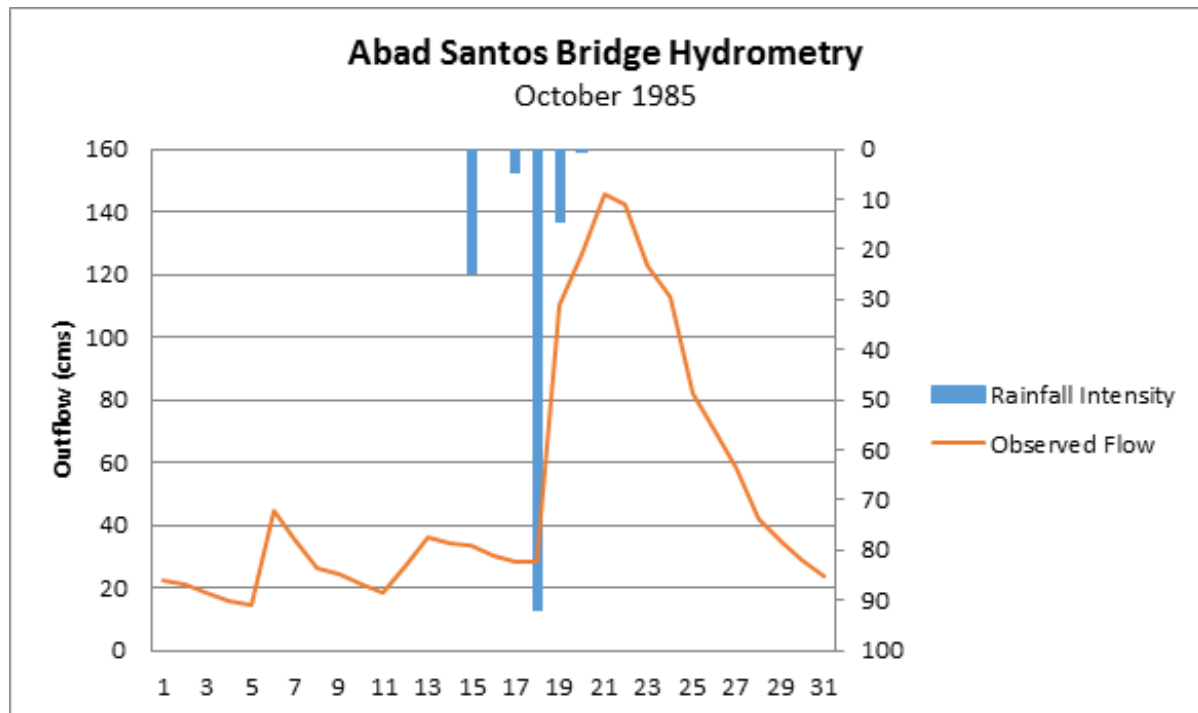


Figure 37. Abad Santos Outflow Hydrograph produced by the HEC-HMS model compared with observed outflow

After calibrating the Abad Santos Bridge HEC-HMS river basin model, its accuracy was measured against the observed values. Figure 37 shows the comparison between the two discharge data.

The Root Mean Square Error (RMSE) method aggregates the individual differences of these two measurements. It was identified at 14.837.

The Pearson correlation coefficient (r_2) assesses the strength of the linear relationship between the observations and the model. This value being close to 1 corresponds to an almost perfect match of the observed discharge and the resulting discharge from the HEC HMS model. Here, it measured 0.9717.

The Nash-Sutcliffe (E) method was also used to assess the predictive power of the model. Here the optimal value is 1. The model attained an efficiency coefficient of 0.9367.

A positive Percent Bias (PBIAS) indicates a model's propensity towards under-prediction. Negative values indicate bias towards over-prediction. Again, the optimal value is 0. In the model, the PBIAS is 0.141.

The Observation Standard Deviation Ratio, RSR, is an error index. A perfect model attains a value of 0. The model has an RSR value of 0.000637.

Results and Discussion

4.1.3 Alejo Santos Bridge, Bulacan HMS Model Calibration Results

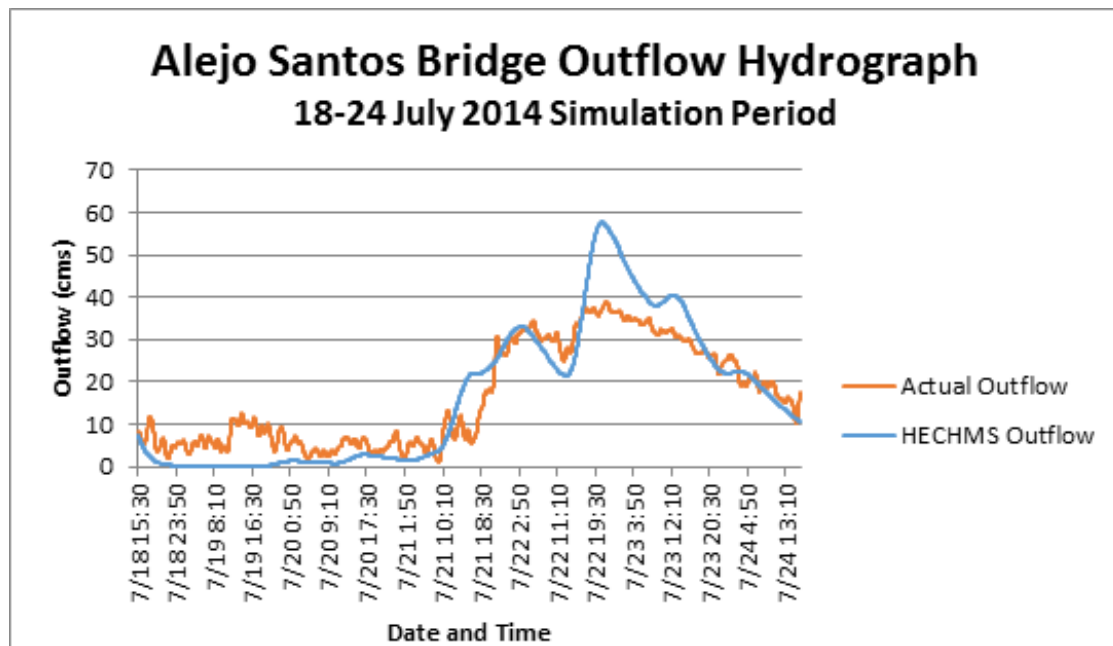


Figure 38. Abad Santos Outflow Hydrograph produced by the HEC-HMS model compared with observed outflow

After calibrating the Alejo Santos HEC-HMS river basin model, its accuracy was measured against the observed values. Figure 38 shows the comparison between the two discharge data.

The Root Mean Square Error (RMSE) method aggregates the individual differences of these two measurements. It was identified at 6.7.

The Pearson correlation coefficient (r^2) assesses the strength of the linear relationship between the observations and the model. This value being close to 1 corresponds to an almost perfect match of the observed discharge and the resulting discharge from the HEC HMS model. Here, it measured 19.5.

The Nash-Sutcliffe (E) method was also used to assess the predictive power of the model. Here the optimal value is 1. The model attained an efficiency coefficient of 0.69.

A positive Percent Bias (PBIAS) indicates a model's propensity towards under-prediction. Negative values indicate bias towards over-prediction. Again, the optimal value is 0. In the model, the PBIAS is 1.21.

The Observation Standard Deviation Ratio, RSR, is an error index. A perfect model attains a value of 0. The model has an RSR value of 0.56.

Results and Discussion

4.1.4 Ilog Baliwag Bridge, Nueva Ecija HMS Calibration Results

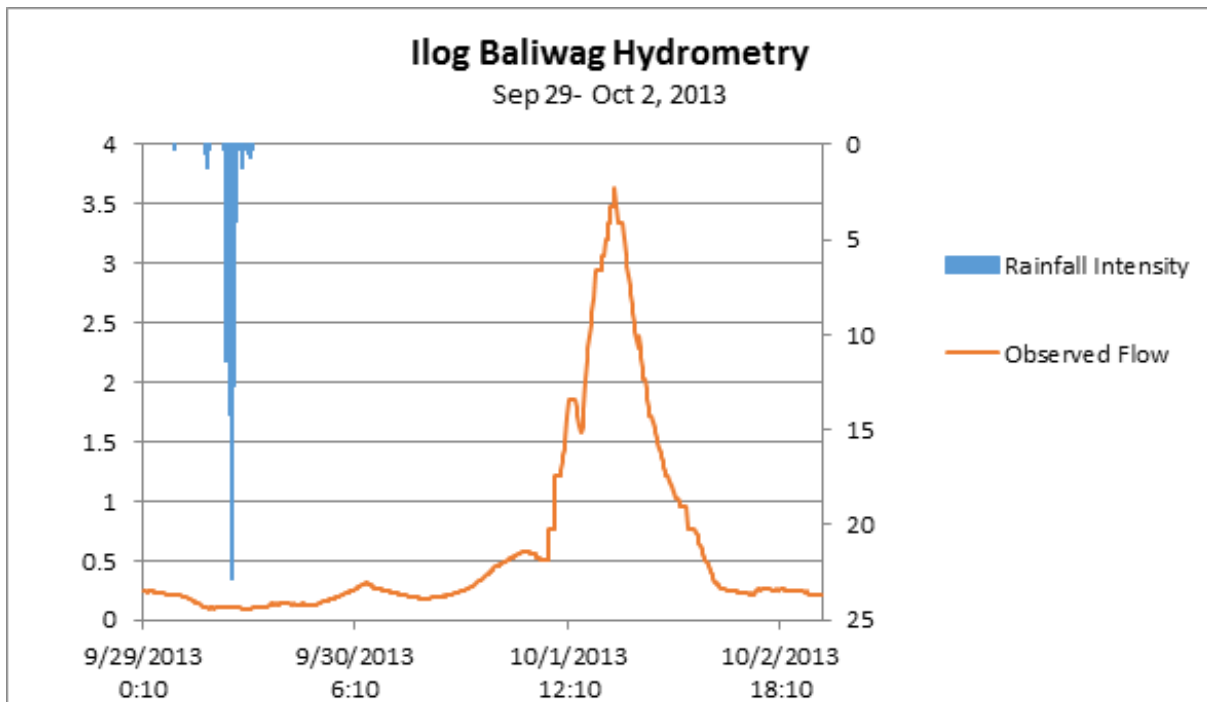


Figure 39. Ilog Baliwag Outflow Hydrograph produced by the HEC-HMS model compared with observed outflow

After calibrating the Ilog Baliwag HEC-HMS river basin model, its accuracy was measured against the observed values. Figure 39 shows the comparison between the two discharge data.

The Root Mean Square Error (RMSE) method aggregates the individual differences of these two measurements. It was identified at 5.3.

The Pearson correlation coefficient (r^2) assesses the strength of the linear relationship between the observations and the model. This value being close to 1 corresponds to an almost perfect match of the observed discharge and the resulting discharge from the HEC HMS model. Here, it measured 0.57.

The Nash-Sutcliffe (E) method was also used to assess the predictive power of the model. Here the optimal value is 1. The model attained an efficiency coefficient of -41.63.

A positive Percent Bias (PBIAS) indicates a model's propensity towards under-prediction. Negative values indicate bias towards over-prediction. Again, the optimal value is 0. In the model, the PBIAS is -88.15.

The Observation Standard Deviation Ratio, RSR, is an error index. A perfect model attains a value of 0. The model has an RSR value of 6.53.

Results and Discussion

4.1.5 Sto. Niño Bridge, Bulacan Calibration Results

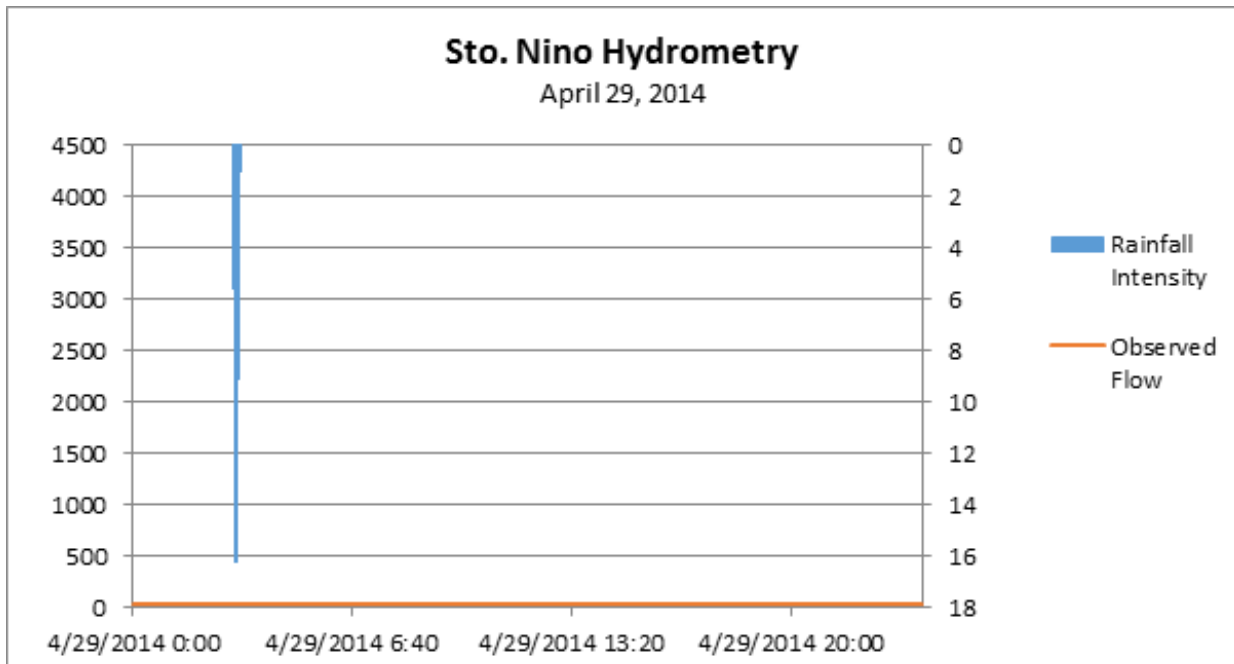


Figure 40. Sto. Niño Outflow Hydrograph produced by the HEC-HMS model compared with observed outflow

After calibrating the Sto. Nino HEC-HMS river basin model, its accuracy was measured against the observed values. Figure 40 shows the comparison between the two discharge data.

The Root Mean Square Error (RMSE) method aggregates the individual differences of these two measurements. It was identified at 621.6.

The Pearson correlation coefficient (r_2) assesses the strength of the linear relationship between the observations and the model. This value being close to 1 corresponds to an almost perfect match of the observed discharge and the resulting discharge from the HEC HMS model. Here, it measured 0.88.

The Nash-Sutcliffe (E) method was also used to assess the predictive power of the model. Here the optimal value is 1. The model attained an efficiency coefficient of -134.50.

A positive Percent Bias (PBIAS) indicates a model's propensity towards under-prediction. Negative values indicate bias towards over-prediction. Again, the optimal value is 0. In the model, the PBIAS is -93.90.

The Observation Standard Deviation Ratio, RSR, is an error index. A perfect model attains a value of 0. The model has an RSR value of 116.



Results and Discussion

The calibrated models of the other discharge points are used in flood forecasting. DREAM project offers the LGUs and other disaster mitigation agencies a water level forecast tool, which can be found on the DREAM website.

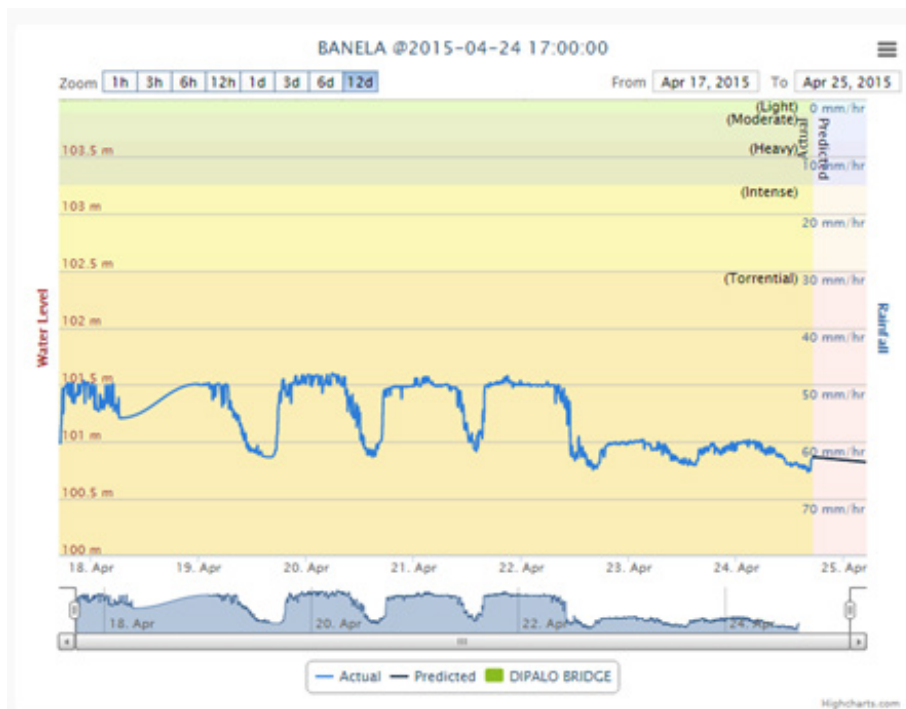


Figure 41. Sample DREAM Water Level Forecast

Given the predicted and real-time actual water level on specific AWLS, possible river flooding can be monitored and information can be disseminated to LGUs. This will help in the early evacuation of the probable affected communities. The calibrated models can also be used for flood inundation mapping.

4.2 Calculated Outflow hydrographs and Discharge Values for different Rainfall Return Periods

4.2.1 Hydrograph using the Rainfall-Runoff Model

4.2.1.1 Cong Dado Dam, Pampanga

In the 5-year return period graph (Figure 42), the peak outflow is 1919.4 cms. This occurs after 1 day, 15 hours, and 40 minutes after the peak precipitation of 26.7 mm.

Results and Discussion

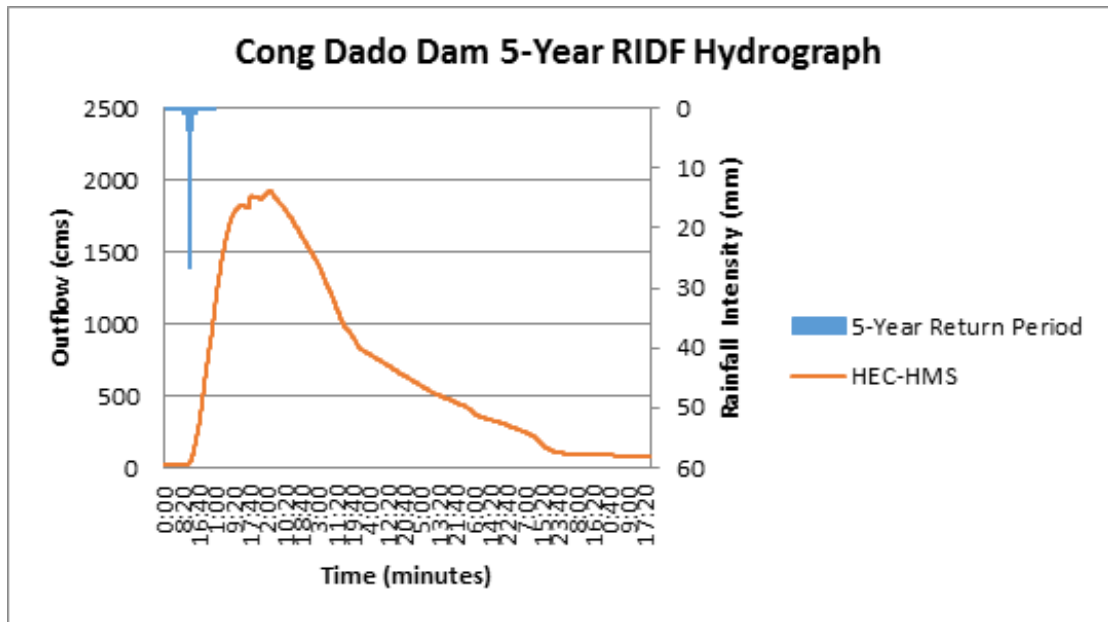


Figure 42. Cong Dado Dam outflow hydrograph generated using the Cabanatuan 5-Year RIDF inputted in WMS and HEC-HMS Basin Model

In the 10-year return period graph (Figure 43), the peak outflow is 2397.9 cms. This occurs after 1 day and 14 hours after the peak precipitation of 32.5 mm.

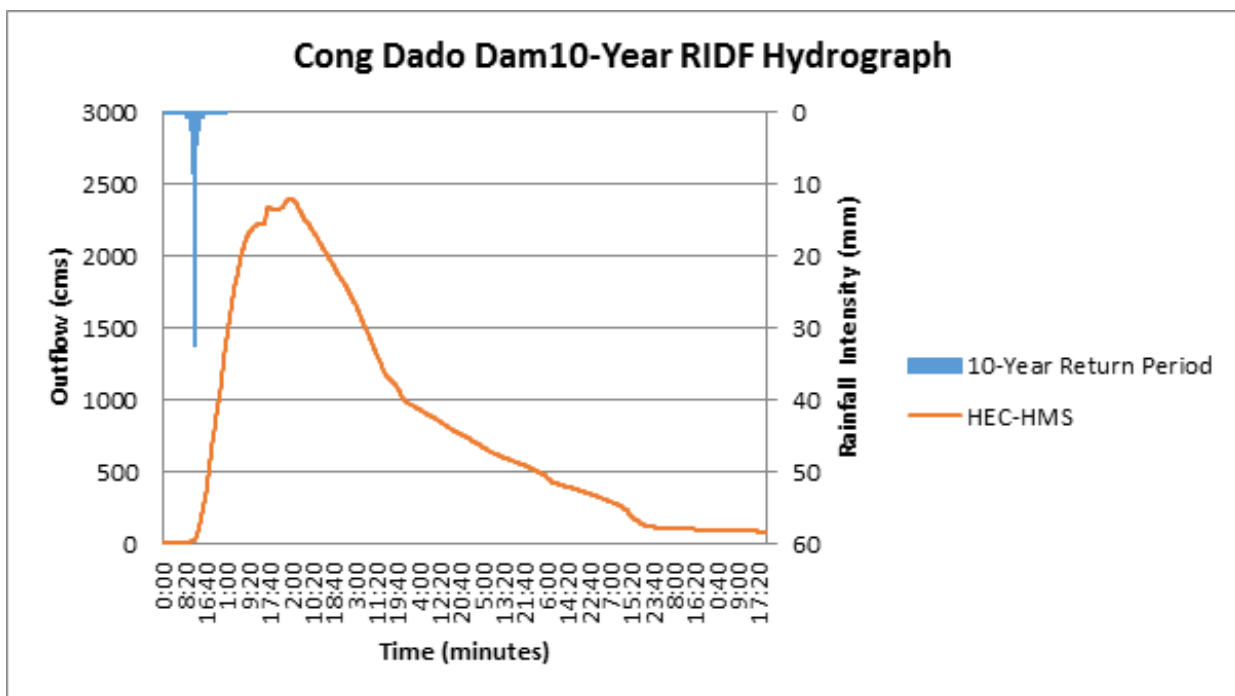


Figure 43. Cong Dado Dam outflow hydrograph generated using the Cabanatuan 10-Year RIDF inputted in WMS and HEC-HMS Basin Model

In the 25-year return period graph (Figure 44), the peak outflow is 3019 cms. This occurs after 1 day, 12 hours, and 30 minutes after the peak precipitation 39.9 mm.



Results and Discussion

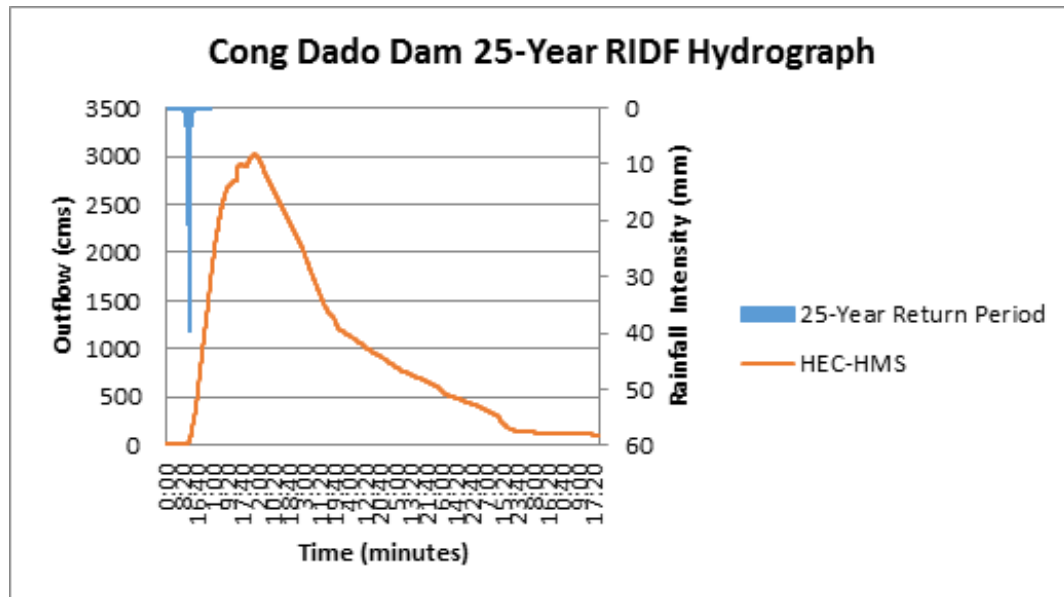


Figure 44. Cong Dado Dam outflow hydrograph generated using the Cabanatuan 25-Year RIDF inputted in WMS and HEC-HMS Basin Model

In the 50-year return period graph (Figure 45), the peak outflow is 3489.3 cms. This occurs after 1 day, 11 hours, 10 minutes after the peak precipitation of 45.4 mm.

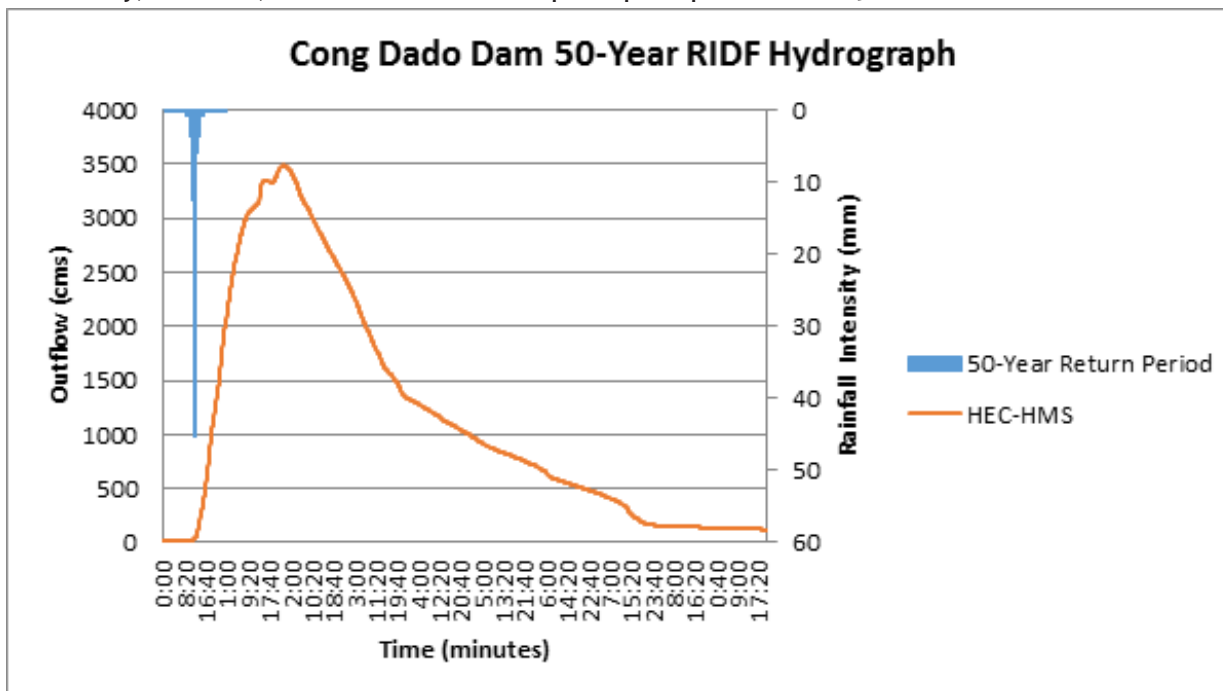


Figure 45. Cong Dado Dam outflow hydrograph generated using the Cabanatuan 50-Year RIDF inputted in WMS and HEC-HMS Basin Model

In the 100-year return period graph (Figure 46), the peak outflow is 3949.4 cms. This occurs after 1 day, 10 hours, and 30 minutes after the peak precipitation of 50.8 mm.

Results and Discussion

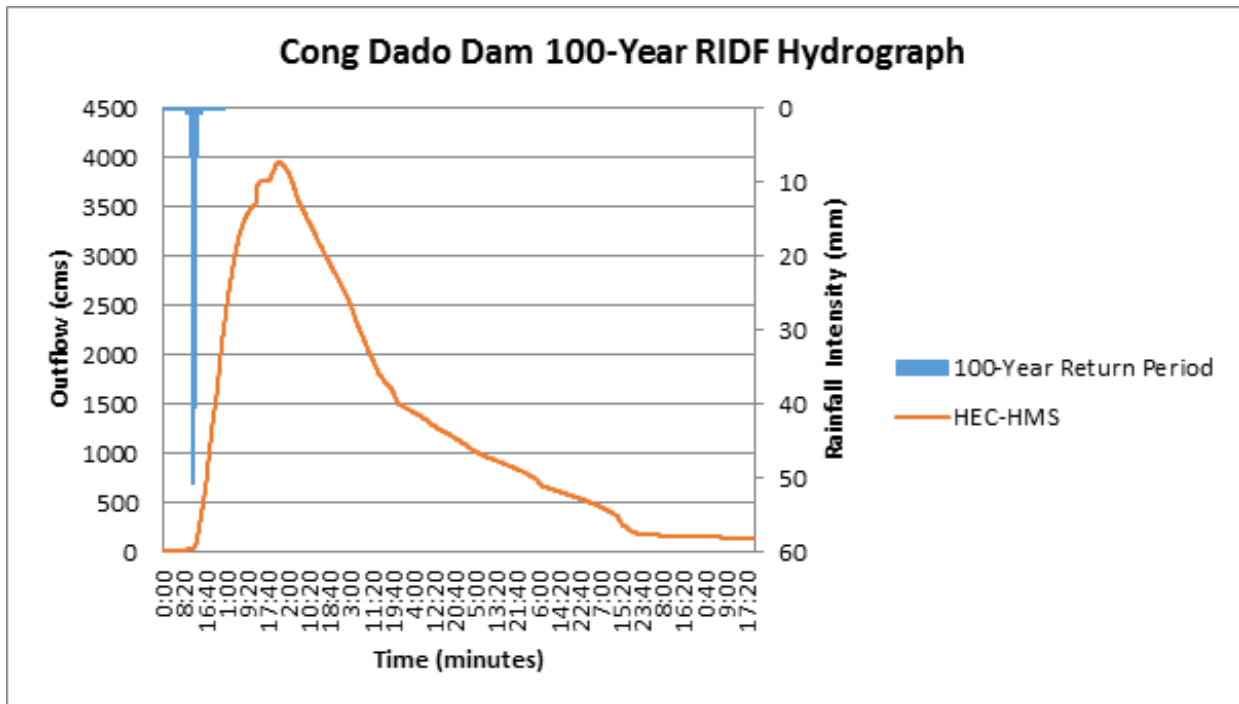


Figure 46. Cong Dado Dam outflow hydrograph generated using the Cabanatuan 100-Year RIDF inputted in WMS and HEC-HMS Basin Model

A summary of the total precipitation, peak rainfall, peak outflow and time to peak of Cong Dado Dam discharge using the Cabanatuan Rainfall Intensity-Duration-Frequency curves (RIDF) in five different return periods is shown in Table 2.

Table 2. Summary of Gamu outflow using Cabanatuan Station Rainfall Intensity Duration Frequency (RIDF)

RIDF Period	Total Precipitation (mm)	Peak rainfall (mm)	Peak outflow (cms)	Time to Peak
5-Year	185.3	26.8	2,466.1	2 days and 2 hours
10-Year	225	31.9	3,169.5	2 days and 20 minutes
25-Year	275.2	38.3	4,085.4	1 day, 22 hours and 30 minutes
50-Year	312.4	43.1	4,774.9	1 day, 21 hours and 40 minutes
100-Year	349.3	47.9	5,459.6	1 day, 21 hours and 10 minutes



Results and Discussion

4.2.1.2 Abad Santos Bridge, Pangasinan

In the 5-year return period graph (Figure 47), the peak outflow is 218.6 cms. This occurs after 2 days and 22 hours after the peak precipitation of 24.79 mm.

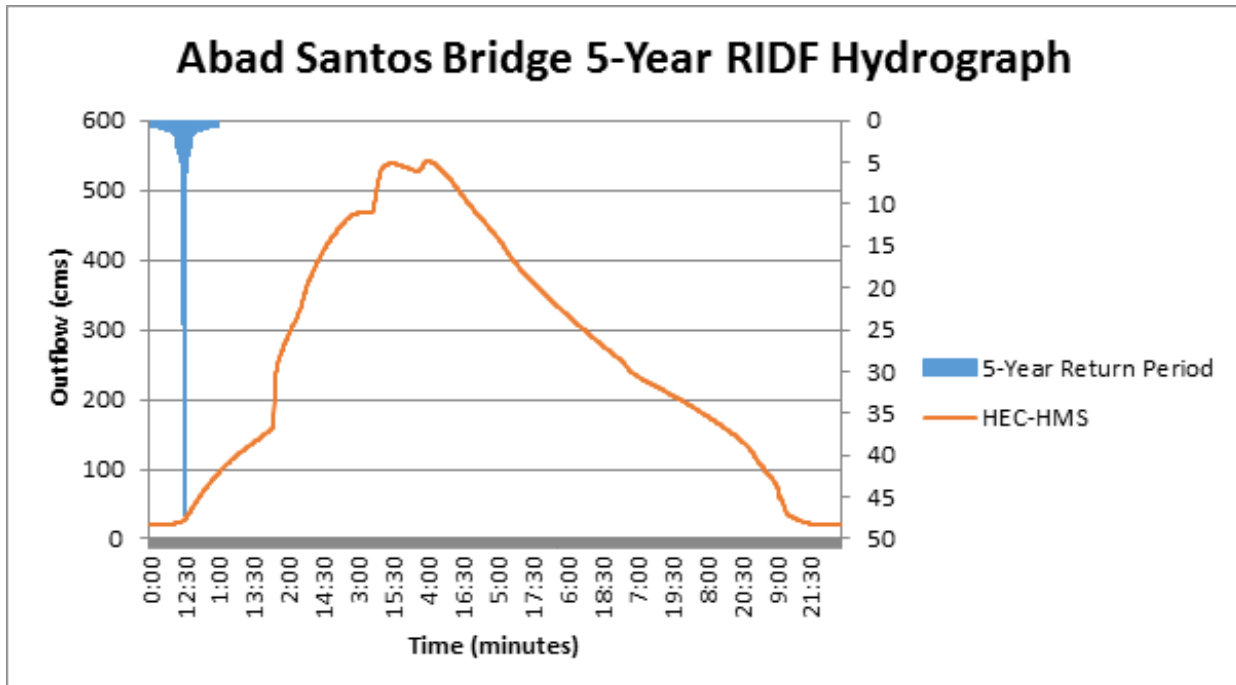


Figure 47. Abad Santos Bridge outflow hydrograph generated using the Cabanatuan 5-Year RIDF inputted in WMS and HEC-HMS Basin Model

In the 10-year return period graph (Figure 48), the peak outflow is 311.2 cms. This occurs after 3 days and 10 hours after the peak precipitation of 30.68 mm.

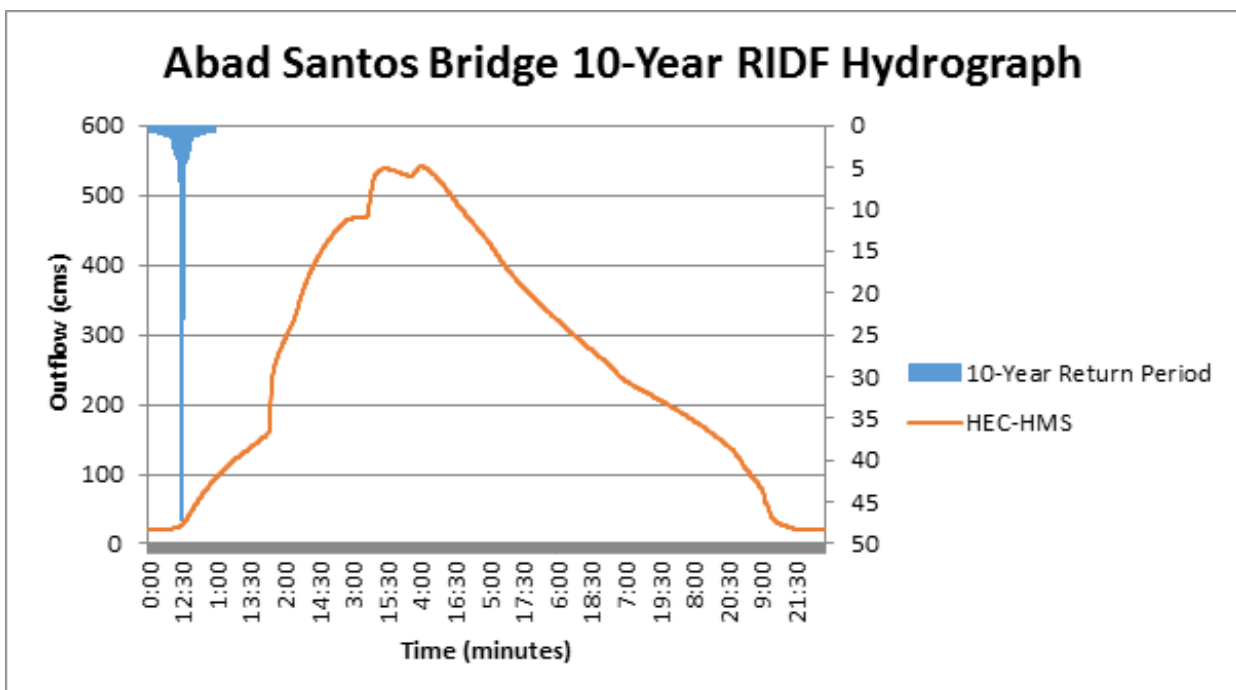


Figure 48. Abad Santos Bridge outflow hydrograph generated using the Cabanatuan 10-Year RIDF inputted in WMS and HEC-HMS Basin Model

Results and Discussion

In the 25-year return period graph (Figure 49), the peak outflow is 434.3 cms. This occurs after 3 days and 9 hours after the peak precipitation of 37.51 mm.

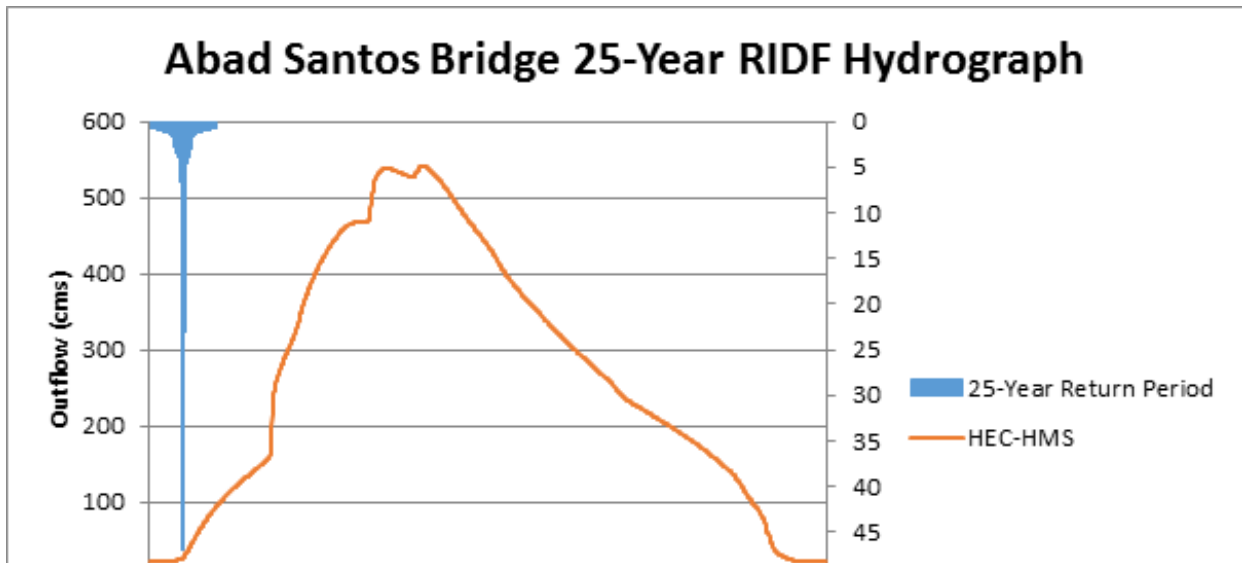


Figure 49. Abad Santos Bridge outflow hydrograph generated using the Cabanatuan 25-Year RIDF inputted in WMS and HEC-HMS Basin Model

In the 50-year return period graph (Figure 50), the peak outflow is 505.0 cms. This occurs after 3 days and 7 hours after the peak precipitation of 42.28 mm.

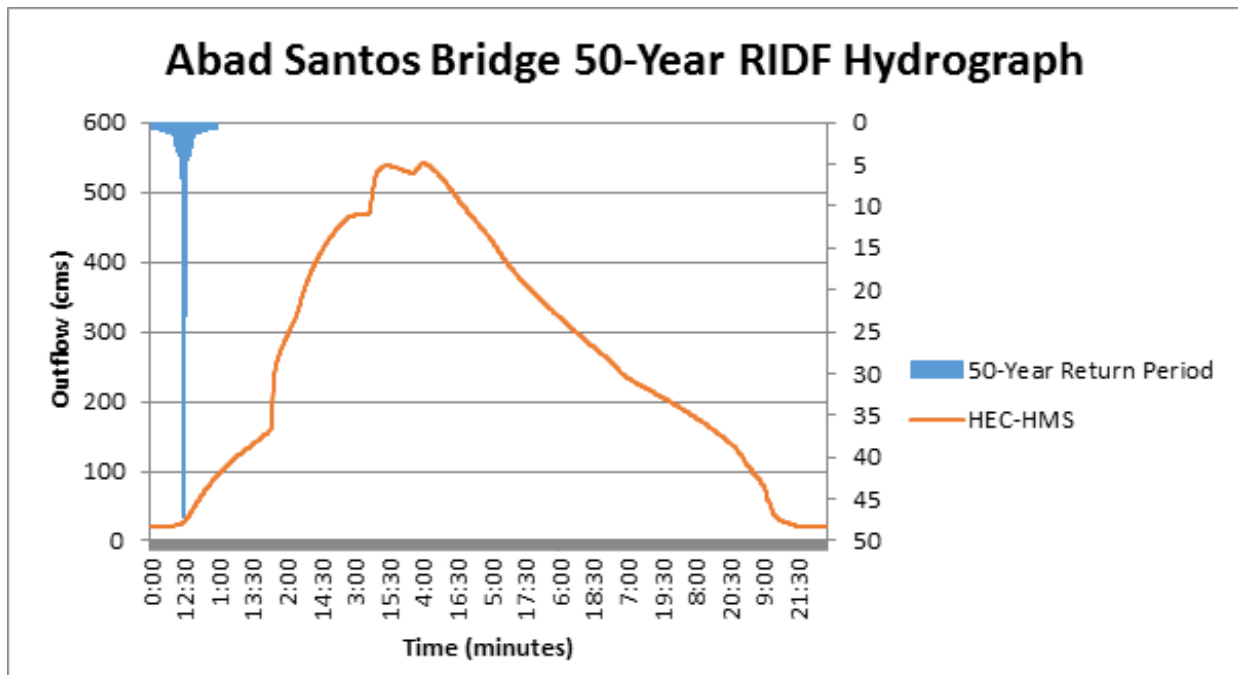


Figure 50. Abad Santos Bridge outflow hydrograph generated using the Cabanatuan 50-Year RIDF inputted in WMS and HEC-HMS Basin Model

In the 100-year return period graph (Figure 51), the peak outflow is 541.2 cms. This occurs after 3 days and 16 hours after the peak precipitation of 47.06 mm.



Results and Discussion

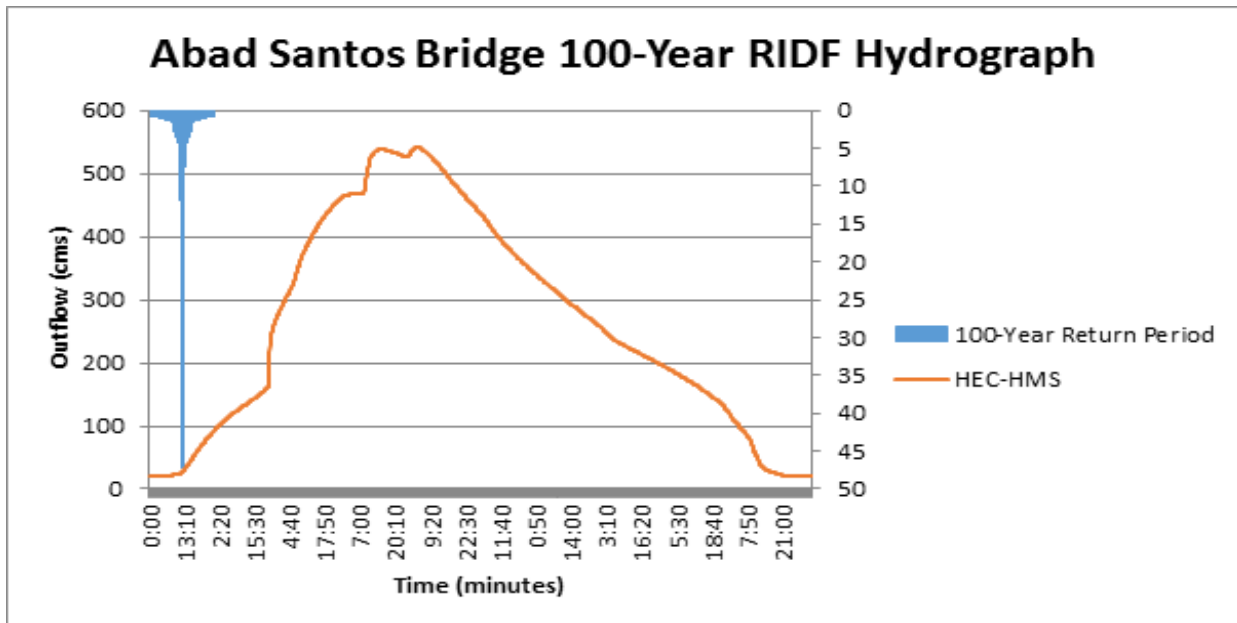


Figure 51. Abad Santos Bridge outflow hydrograph generated using the Cabanatuan 100-Year RIDF inputted in WMS and HEC-HMS Basin Model

A summary of the total precipitation, peak rainfall, peak outflow and time to peak of Abad Santos discharge using the Cabanatuan Rainfall Intensity-Duration-Frequency curves (RIDF) in five different return periods is shown in Table 3.

Table 3. Summary of Abad Santos outflow using Cabanatuan Station Rainfall Intensity Duration Frequency (RIDF)

RIDF Period	Total Precipitation (mm)	Peak rainfall (mm)	Peak outflow (cms)	Time to Peak
5-Year	184.69	24.79	218.6	2 days
10-Year	233.64	30.68	311.2	3 days
25-Year	291.10	37.51	403.8	3 days
50-Year	331.95	42.28	471.3	3 days
100-Year	372.50	47.06	541.2	3 days

4.2.1.3 Alejo Santos Bridge, Bulacan

In the 5-year return period graph (Figure 52), the peak outflow is 119.4 cms. This occurs after 10 hours and 40 minutes after the peak precipitation of 31.4 mm.

Results and Discussion

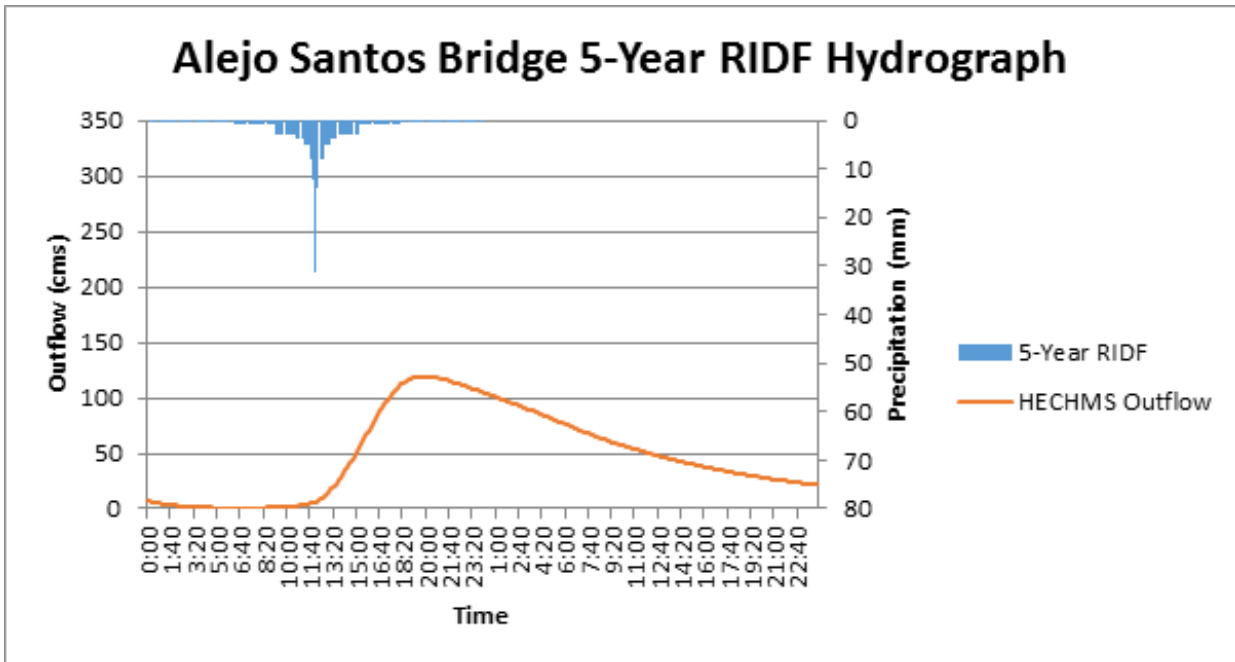


Figure 52. Alejo Santos Bridge outflow hydrograph generated using the Cabanatuan 5-Year RIDF inputted in WMS and HEC-HMS Basin Model

In the 10-year return period graph (Figure 53), the peak outflow is 166.1 cms. This occurs after 10 hours and 10 minutes after the peak precipitation of 37 mm.

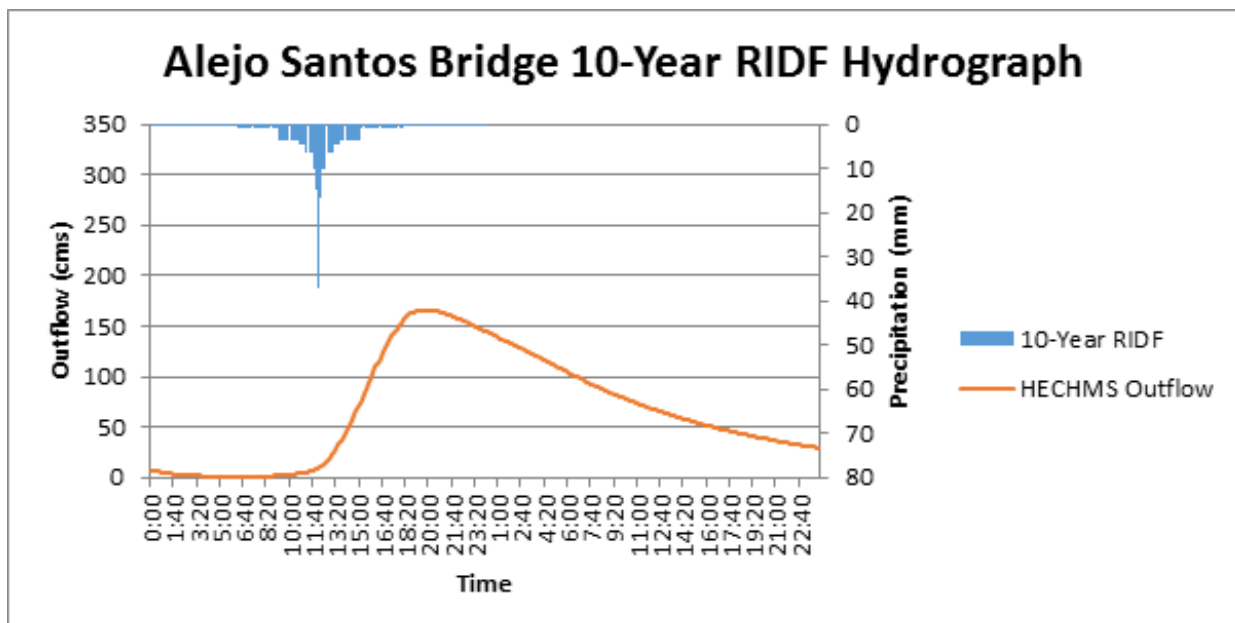


Figure 53. Alejo Santos Bridge outflow hydrograph generated using the Cabanatuan 10-Year RIDF inputted in WMS and HEC-HMS Basin Model

In the 25-year return period graph (Figure 54), the peak outflow is 230.2 cms. This occurs after 9 hours and 40 minutes after the peak precipitation of 44 mm.



Results and Discussion

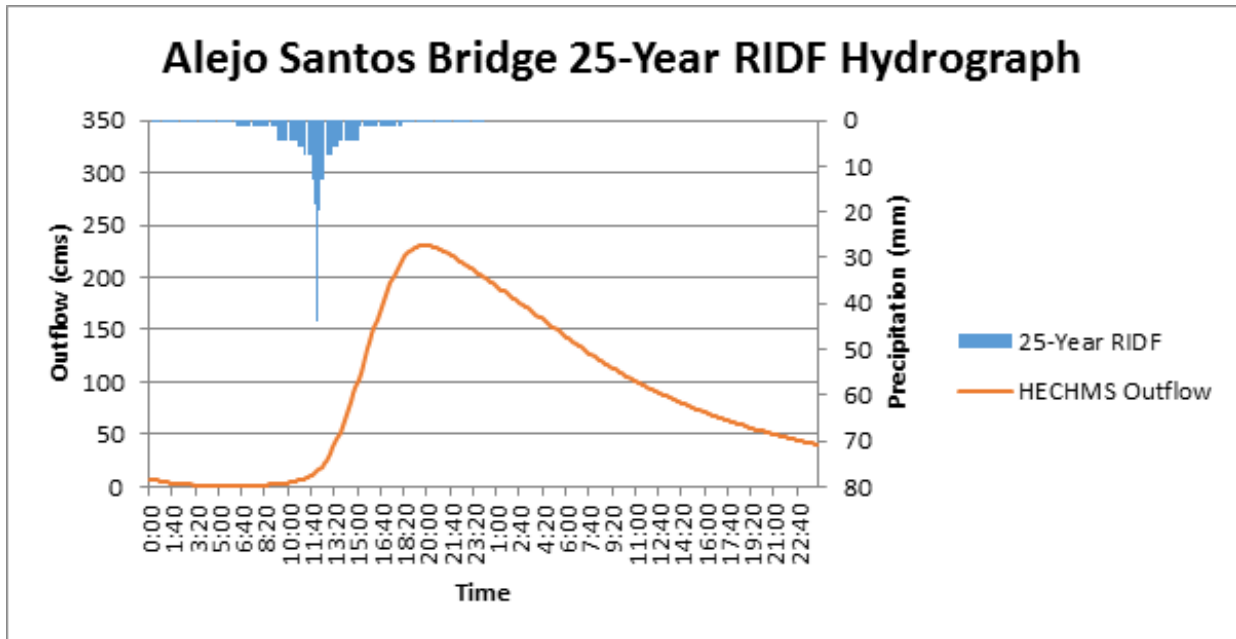


Figure 54. Alejo Santos Bridge outflow hydrograph generated using the Cabanatuan 25-Year RIDF inputted in WMS and HEC-HMS Basin Model

In the 50-year return period graph (Figure 55), the peak outflow is 272.2 cms. This occurs after 9 hours and 20 minutes after the peak precipitation of 49.2 mm.

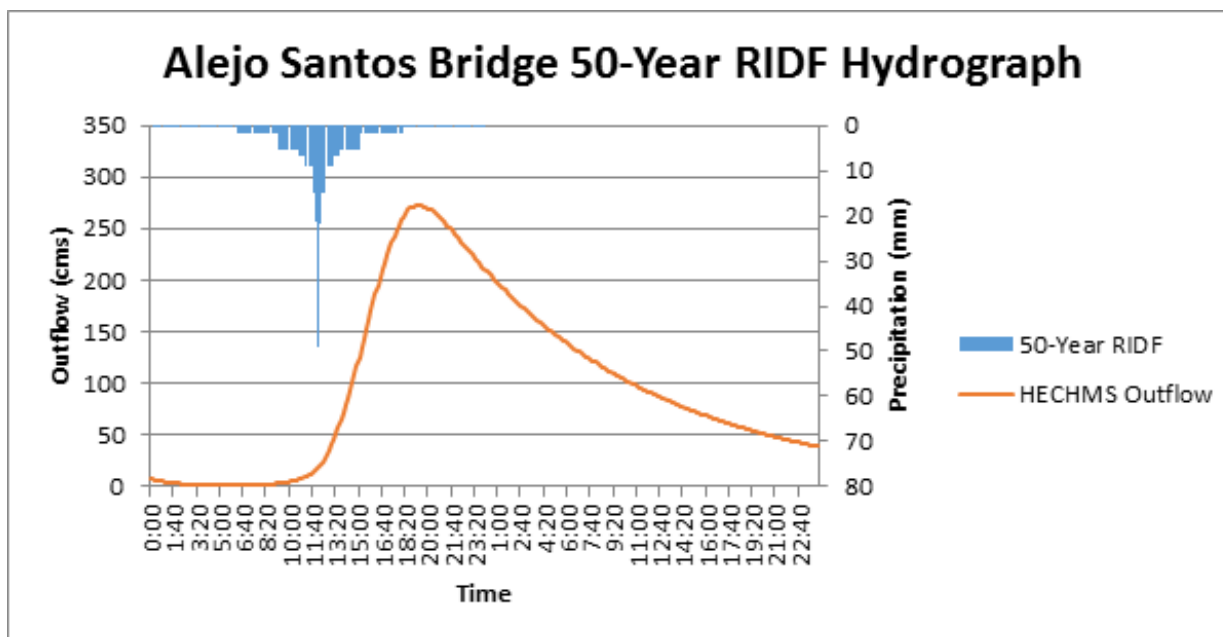


Figure 55. Alejo Santos Bridge outflow hydrograph generated using the Cabanatuan 50-Year RIDF inputted in WMS and HEC-HMS Basin Model

In the 100-year return period graph (Figure 56), the peak outflow is 330.2 cms. This occurs after 9 hours after the peak precipitation of 54.4 mm.

Results and Discussion

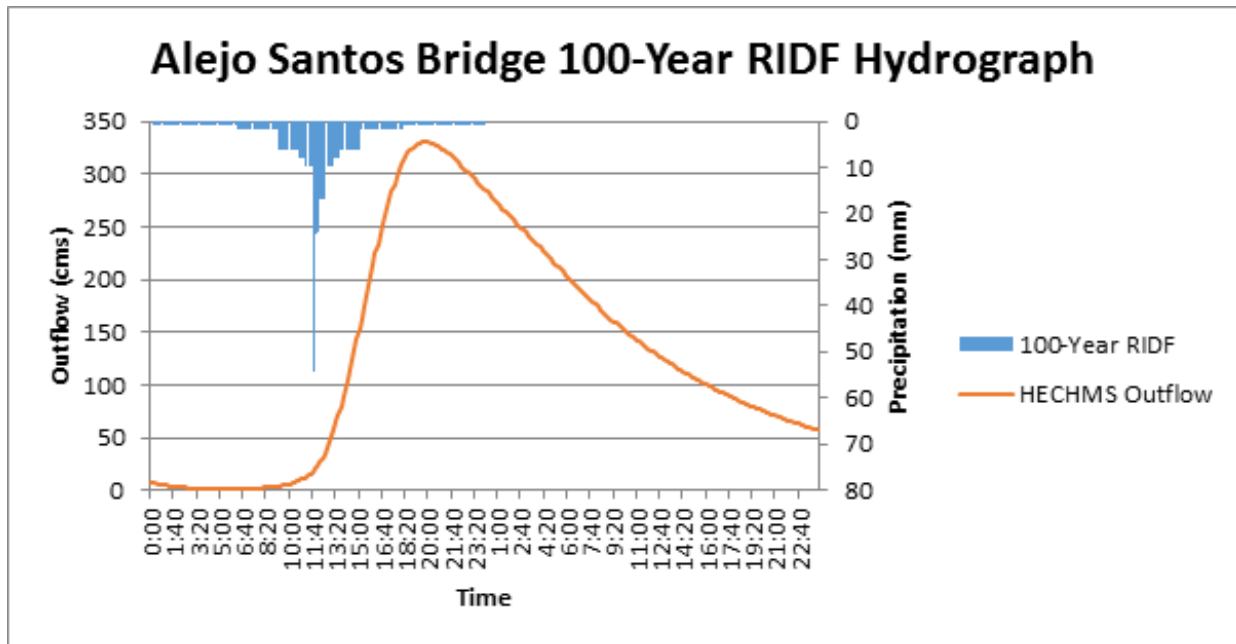


Figure 56. Alejo Santos Bridge outflow hydrograph generated using the Cabanatuan 100-Year RIDF inputted in WMS and HEC-HMS Basin Model

A summary of the total precipitation, peak rainfall, peak outflow and time to peak of Alejo Santos discharge using the Cabanatuan Rainfall Intensity Duration Frequency curves (RIDF) in five different return periods is shown in Table 4.

Table 4. Summary of Alejo Santos outflow using Cabanatuan Station Rainfall Intensity Duration Frequency (RIDF)

RIDF Period	Total Precipitation (mm)	Peak rainfall (mm)	Peak outflow (cms)	Time to Peak
5-Year	243.1	31.4	119.4	7 hours, 40 minutes
10-Year	300.7	37	166.1	7 hours, 40 minutes
25-Year	373.6	44	230.2	7 hours, 40 minutes
50-Year	427.6	49.2	272.2	7 hours, 10 minutes
100-Year	481.2	54.4	330.2	7 hours, 40 minutes



Results and Discussion

4.2.1.4 Ilog Baliwag Bridge, Nueva Ecija

In the 5-year return period graph (Figure 57), the peak outflow is 19.5 cms. This occurs after 1 day, 23 hours and 20 minutes after the peak precipitation of 26.8 mm.

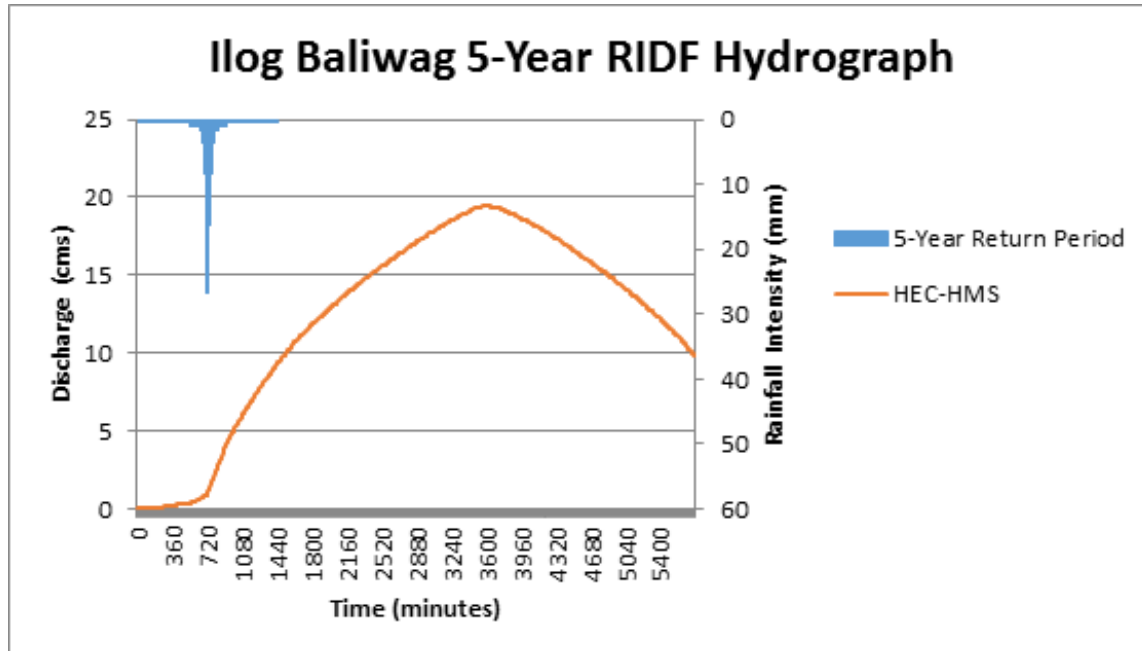


Figure 57. Ilog Baliwag Bridge outflow hydrograph generated using the Cabanatuan 5 -Year RIDF inputted in WMS and HEC-HMS Basin Model

In the 10-year return period graph (Figure 58), the peak outflow is 2362.9 cms. This occurs after 13 hours and 50 minutes after the peak precipitation of 63.8 mm.

Results and Discussion

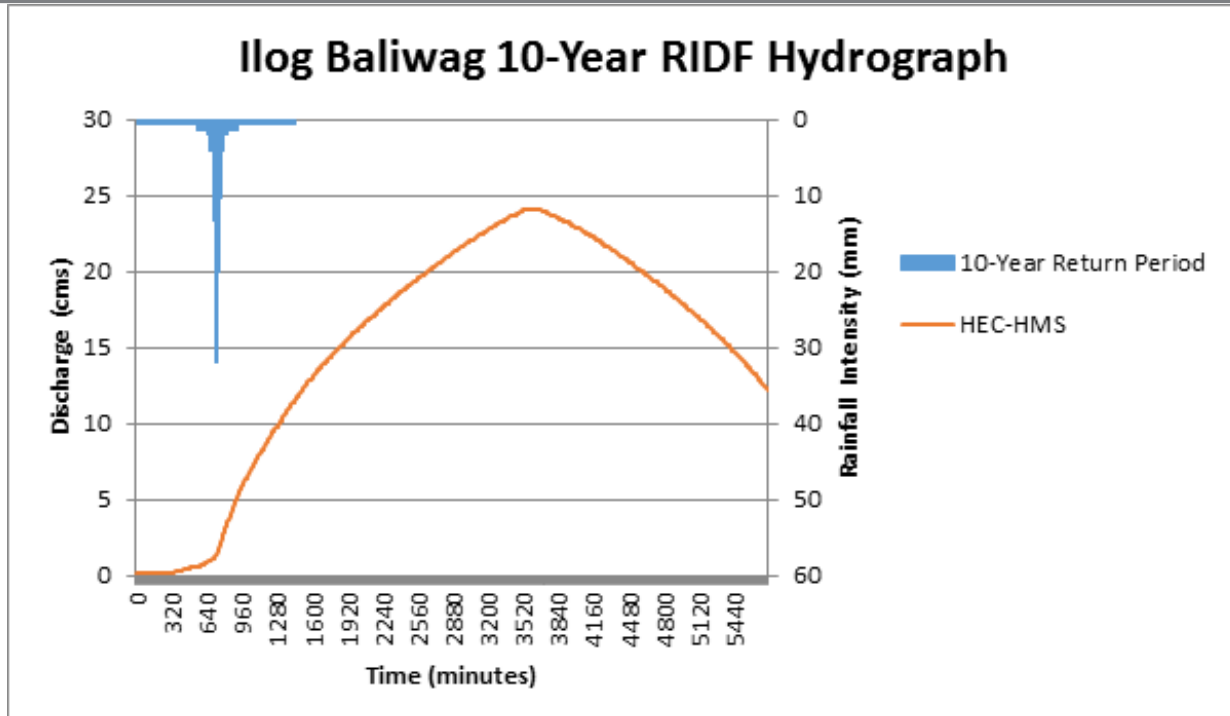


Figure 58. Ilog Baliwag Bridge outflow hydrograph generated using the Cabanatuan 10 -Year RIDF inputted in WMS and HEC-HMS Basin Model

In the 25-year return period graph (Figure 59), the peak outflow is 29.9 cms. This occurs after 1 day, 23 hours and 10 minutes after the peak precipitation of 38.3 mm.

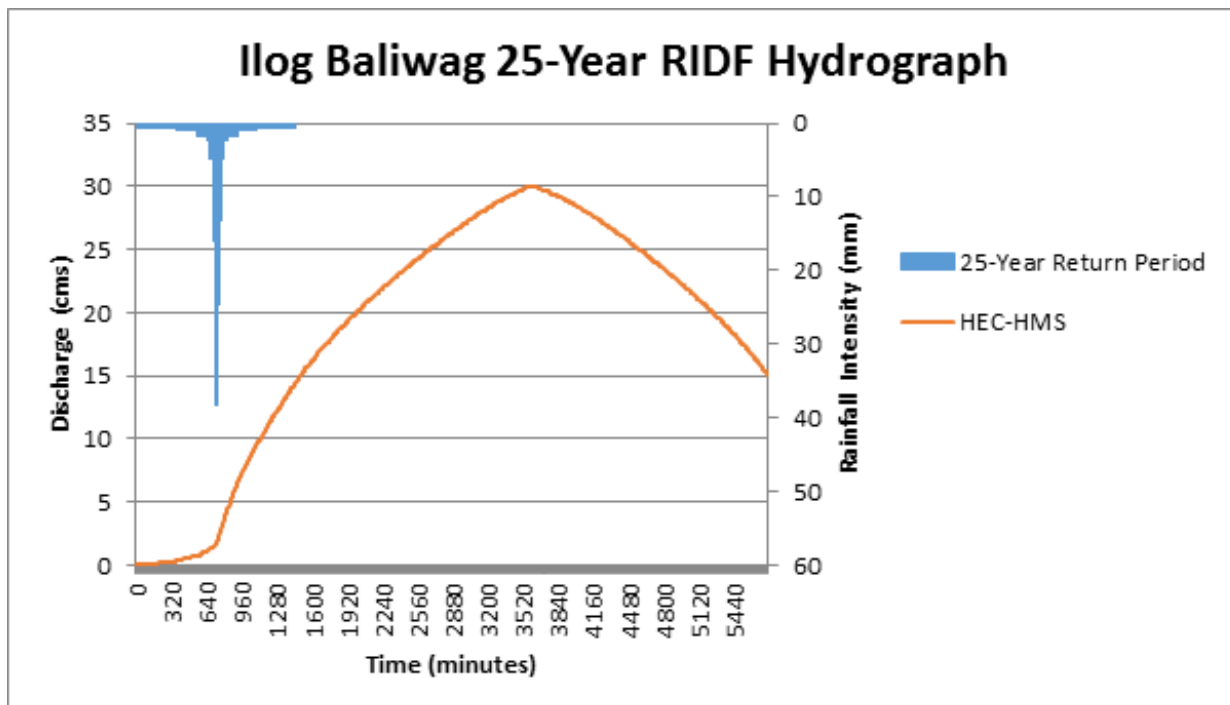


Figure 59. Ilog Baliwag Bridge outflow hydrograph generated using the Cabanatuan 25 -Year RIDF inputted in WMS and HEC-HMS Basin Model



Results and Discussion

In the 50-year return period graph (Figure 60), the peak outflow is 34.2 cms. This occurs after 1 day, and 23 hours after the peak precipitation of 43.1 mm.

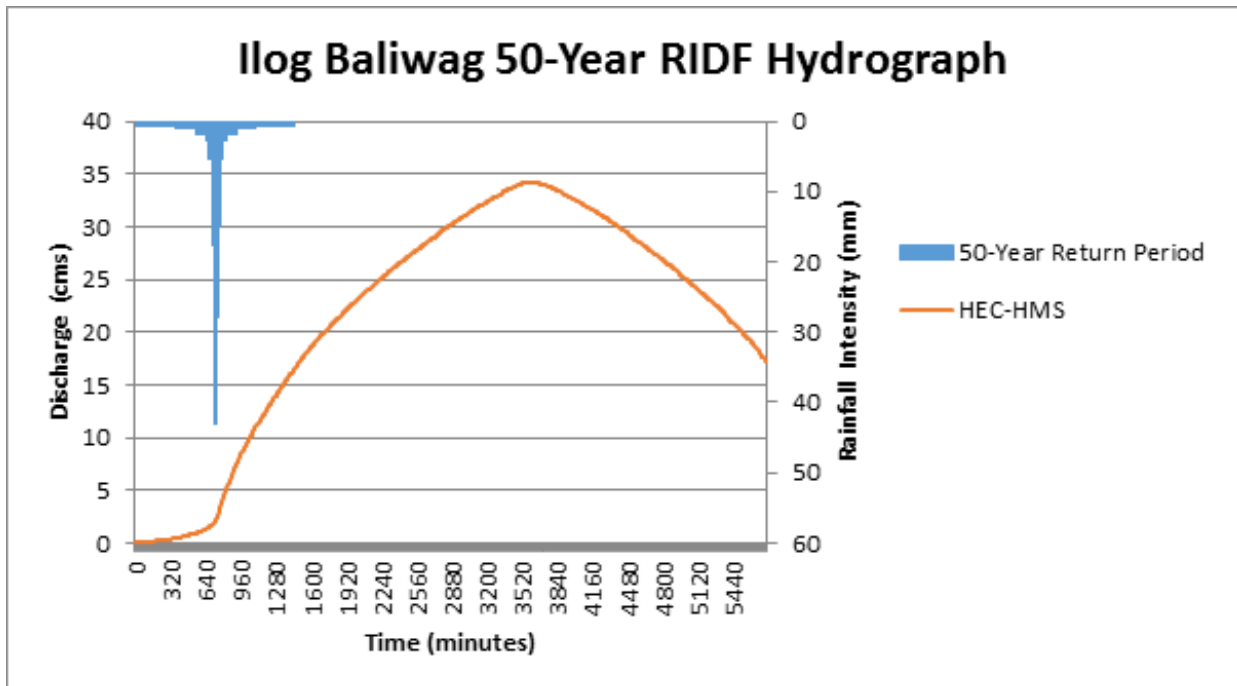


Figure 60. Ilog Baliwag Bridge outflow hydrograph generated using the Cabanatuan 50 -Year RIDF inputted in WMS and HEC-HMS Basin Model

In the 100-year return period graph (Figure 61), the peak outflow is 38.5 cms. This occurs after 1 day, and 23 hours after the peak precipitation of 47.9 mm.

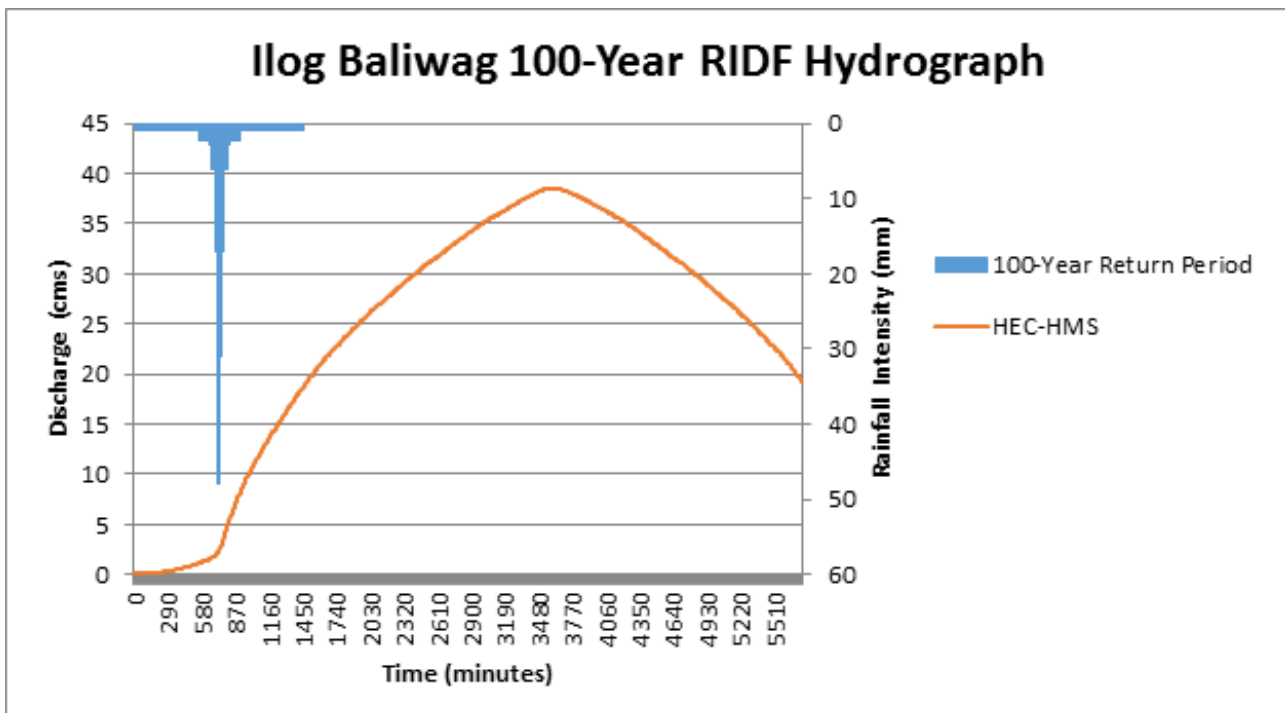


Figure 61. Ilog Baliwag Bridge outflow hydrograph generated using the Cabanatuan 100 -Year RIDF inputted in WMS and HEC-HMS Basin Model

Results and Discussion

A summary of the total precipitation, peak rainfall, peak outflow and time to peak of Ilog Baliwag discharge using the Cabanatuan Rainfall Intensity-Duration-Frequency curves (RIDF) in five different return periods is shown in Table 5.

Table 5. Summary of Baliwag outflow using Cabanatuan Station Rainfall Intensity Duration Frequency (RIDF)

RIDF Period	Total Precipitation (mm)	Peak rainfall (mm)	Peak outflow (cms)	Time to Peak
5-Year	185.3	26.8	19.5	1 day, 23 hours and 20 minutes
10-Year	225	31.9	24.1	1 day, 23 hours and 20 minutes
25-Year	275.2	38.3	29.9	1 day, 23 hours and 10 minutes
50-Year	312.4	43.1	34.2	1 day, and 23 hours
100-Year	349.3	47.9	38.5	1 day, and 23 hours

4.2.1.5 Sto. Niño Bridge, Bulacan

In the 5-year return period graph (Figure 62), the peak outflow is 37113.2 cms. This occurs after 4 hours and 40 minutes after the peak precipitation of 26.8 mm.

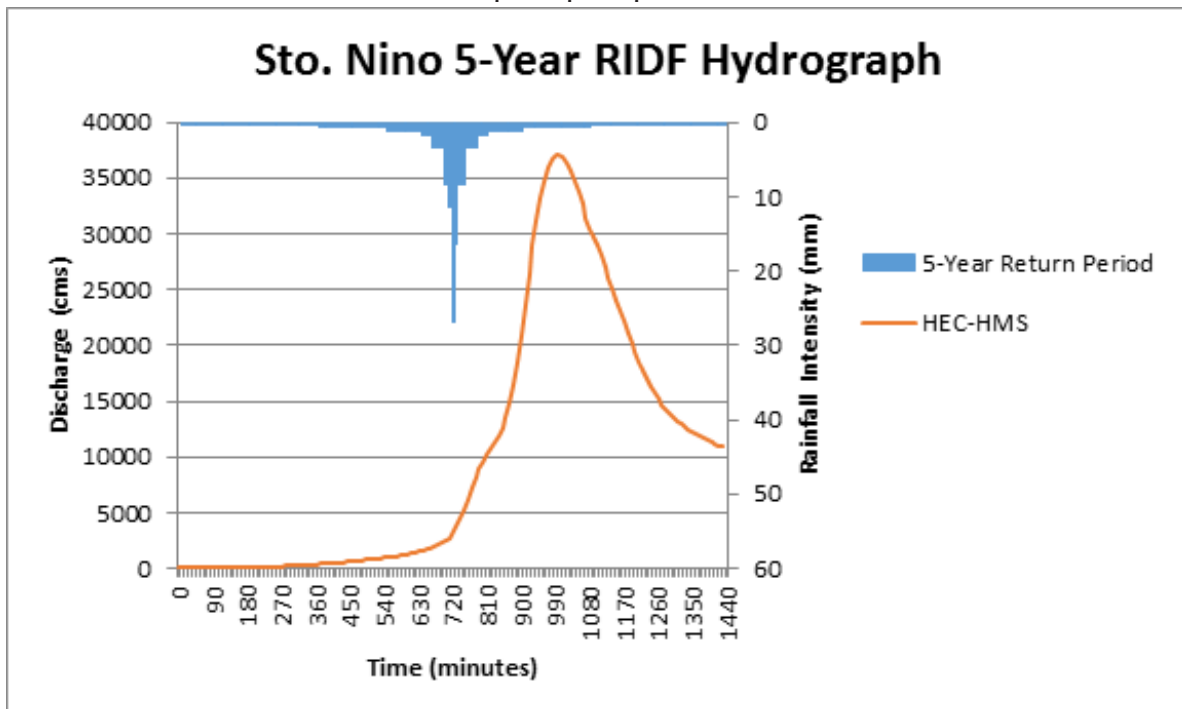


Figure 62. Sto. Niño Bridge Outflow hydrograph generated using the Cabanatuan 5-Year RIDF inputted in HEC-HMS

In the 10-year return period graph (Figure 63), the peak outflow is 47953.2 cms. This occurs after 4 hours and 30 minutes after the peak precipitation of 31.9 mm.



Results and Discussion

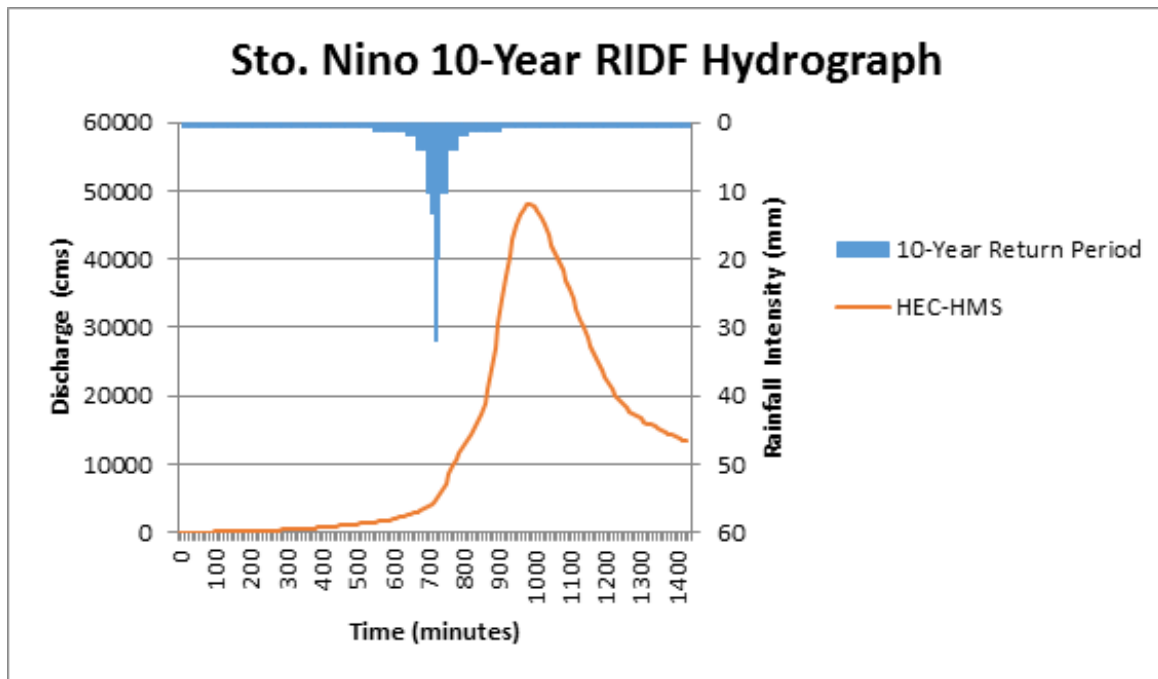


Figure 63. Sto. Niño Bridge Outflow hydrograph generated using the Cabanatuan 10-Year RIDF inputted in HEC-HMS

In the 25-year return period graph (Figure 64), the peak outflow is 61988.8 cms. This occurs after 4 hours and 20 minutes after the peak precipitation of 38.3 mm.

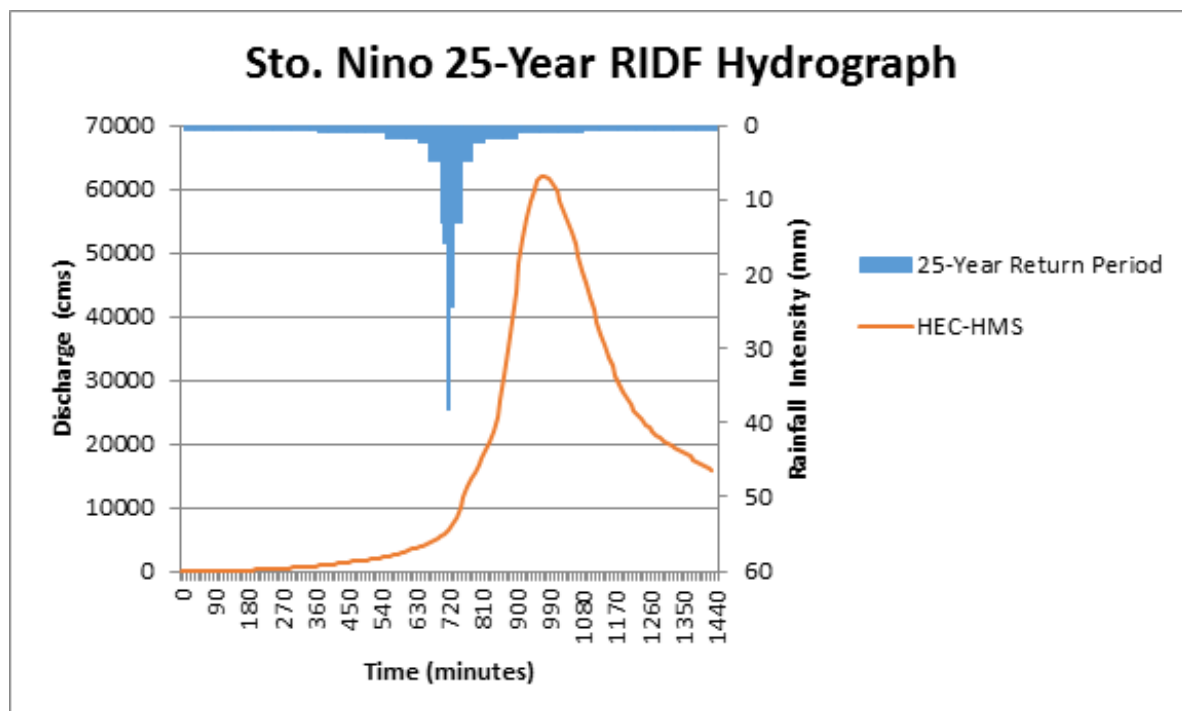


Figure 64. Sto. Niño Bridge Outflow hydrograph generated using the Cabanatuan 25-Year RIDF inputted in HEC-HMS

In the 50-year return period graph (Figure 65), the peak outflow is 72658.8 cms. This occurs after 4 hours and 10 minutes after the peak precipitation of 43.1 mm.

Results and Discussion

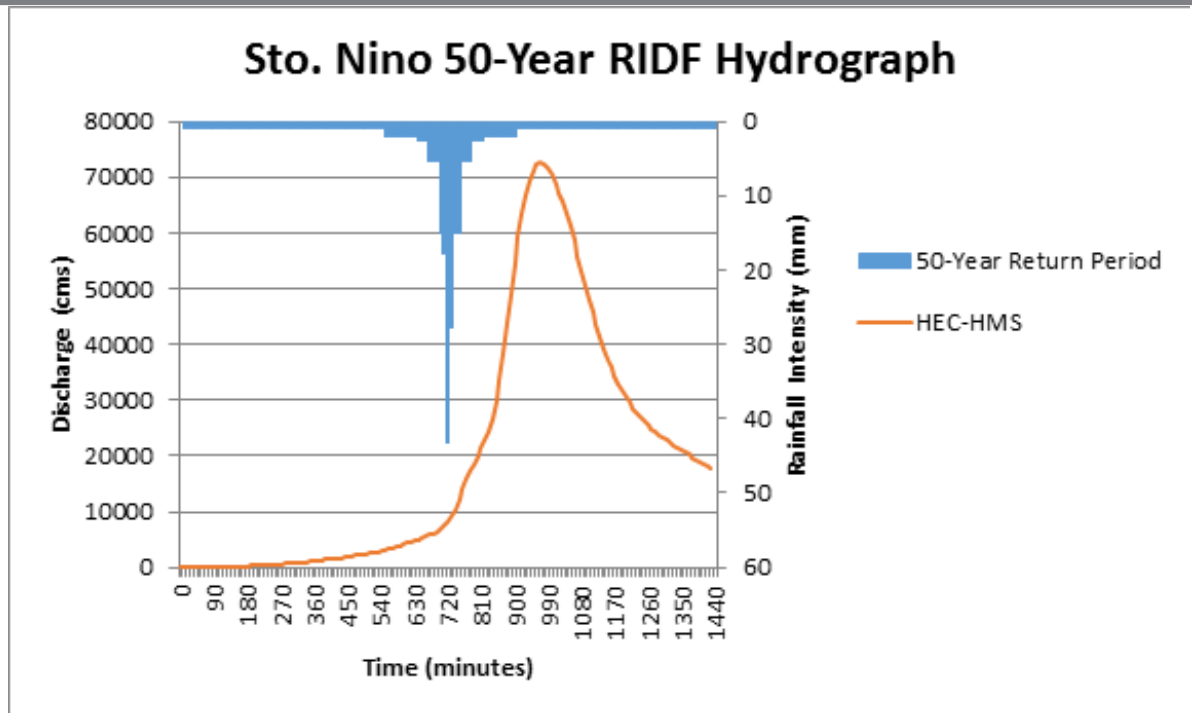


Figure 65. Sto. Niño Bridge Outflow hydrograph generated using the Cabanatuan 50-Year RIDF inputted in HEC-HMS

In the 100-year return period graph (Figure 66), the peak outflow is 83066.6 cms. This occurs after 4 hours and 10 minutes after the peak precipitation of 47.9 mm.

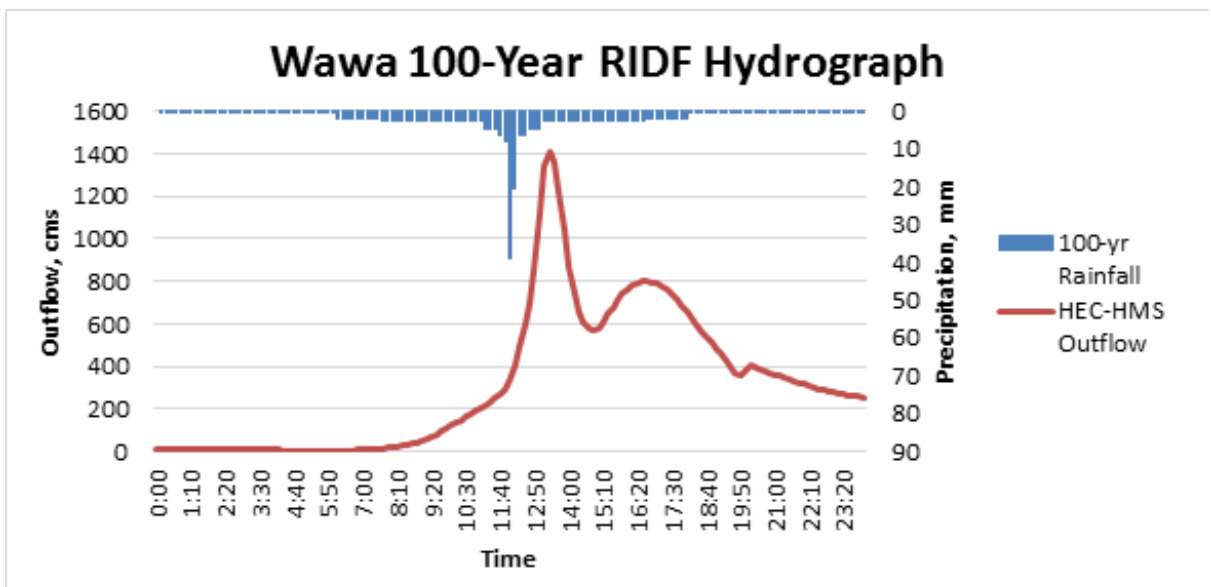


Figure 66. Sto. Niño Bridge Outflow hydrograph generated using the Cabanatuan 100-Year RIDF inputted in HEC-HMS

A summary of the total precipitation, peak rainfall, peak outflow and time to peak of Sto. Niño discharge using the Cabanatuan Rainfall Intensity-Duration-Frequency curves (RIDF) in five different return periods is shown in Table 6.



Results and Discussion

Table 6. Summary of Sto. Niño outflow using Cabanatuan Station Rainfall Intensity Duration Frequency (RIDF)

RIDF Period	Total Precipitation (mm)	Peak rainfall (mm)	Peak outflow (cms)	Time to Peak
5-Year	185.3	26.8	37113.2	4 hours and 40 mins
10-Year	225	31.9	47953.2	4 hours and 30 mins
25-Year	275.2	38.3	61988.8	4 hours and 20 mins
50-Year	312.4	43.1	72658.8	4 hours and 10 mins
100-Year	349.3	47.9	83066.6	4 hours and 10 mins

Results and Discussion

4.2.2 Discharge Data using Dr. Horritt’s Recommended Hydrological Method

The river discharge values using Dr. Horritt’s recommended hydrological method are shown in Figure 67 and the peak discharge values are summarized in Table 7.

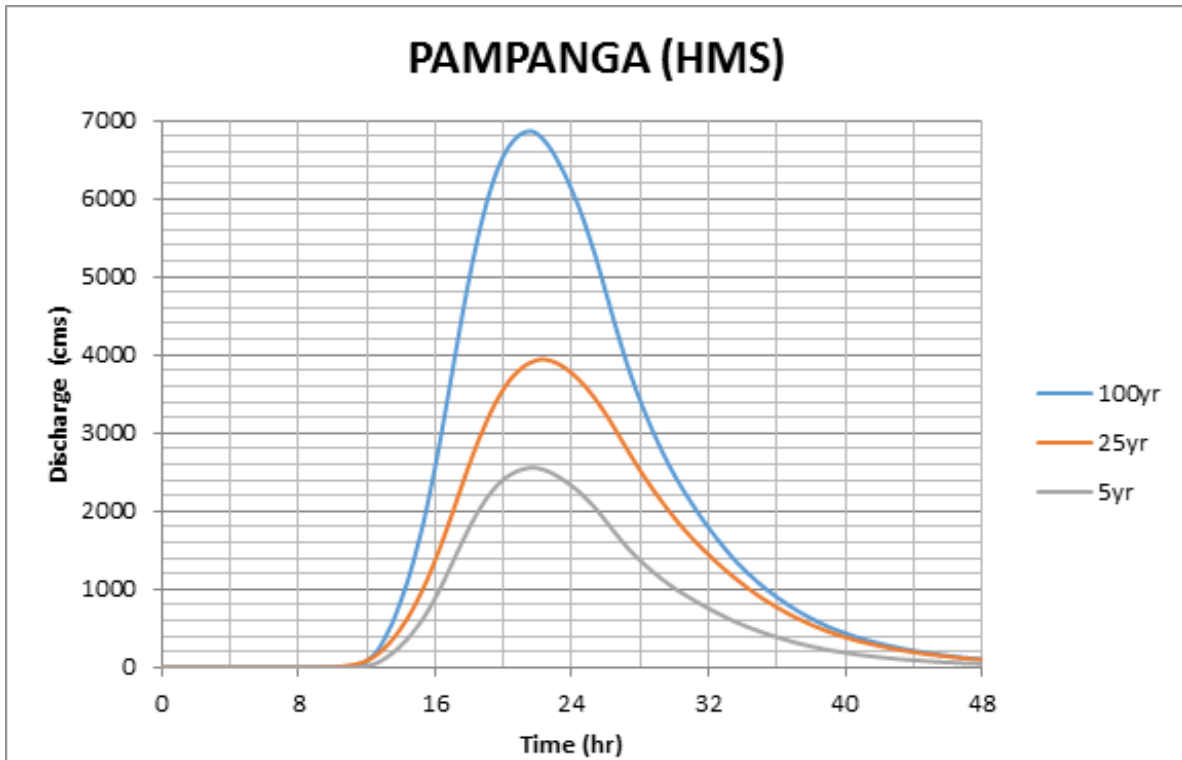


Figure 67. Outflow hydrograph generated for Pampanga using the Science Garden, Iba, and Cabanatuan stations’ 5-, 25-, 100-Year Rainfall Intensity Duration Frequency in HEC-HMS

Table 7. Summary of Pampanga river discharge using the recommended hydrological method by Dr. Horritt

RIDF Period	Peak discharge (cms)	Time-to-peak
5-Year	2,558.3	21 hours, 40 minutes
25-Year	3,943.7	22 hours, 20 minutes
100-Year	6,863.3	21 hours, 30 minutes

The comparison of discharge values obtained from HEC-HMS, QMED, and from the bankful discharge method, Qbankful, are shown in Table 8. Using values from the DTM of Pampanga, the bankful discharge for the river was computed.



Results and Discussion

Table 8. Validation of river discharge estimate using the bankful method

Discharge Point	Qbankful, cms	QMED, cms	Validation
Pampanga	2,091.64	2,251.3	Pass

The value from the HEC-HMS discharge estimate was able to satisfy the condition for validating the computed discharge using the bankful method. The computed value was used for the discharge point that did not have actual discharge data. The actual discharge data were also used for some areas in the floodplain that were modeled. It is recommended, therefore, to use the actual value of the river discharge for higher-accuracy modeling.

4.3 Flood Hazard and Flow Depth Maps

The following images are the hazard and flow depth maps for the 5-, 25-, and 100-year rain return scenarios of the Pampanga river basin.

Results and Discussion

Flood Hazard Maps and Flow Depth Maps

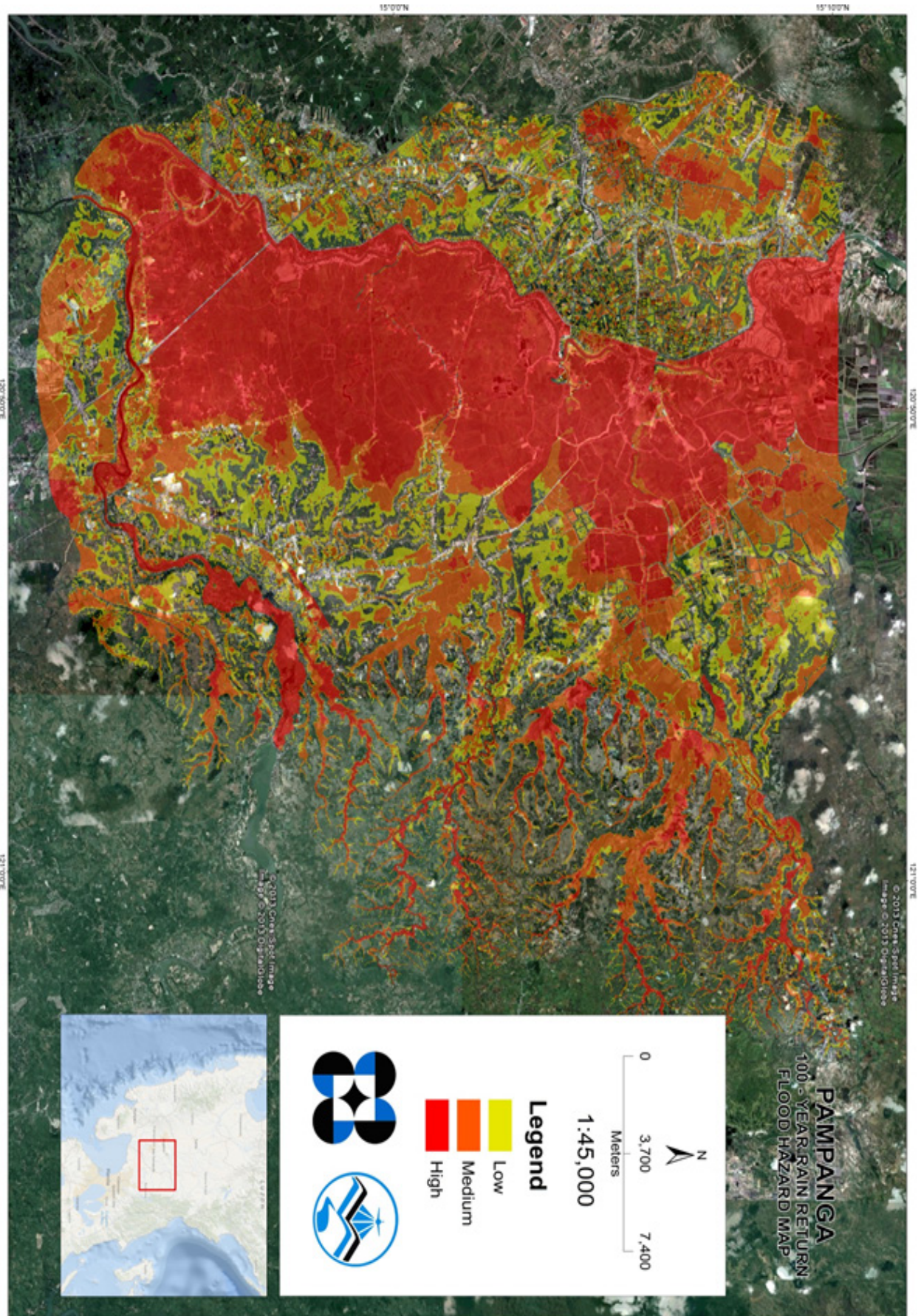


Figure 68. 100-year Flood Hazard Map for Pampanga River Basin

Results and Discussion

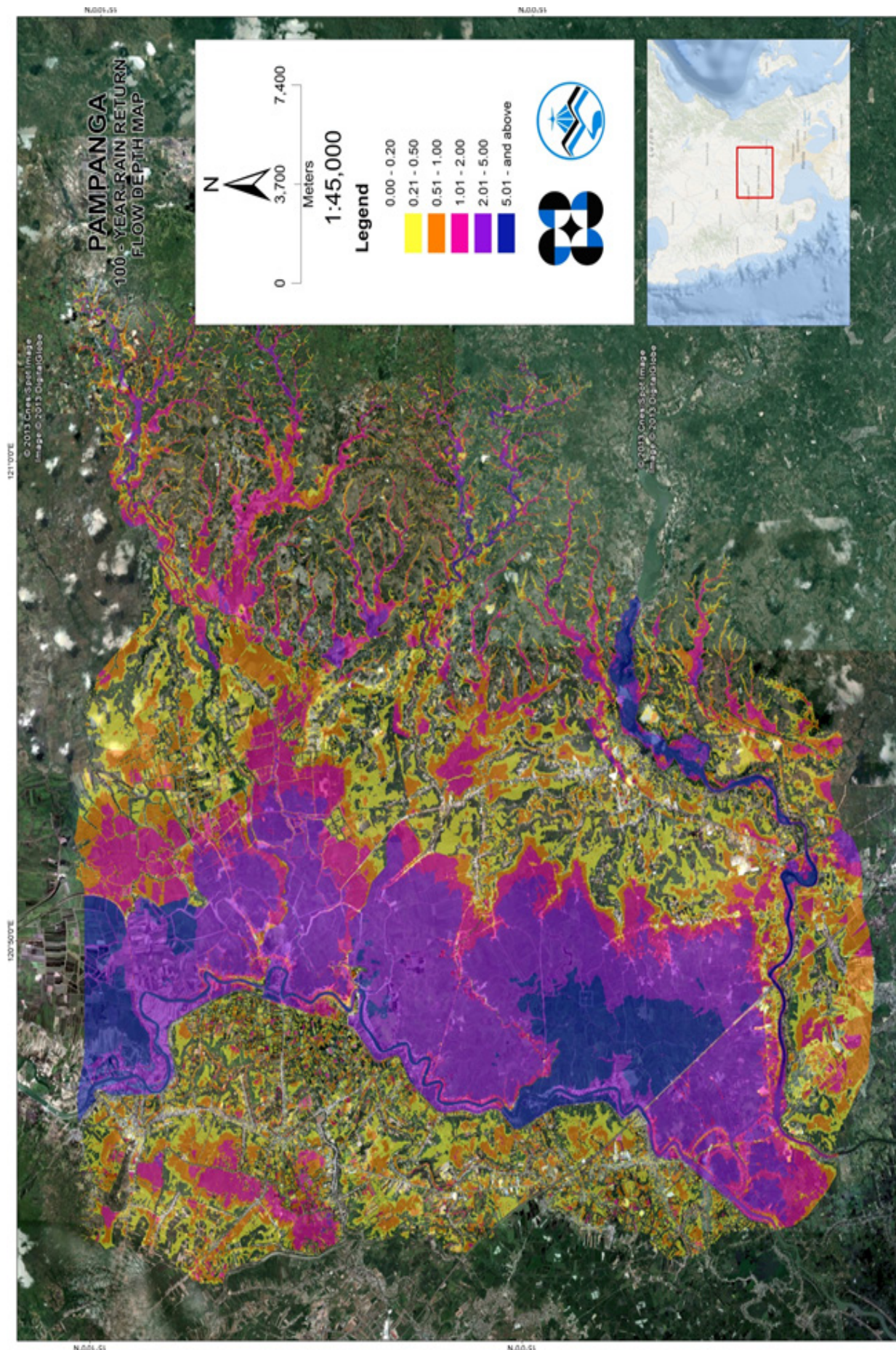


Figure 69. 100-year Flow Depth Map for Pampanga River Basin

Results and Discussion

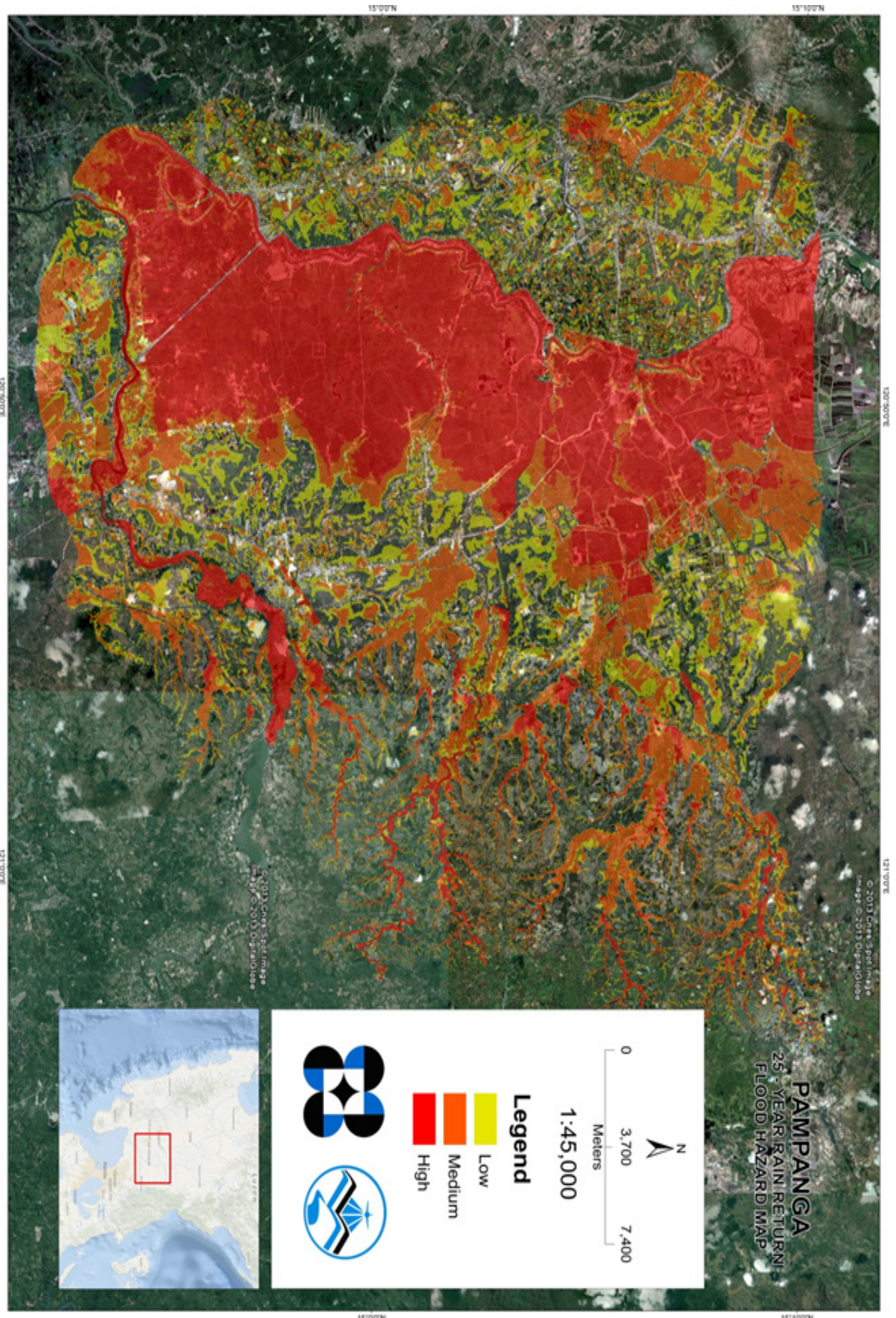


Figure 70. 25-year Flood Hazard Map for Pampanga River Basin



Results and Discussion

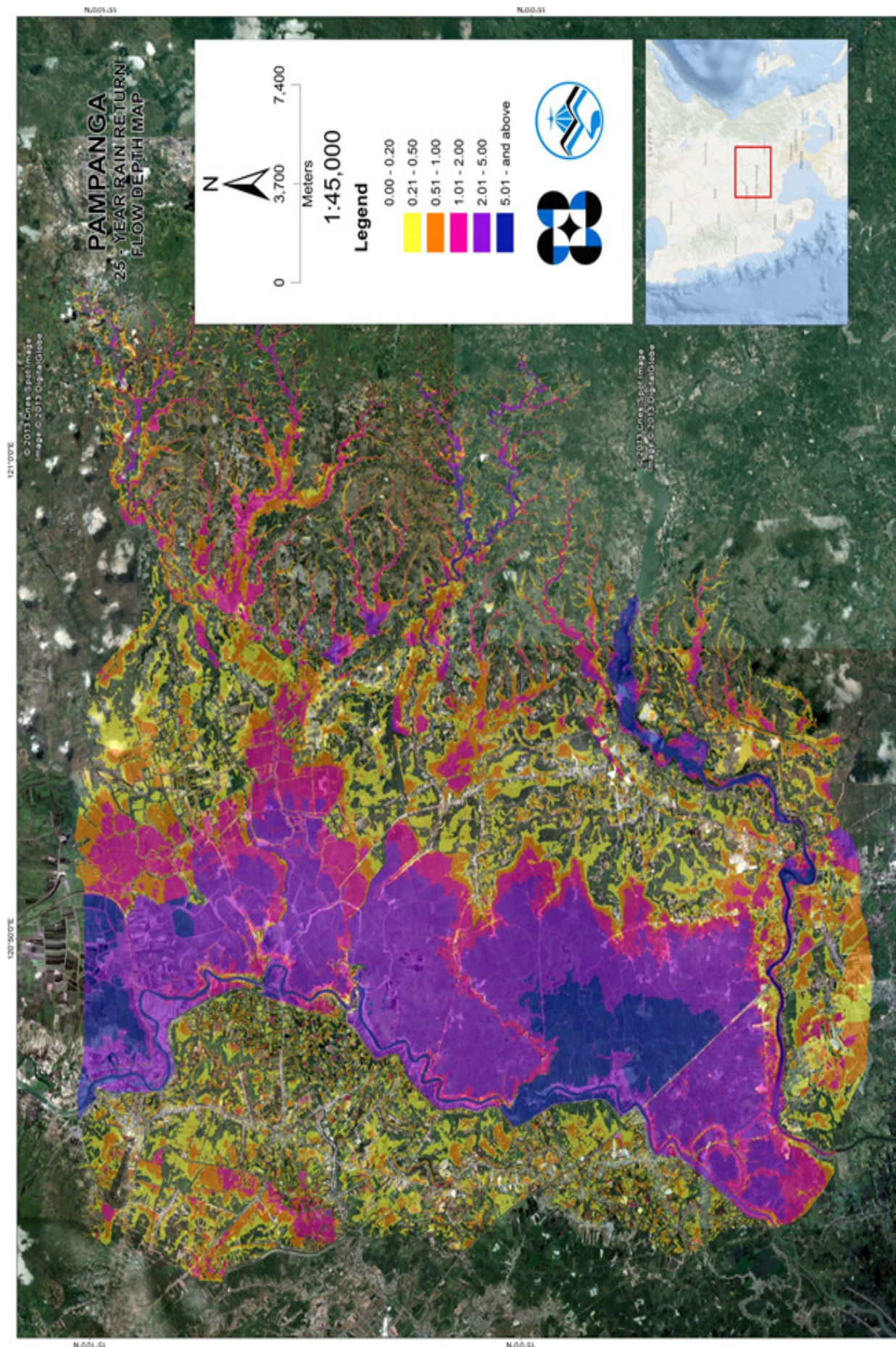


Figure 71. 25-year Flow Depth Map for Pampanga River Basin

Results and Discussion

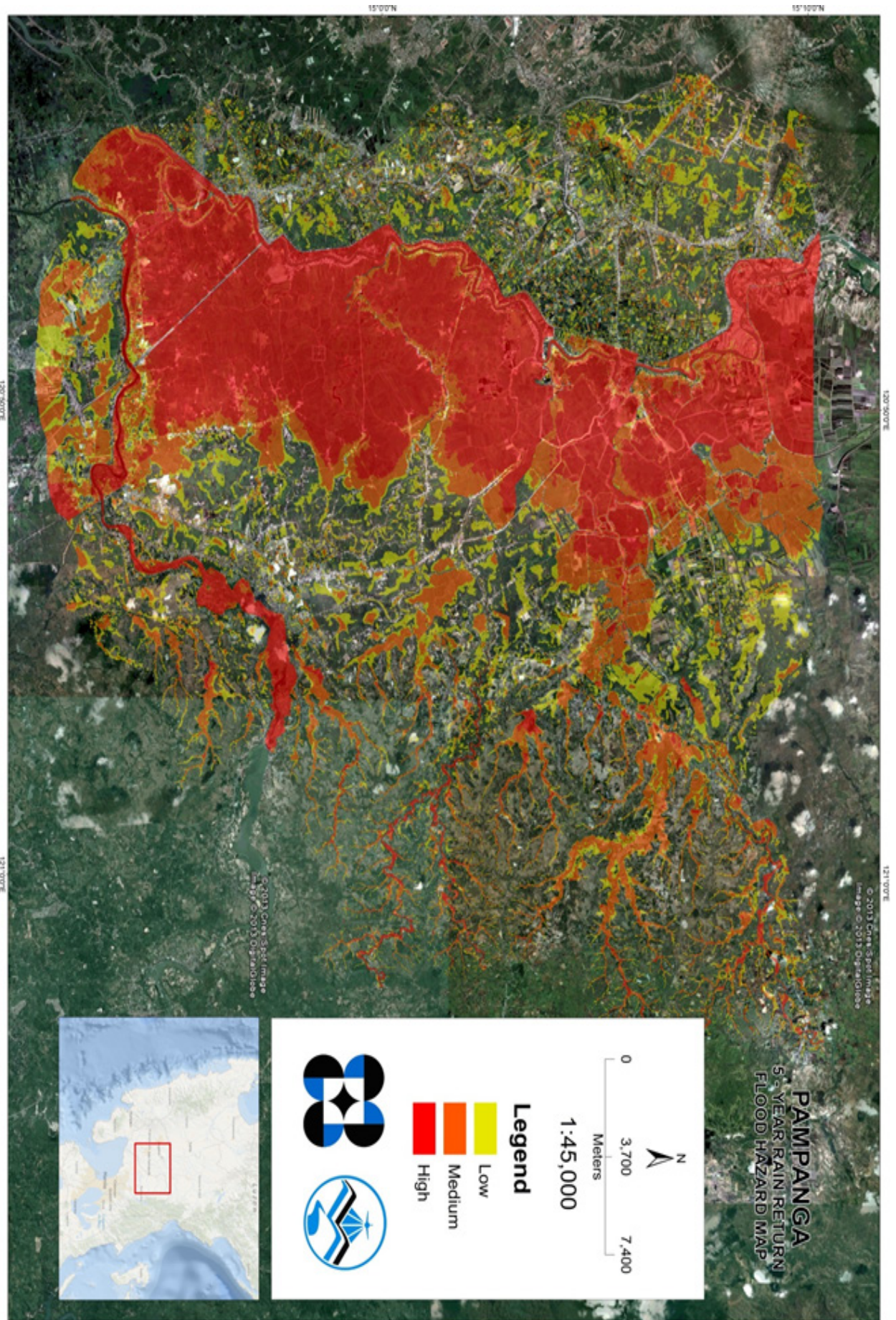


Figure 72. 5-year Flood Hazard Map for Pampanga River Basin



Results and Discussion

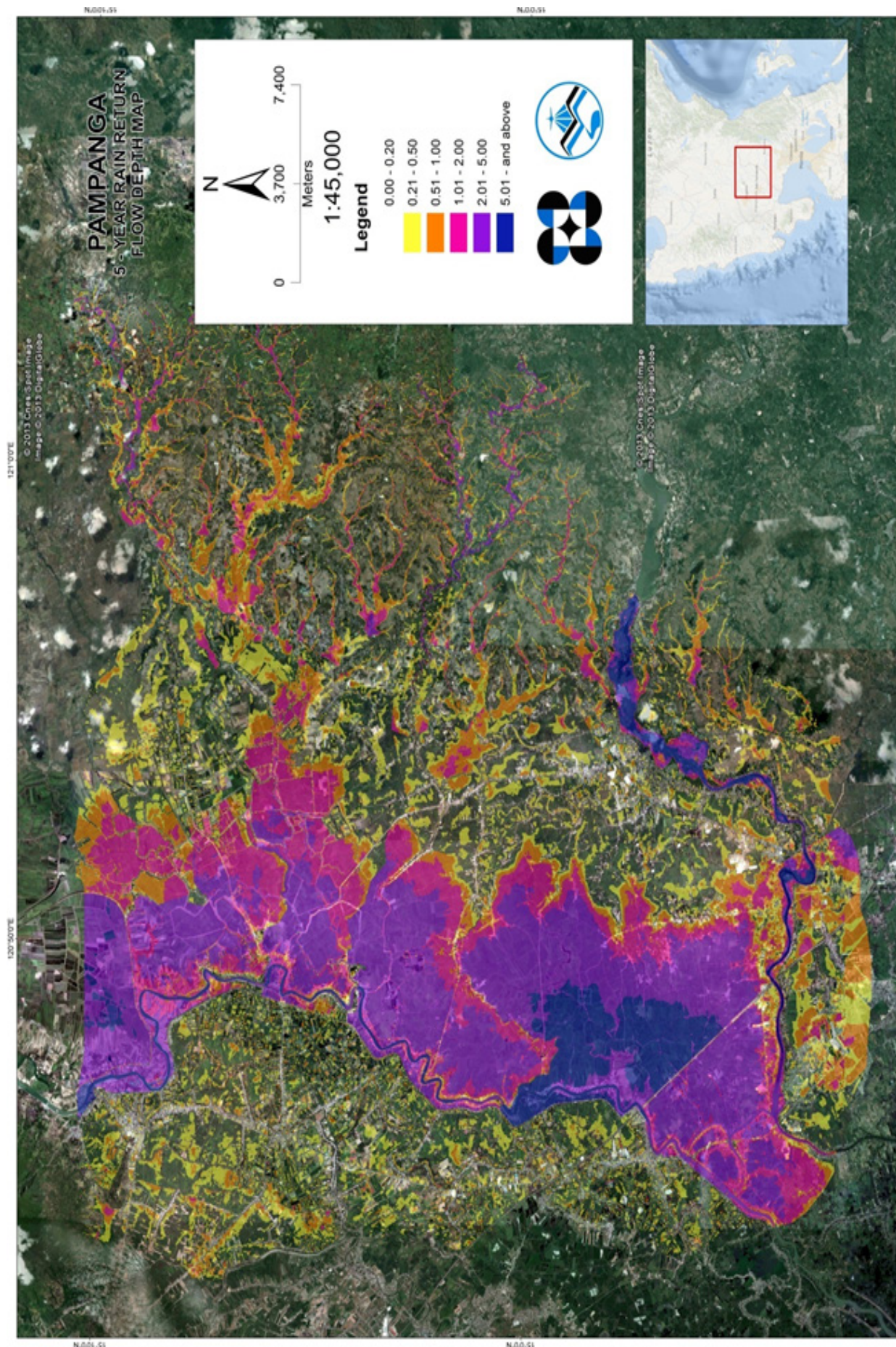


Figure 73. 5-year FFlow Depth Map for Pampanga River Basin

Bibliography

- Aquaveo. (2012). Watershed Modeling - HEC HMS Interface. Aquaveo.
- Feldman, A. D. (2000). Hydrologic Modeling System HEC-HMS Technical Reference Manual. Davis, CA: US Army Corps of Engineers - Hydrologic Engineering Center.
- FLO-2D Software, I. Flo-2D Reference Manual. FLO-2D Software, Inc.
- Hilario, F. (2007). Pampanga River Basin. Lecture presented at 2nd Asia Water Cycle Symposium (AWCI) International Task Team (ITT) in University of Tokyo, Tokyo.
- Merwade, V. (2012). Terrain Processing and HMS- Model Development using GeoHMS. Lafayette, Indiana.
- Santillan, J. (2011). Profile and Cross Section Surveys, Inflow measurement and flood modeling of Surigao River, Surigao City for Flood Hazard Assessment Purposes. Quezon City: Training Center for Applied Geodesy and Photogrammetry (TCAGP).
- Scharffenberg, W. A., & Fleming, M. J. (2010). Hydrologic Modeling System HEC-HMS User's Manual. Davis, California: U.S Army Corps of Engineers - Hydrologic Engineering Center.
- www.abs-cbnnews.com (2009). The Pampanga River Basin. Retrieved October 29, 2015, from <http://www.abs-cbnnews.com/research/10/23/09/pampanga-river-basin>



Appendix



Appendix A. Cong Dado Dam Model Basin Parameters

Basin Number	SCS Curve Number Loss			Clark Unit Hydrograph Transform		Recession Baseflow				
	Initial Abstraction (mm)	Curve Number	Impervious (%)	Time of Concentration (HR)	Storage Coefficient (HR)	Initial Type	Initial Discharge (M ³ /S)	Recession Constant	Threshold Type	Ratio to Peak
10B	0.13636	82.88708	0	87.48	0.94505	Discharge	0.30996	0.9	Ratio to Peak	0
11B	0.13636	73.31813	0	35.58	0.23915	Discharge	0.13467	0.9	Ratio to Peak	0
12B	0.091364	84.3997	0	33.18	0.2064	Discharge	0.009474	0.9	Ratio to Peak	0
13B	0.091364	84.3997	0	31.86	0.18885	Discharge	0.024477	0.9	Ratio to Peak	0
14B	0.091364	63.24497	0	43.44	0.3458	Discharge	0.22783	0.9	Ratio to Peak	0
15B	0.090909	46.0362	0	35.16	0.2336	Discharge	0.014757	0.9	Ratio to Peak	0
16B	0.13636	61.72139	0	35.76	0.2417	Discharge	0.076756	0.9	Ratio to Peak	0
17B	0.13636	92.5218	0	83.58	0.89165	Discharge	0.20706	0.9	Ratio to Peak	0
18B	0.13636	89.92404	0	139.62	1.65325	Discharge	1.3416	0.9	Ratio to Peak	0
19B	0.13636	89.93501	0	281.58	3.5837	Discharge	1.8843	0.9	Ratio to Peak	0
1B	0.091364	86.18634	0	30.78	0.1737	Discharge	0.098732	0.9	Ratio to Peak	0



Appendix

Basin Number	SCS Curve Number Loss			Clark Unit Hydrograph Transform		Recession Baseflow Initial Type	Initial Discharge (M ³ /S)	Recession Constant	Threshold Type	Ratio to Peak
	Initial Abstraction (mm)	Curve Number	Impervious (%)	Time of Concentration (HR)	Storage Coefficient (HR)					
20B	0.091364	94.04538	0	46.44	0.38645	Discharge	0.025773	0.9	Ratio to Peak	0
21B	0.091364	61.3816	0	25.5	0.10195	Discharge	0.013566	0.9	Ratio to Peak	0
22B	0.13636	79.43437	0	48.84	0.41915	Discharge	0.084642	0.9	Ratio to Peak	0
23B	0.13636	84.93679	0	61.38	0.58945	Discharge	0.36144	0.9	Ratio to Peak	0
24B	0.13636	86.70151	0	36.24	0.24825	Discharge	0.046874	0.9	Ratio to Peak	0
25B	0.13636	84.3997	0	27.06	0.1229	Discharge	0.016163	0.9	Ratio to Peak	0
26B	0.13636	79.82896	0	41.04	0.3129	Discharge	0.093791	0.9	Ratio to Peak	0
27B	0.13636	80.30029	0	48.12	0.4099	Discharge	0.16647	0.9	Ratio to Peak	0
28B	0.091364	82.96381	0	38.58	0.2799	Discharge	0.090173	0.9	Ratio to Peak	0
29B	0.090909	88.90467	0	161.46	1.9507	Discharge	0.3999	0.9	Ratio to Peak	0
2B	0.090909	84.95871	0	37.2	0.26115	Discharge	0.38556	0.9	Ratio to Peak	0



Appendix

Basin Number	SCS Curve Number Loss			Clark Unit Hydrograph Transform		Recession Baseflow Initial Type	Initial Discharge (M ³ /S)	Recession Constant	Threshold Type	Ratio to Peak
	Initial Abstraction (mm)	Curve Number	Impervious (%)	Time of Concentration (HR)	Storage Coefficient (HR)					
30B	0.090909	92.0724	0	56.52	0.52385	Discharge	0.042815	0.9	Ratio to Peak	0
31B	0.090909	86.95361	0	55.68	0.5125	Discharge	0.036332	0.9	Ratio to Peak	0
32B	0.090909	84.95871	0	172.02	2.0939	Discharge	2.8733	0.9	Ratio to Peak	0
33B	0.090909	92.0724	0	113.34	1.2959	Discharge	0.32437	0.9	Ratio to Peak	0
34B	0.090909	84.3997	0	33.06	0.20485	Discharge	0.056282	0.9	Ratio to Peak	0
35B	0.090909	84.3997	0	37.02	0.2583	Discharge	0.14549	0.9	Ratio to Peak	0
36B	0.090909	84.3997	0	35.16	0.2334	Discharge	0.19307	0.9	Ratio to Peak	0
37B	0.090909	84.3997	0	24.42	0.08705	Discharge	0.021993	0.9	Ratio to Peak	0
38B	0.090909	72.45221	0	39.54	0.29255	Discharge	0.11394	0.9	Ratio to Peak	0
39B	0.090909	89.75963	0	36.9	0.2571	Discharge	0.047716	0.9	Ratio to Peak	0
3B	0.090909	84.86006	0	26.58	0.1168	Discharge	0.097028	0.9	Ratio to Peak	0



Appendix

Basin Number	SCS Curve Number Loss			Clark Unit Hydrograph Transform		Recession Baseflow Initial Type	Initial Discharge (M ³ /S)	Recession Constant	Threshold Type	Ratio to Peak
	Initial Abstraction (mm)	Curve Number	Impervious (%)	Time of Concentration (HR)	Storage Coefficient (HR)					
40B	0.090909	92.0724	0	109.02	1.2372	Discharge	0.16591	0.9	Ratio to Peak	0
41B	0.090909	92.0724	0	75.36	0.77995	Discharge	0.099256	0.9	Ratio to Peak	0
42B	0.090909	85.79175	0	67.44	0.6725	Discharge	0.22458	0.9	Ratio to Peak	0
43B	0.090909	65.766	0	32.28	0.19415	Discharge	0.077976	0.9	Ratio to Peak	0
44B	0.090909	82.58017	0	68.64	0.6888	Discharge	0.34963	0.9	Ratio to Peak	0
45B	0.090909	92.0724	0	36.96	0.25815	Discharge	0.010784	0.9	Ratio to Peak	0
46B	0.090909	88.92659	0	65.52	0.6461	Discharge	0.27837	0.9	Ratio to Peak	0
47B	0.090909	86.07673	0	76.86	0.8001	Discharge	1.4551	0.9	Ratio to Peak	0
48B	0.090909	84.3997	0	23.64	0.077	Discharge	0.016839	0.9	Ratio to Peak	0
49B	0.090909	88.23605	0	43.8	0.35045	Discharge	0.064652	0.9	Ratio to Peak	0
4B	0.090909	85.13409	0	23.28	0.07155	Discharge	0.022205	0.9	Ratio to Peak	0

Appendix

Basin Number	SCS Curve Number Loss			Clark Unit Hydrograph Transform		Recession Baseflow Initial Type	Initial Discharge (M ³ /S)	Recession Constant	Threshold Type	Ratio to Peak
	Initial Abstraction (mm)	Curve Number	Impervious (%)	Time of Concentration (HR)	Storage Coefficient (HR)					
50B	0.090909	86.06577	0	37.5	0.26535	Discharge	0.13482	0.9	Ratio to Peak	0
51B	0.090909	84.3997	0	39	0.2857	Discharge	0.11633	0.9	Ratio to Peak	0
52B	0.090909	84.3997	0	25.26	0.0991	Discharge	0.031782	0.9	Ratio to Peak	0
53B	0.090909	53.30334	0	41.04	0.31295	Discharge	0.044241	0.9	Ratio to Peak	0
54B	0.090909	85.6931	0	49.08	0.4228	Discharge	0.26059	0.9	Ratio to Peak	0
55B	0.090909	84.3997	0	24.6	0.09005	Discharge	0.020219	0.9	Ratio to Peak	0
56B	0.090909	84.3997	0	27.3	0.1266	Discharge	0.036226	0.9	Ratio to Peak	0
57B	0.090909	84.55315	0	52.68	0.47185	Discharge	0.17207	0.9	Ratio to Peak	0
58B	0.090909	84.87102	0	34.86	0.2289	Discharge	0.071433	0.9	Ratio to Peak	0
59B	0.090909	82.96381	0	80.52	0.85045	Discharge	0.56062	0.9	Ratio to Peak	0
5B	0.090909	85.41907	0	31.98	0.18985	Discharge	0.088117	0.9	Ratio to Peak	0



Appendix

Basin Number	SCS Curve Number Loss			Clark Unit Hydrograph Transform		Recession Baseflow Initial Type	Initial Discharge (M ³ /S)	Recession Constant	Threshold Type	Ratio to Peak
	Initial Abstraction (mm)	Curve Number	Impervious (%)	Time of Concentration (HR)	Storage Coefficient (HR)					
60B	0.090909	84.3997	0	34.86	0.22925	Discharge	0.088561	0.9	Ratio to Peak	0
61B	0.090909	86.5919	0	61.26	0.58825	Discharge	0.4023	0.9	Ratio to Peak	0
62B	0.090909	85.8904	0	29.28	0.1536	Discharge	0.12152	0.9	Ratio to Peak	0
63B	0.090909	85.87944	0	36.84	0.2559	Discharge	0.25112	0.9	Ratio to Peak	0
64B	0.090909	84.3997	0	34.2	0.22035	Discharge	0.1145	0.9	Ratio to Peak	0
65B	0.090909	85.30946	0	27.48	0.12855	Discharge	0.11711	0.9	Ratio to Peak	0
66B	0.090909	83.44609	0	40.68	0.3086	Discharge	0.39899	0.9	Ratio to Peak	0
67B	0.090909	84.3997	0	38.46	0.27845	Discharge	0.12823	0.9	Ratio to Peak	0
68B	0.090909	84.3997	0	33.84	0.2154	Discharge	0.099299	0.9	Ratio to Peak	0
69B	0.090909	85.19985	0	72.84	0.74525	Discharge	0.98557	0.9	Ratio to Peak	0
6B	0.090909	85.8904	0	391.92	5.08395	Discharge	6.4153	0.9	Ratio to Peak	0

Appendix

Basin Number	SCS Curve Number Loss			Clark Unit Hydrograph Transform		Recession Baseflow	Initial Discharge (M3/S)	Recession Constant	Threshold Type	Ratio to Peak
	Initial Abstraction (mm)	Curve Number	Impervious (%)	Time of Concentration (HR)	Storage Coefficient (HR)					
70B	0.090909	86.10962	0	37.26	0.26205	Discharge	0.16822	0.9	Ratio to Peak	0
71B	0.090909	84.3997	0	29.34	0.1543	Discharge	0.059319	0.9	Ratio to Peak	0
72B	0.090909	85.16697	0	33.06	0.20505	Discharge	0.10136	0.9	Ratio to Peak	0
73B	0.090909	85.13409	0	28.14	0.1378	Discharge	0.082655	0.9	Ratio to Peak	0
74B	0.090909	98.9373	0	26.76	0.119	Discharge	0.014167	0.9	Ratio to Peak	0
78B	0.090909	86.1973	0	36.24	0.2481	Discharge	0.043243	0.9	Ratio to Peak	0
79B	0.090909	94.00154	0	52.92	0.4749	Discharge	0.19102	0.9	Ratio to Peak	0
7B	0.090909	88.24701	0	140.82	1.67015	Discharge	0.34849	0.9	Ratio to Peak	0
81B	0.090909	85.22178	0	38.58	0.27965	Discharge	0.045571	0.9	Ratio to Peak	0
82B	0.090909	84.89295	0	34.5	0.2243	Discharge	0.10085	0.9	Ratio to Peak	0
83B	0.090909	97.00485	0	43.8	0.35095	Discharge	0.023127	0.9	Ratio to Peak	0



Appendix

Basin Number	SCS Curve Number Loss			Clark Unit Hydrograph Transform		Recession Baseflow	Initial Discharge (M ³ /S)	Recession Constant	Threshold Type	Ratio to Peak
	Initial Abstraction (mm)	Curve Number	Impervious (%)	Time of Concentration (HR)	Storage Coefficient (HR)					
84B	0.090909	89.93501	0	63.48	0.61855	Discharge	0.10472	0.9	Ratio to Peak	0
86B	0.090909	71.8932	0	262.56	3.3253	Discharge	0.91982	0.9	Ratio to Peak	0
87B	0.090909	69.62427	0	179.88	2.20105	Discharge	0.33576	0.9	Ratio to Peak	0
88B	0.090909	91.51339	0	123.72	1.4371	Discharge	0.62054	0.9	Ratio to Peak	0
8B	0.090909	78.30538	0	63.78	0.62265	Discharge	0.33662	0.9	Ratio to Peak	0
9B	0.090909	86.58094	0	175.98	2.14805	Discharge	1.3517	0.9	Ratio to Peak	0

Appendix B. Abad Santos Bridge Model Basin Parameters

Basin Number	SCS Curve Number Loss			Clark Unit Hydrograph Transform		Recession Baseflow				
	Initial Abstraction (mm)	Curve Number	Impervious (%)	Time of Concentration (HR)	Storage Coefficient (HR)	Initial Type	Initial Discharge (M3/S)	Recession Constant	Threshold Type	Ratio to Peak
80B	0.0909091	77.647724	0	58.56	0.3061	Discharge	0.71673	1	Ratio to Peak	0.00
81B	0.0909091	78.404033	0	77.16	0.5593	Discharge	0.36762	1	Ratio to Peak	0.00
82B	0.0909091	78.1015094	0	69	0.4486	Discharge	0.81354	1	Ratio to Peak	0.00
83B	0.0909091	89.244462	0	87.6	0.7019	Discharge	0.18656	1	Ratio to Peak	0.00
84B	0.0909091	82.7402046	0	126.96	1.2371	Discharge	0.84478	1	Ratio to Peak	0.00
85B	0.0909091	77.647724	0	51.84	0.2149	Discharge	0.41344	1	Ratio to Peak	0.00
89B	0.0909091	77.647724	0	49.2	0.1796	Discharge	0.13491	1	Ratio to Peak	0.00
90B	0.0909091	78.656136	0	80.88	0.6107	Discharge	1.1979	1	Ratio to Peak	0.00
91B	0.0909091	77.647724	0	78.12	0.5733	Discharge	1.0165	1	Ratio to Peak	0.00
92B	0.0909091	77.647724	0	80.4	0.6037	Discharge	2.0832	1	Ratio to Peak	0.00
94B	0.0909091	73.4123936	0	62.4	0.3587	Discharge	0.31516	1	Ratio to Peak	0.00



Appendix

Basin Number	SCS Curve Number Loss			Clark Unit Hydrograph Transform		Recession Baseflow	Initial Discharge (M ³ /S)	Recession Constant	Threshold Type	Ratio to Peak
	Initial Abstraction (mm)	Curve Number	Impervious (%)	Time of Concentration (HR)	Storage Coefficient (HR)					
95B	0.0909091	76.4376296	0	77.4	0.563	Discharge	1.5154	1	Ratio to Peak	0.00
96B	0.0909091	77.647724	0	52.44	0.2235	Discharge	0.54907	1	Ratio to Peak	0.00
97B	0.0909091	78.969	0	216.36	2.4523	Discharge	12.545	1	Ratio to Peak	0.00

Appendix C. Alejo Santos Model Basin Parameters

Basin Number	SCS Curve Number Loss			Clark Unit Hydrograph Transform		Recession Baseflow				
	Initial Abstraction (mm)	Curve Number	Impervious (%)	Time of Concentration (HR)	Storage Coefficient (HR)	Initial Type	Initial Discharge (M ³ /S)	Recession Constant	Threshold Type	Ratio to Peak
28B	0.584375	58.643	0.0	4.8904	2.585625	0.56628	0.5	0	Ratio to Peak	0.00
29B	11.775203	58.643	0.0	12.466	8.262765	5.4283	0.5	0.00	Ratio to Peak	0.00
30B	0.5991293	58.643	0.0	2.1586	62.7249	2.0218	0.5	0.00	Ratio to Peak	0.00
31B	12.3028235	58.643	0.0	5.8717	3.321675	2.0101	0.5	0.00	Ratio to Peak	0.00
32B	1.3280	58.643	0.0	7.5371	1.733865	1.8231	0.5	0.00	Ratio to Peak	0.00
33B	12.131064	58.643	0.0	14.1184	9.499665	3.2782	0.45054	0.00	Ratio to Peak	0.00
34B	0.584375	58.643	0.0	7.4131	4.478565	3.5753	0.5	0.00	Ratio to Peak	0.00
35B	1.9821252	58.643	0.0	6.5707	2.38161	2.0716	0.5	0.00	Ratio to Peak	0.00
36B	1.3280	58.643	0.0	2.6168	2.855685	0.47149	0.49938	0.00	Ratio to Peak	0.00
37B	1.9821252	58.643	0.0	6.8011	2.609145	1.2214	0.45096	0.00	Ratio to Peak	0.00
38B	0.584375	58.643	0.0	7.7141	4.703055	2.7095	0.5	0.00	Ratio to Peak	0.00



Appendix

Basin Number	SCS Curve Number Loss			Clark Unit Hydrograph Transform		Recession Baseflow	Initial Discharge (M ³ /S)	Recession Constant	Threshold Type	Ratio to Peak
	Initial Abstraction (mm)	Curve Number	Impervious (%)	Time of Concentration (HR)	Storage Coefficient (HR)					
39B	0.584375	58.643	0.0	8.1019	4.992225	2.3231	0.5	0.00	Ratio to Peak	0
40B	0.584375	58.643	0.0	4.9248	2.614395	1.2746	0.45	0.00	Ratio to Peak	0
41B	0.584375	58.643	0.0	5.5443	3.078915	1.1169	0.5	0.00	Ratio to Peak	0
42B	0.584375	58.643	0.0	6.3715	3.699675	2.5603	1	0.00	Ratio to Peak	0
43B	0.584375	58.643	0.0	7.4731	4.523715	2.5489	0.9	0.00	Ratio to Peak	0

Appendix D. Ilog Baliwag Model basin Parameters

Basin Number	SCS Curve Number Loss			Clark Unit Hydrograph Transform		Recession Baseflow				
	Initial Abstraction (mm)	Curve Number	Impervious (%)	Time of Concentration (HR)	Storage Coefficient (HR)	Initial Type	Initial Discharge (M ³ /S)	Recession Constant	Threshold Type	Ratio to Peak
41B	1	92.0724	0	94.25	0.77995	0.0992561	0.9	0	Ratio to Peak	0.00



Appendix E. Sto Nino Model Basin Parameters

Basin Number	SCS Curve Number Loss			Clark Unit Hydrograph Transform		Recession Baseflow				
	Initial Abstraction (mm)	Curve Number	Impervious (%)	Time of Concentration (HR)	Storage Coefficient (HR)	Initial Type	Initial Discharge (M ³ /S)	Recession Constant	Threshold Type	Ratio to Peak
10B	1.5	82.887082	0	1.1664	0.18901	0.30996	0.9	0	Ratio to Peak	0.00
11B	1.5	73.318129	0	0.4744	0.04783	0.13467	0.9	0	Ratio to Peak	0.00
12B	1.005	84.3997	0	0.4424	0.04128	0.0094742	0.9	0	Ratio to Peak	0.00
13B	1.005	84.3997	0	0.4248	0.03777	0.0244767	0.9	0	Ratio to Peak	0.00
14B	1.005	63.24497	0	0.5792	0.06916	0.22783	0.9	0	Ratio to Peak	0.00
15B	1	46.0362	0	0.4688	0.04672	0.0147569	0.9	0	Ratio to Peak	0.00
16B	1.5	61.721391	0	0.4768	0.04834	0.0767557	0.9	0	Ratio to Peak	0.00
17B	1.5	92.521801	0	1.1144	0.17833	0.20706	0.9	0	Ratio to Peak	0.00
18B	1.5	89.924044	0	1.8616	0.33065	1.3416	0.9	0	Ratio to Peak	0.00
19B	1.5	89.935005	0	3.7544	0.71674	1.8843	0.9	0	Ratio to Peak	0.00
1B	1.005	86.186343	0	0.4104	0.03474	0.098732	0.9	0	Ratio to Peak	0.00

Appendix

Basin Number	SCS Curve Number Loss			Clark Unit Hydrograph Transform		Recession Baseflow Initial Type	Initial Discharge (M ₃ /S)	Recession Constant	Threshold Type	Ratio to Peak
	Initial Abstraction (mm)	Curve Number	Impervious (%)	Time of Concentration (HR)	Storage Coefficient (HR)					
20B	1.005	94.04538	0	0.6192	0.07729	0.0257731	0.9	0	Ratio to Peak	0
21B	1.005	61.3816	0	0.34	0.02039	0.0135664	0.9	0	Ratio to Peak	0
22B	1.5	79.434367	0	0.6512	0.08383	0.0846418	0.9	0	Ratio to Peak	0
23B	1.5	84.936789	0	0.8184	0.11789	0.36144	0.9	0	Ratio to Peak	0
24B	1.5	86.70151	0	0.4832	0.04965	0.0468738	0.9	0	Ratio to Peak	0
25B	1.5	84.3997	0	0.3608	0.028161	0.0161628	0.9	0	Ratio to Peak	0
26B	1.5	79.828963	0	0.5472	0.028161	0.0937908	0.9	0	Ratio to Peak	0
27B	1.5	80.300286	0	0.6416	0.08198	0.16647	0.9	0	Ratio to Peak	0
28B	1.005	82.963809	0	0.5144	0.05598	0.090173	0.9	0	Ratio to Peak	0
29B	1	88.904671	0	2.1528	0.39014	0.3999	0.9	0	Ratio to Peak	0
2B	1	84.958711	0	0.496	0.05223	0.38556	0.9	0	Ratio to Peak	0



Appendix

Basin Number	SCS Curve Number Loss			Clark Unit Hydrograph Transform		Recession Baseflow Initial Type	Initial Discharge (M ³ /S)	Recession Constant	Threshold Type	Ratio to Peak
	Initial Abstraction (mm)	Curve Number	Impervious (%)	Time of Concentration (HR)	Storage Coefficient (HR)					
30B	1	92.0724	0	0.7536	0.10477	0.0428151	0.9	0	Ratio to Peak	0
31B	1	86.953613	0	0.7424	0.1025	0.036332	0.9	0	Ratio to Peak	0
32B	1	84.958711	0	2.2936	0.41878	2.8733	0.9	0	Ratio to Peak	0
33B	1	92.0724	0	1.5112	0.25918	0.32437	0.9	0	Ratio to Peak	0
34B	1	84.3997	0	0.4408	0.04097	0.0562818	0.9	0	Ratio to Peak	0
35B	1	84.3997	0	0.4936	0.05166	0.14549	0.9	0	Ratio to Peak	0
36B	1	84.3997	0	0.4688	0.04668	0.19307	0.9	0	Ratio to Peak	0
37B	1	84.3997	0	0.3256	0.01741	0.0219926	0.9	0	Ratio to Peak	0
38B	1	72.45221	0	0.5272	0.05851	0.11394	0.9	0	Ratio to Peak	0
39B	1	89.759629	0	0.492	0.05142	0.0477162	0.9	0	Ratio to Peak	0
3B	1	84.860062	0	0.3544	0.02336	0.0970275	0.9	0	Ratio to Peak	0

Appendix

Basin Number	SCS Curve Number Loss			Clark Unit Hydrograph Transform		Recession Baseflow		Initial Discharge (M ₃ /S)	Recession Constant	Threshold Type	Ratio to Peak
	Initial Abstraction (mm)	Curve Number	Impervious (%)	Time of Concentration (HR)	Storage Coefficient (HR)	Initial Type					
40B	1	92.0724	0	1.4536	0.24744	0.16591	0	0.9	0	Ratio to Peak	0
41B	1	92.0724	0	1.2567	0.15599	0.0992561	0	0.9	0	Ratio to Peak	0
42B	1	85.791747	0	0.8992	0.1345	0.22458	0	0.9	0	Ratio to Peak	0
43B	1	65.766	0	0.4304	0.03883	0.0779761	0	0.9	0	Ratio to Peak	0
44B	1	82.580174	0	0.9152	0.13776	0.34963	0	0.9	0	Ratio to Peak	0
45B	1	92.0724	0	0.4928	0.05163	0.0107841	0	0.9	0	Ratio to Peak	0
46B	1	88.926593	0	0.8736	0.12922	0.27837	0	0.9	0	Ratio to Peak	0
47B	1	86.076733	0	1.0248	0.16002	1.4551	0	0.9	0	Ratio to Peak	0
48B	1	84.3997	0	0.3152	0.077	0.0168394	0	0.9	0	Ratio to Peak	0
49B	1	88.23605	0	0.584	0.07009	0.064652	0	0.9	0	Ratio to Peak	0
4B	1	85.134087	0	0.3104	0.07155	0.022205	0	0.9	0	Ratio to Peak	0



Appendix

Basin Number	SCS Curve Number Loss			Clark Unit Hydrograph Transform		Recession Baseflow Initial Type	Initial Discharge (M ³ /S)	Recession Constant	Threshold Type	Ratio to Peak
	Initial Abstraction (mm)	Curve Number	Impervious (%)	Time of Concentration (HR)	Storage Coefficient (HR)					
50B	1	86.065772	0	0.5	0.05307	0.13482	0.9	0	Ratio to Peak	0
51B	1	84.3997	0	0.52	0.05714	0.11633	0.9	0	Ratio to Peak	0
52B	1	84.3997	0	0.3368	0.01982	0.0317822	0.9	0	Ratio to Peak	0
53B	1	53.303343	0	0.5472	0.06259	0.044241	0.9	0	Ratio to Peak	0
54B	1	85.693098	0	0.6544	0.08456	0.26059	0.9	0	Ratio to Peak	0
55B	1	84.3997	0	0.328	0.01801	0.0202186	0.9	0	Ratio to Peak	0
56B	1	84.3997	0	0.364	0.02532	0.0362257	0.9	0	Ratio to Peak	0
57B	1	84.553154	0	0.7024	0.09437	0.17207	0.9	0	Ratio to Peak	0
58B	1	84.871023	0	0.4648	0.04578	0.0714334	0.9	0	Ratio to Peak	0
59B	1	82.963809	0	1.0736	0.17009	0.56062	0.9	0	Ratio to Peak	0
5B	1	85.419073	0	0.4264	0.03797	0.0881171	0.9	0	Ratio to Peak	0

Appendix

Basin Number	SCS Curve Number Loss			Clark Unit Hydrograph Transform		Recession Baseflow		Initial Discharge (M ₃ /S)	Recession Constant	Threshold Type	Ratio to Peak
	Initial Abstraction (mm)	Curve Number	Impervious (%)	Time of Concentration (HR)	Storage Coefficient (HR)	Initial Type					
60B	1	84.3997	0	0.4648	0.04585	0.0885612	0	0.9	0	Ratio to Peak	0
61B	1	86.5919	0	0.8168	0.11765	0.4023	0	0.9	0	Ratio to Peak	0
62B	1	85.890396	0	0.3904	0.03072	0.12152	0	0.9	0	Ratio to Peak	0
63B	1	85.879435	0	0.4912	0.05118	0.25112	0	0.9	0	Ratio to Peak	0
64B	1	84.3997	0	0.456	0.04407	0.1145	0	0.9	0	Ratio to Peak	0
65B	1	85.309463	0	0.3664	0.02571	0.11711	0	0.9	0	Ratio to Peak	0
66B	1	83.446093	0	0.5424	0.06172	0.39899	0	0.9	0	Ratio to Peak	0
67B	1	84.3997	0	0.5128	0.05569	0.12823	0	0.9	0	Ratio to Peak	0
68B	1	84.3997	0	0.4512	0.04308	0.0992991	0	0.9	0	Ratio to Peak	0
69B	1	85.199853	0	0.9712	0.14905	0.98557	0	0.9	0	Ratio to Peak	0
6B	1	85.890396	0	5.2256	1.01679	6.4153	0	0.9	0	Ratio to Peak	0
70B	1	86.109616	0	0.4968	0.05241	0.16822	0	0.9	0	Ratio to Peak	0



Appendix

Basin Number	SCS Curve Number Loss			Clark Unit Hydrograph Transform		Recession Baseflow	Initial Discharge (M3/S)	Recession Constant	Threshold Type	Ratio to Peak
	Initial Abstraction (mm)	Curve Number	Impervious (%)	Time of Concentration (HR)	Storage Coefficient (HR)					
71B	1	84.3997	0	0.3912	0.03086	0.0593194	0.9	0	Ratio to Peak	0
72B	1	85.16697	0	0.4408	0.04101	0.10136	0.9	0	Ratio to Peak	0
73B	1	85.134087	0	0.3752	0.02756	0.0826554	0.9	0	Ratio to Peak	0
74B	1	98.9373	0	0.3568	0.0238	0.0141666	0.9	0	Ratio to Peak	0
78B	1	86.197304	0	0.4832	0.04962	0.0432428	0.9	0	Ratio to Peak	0
79B	1	94.001536	0	0.7056	0.09498	0.19102	0.9	0	Ratio to Peak	0
7B	1	88.247011	0	1.8776	0.33403	0.34849	0.9	0	Ratio to Peak	0
86B	1	71.893199	0	3.5008	0.66506	0.91982	0.9	0	Ratio to Peak	0
87B	1	69.624272	0	2.3984	0.44021	0.33576	0.9	0	Ratio to Peak	0
88B	1	91.513389	0	1.6496	0.28742	0.62054	0.9	0	Ratio to Peak	0
8B	1	78.305384	0	0.8504	0.12453	0.33662	0.9	0	Ratio to Peak	0
9B	1	86.580939	0	2.3464	0.42961	1.3517	0.9	0	Ratio to Peak	0

Appendix

Appendix F. Cong Dado Dam Model Reach Parameters

Reach Number	Muskingum Cunge Channel Routing						
	Time Step Method	Length (m)	Slope	Manning's n	Shape	Width	Side Slope
908R	Automatic Fixed Interval	52105.14	0.1322	0.51758	Trapezoid	30	45
909R	Automatic Fixed Interval	33143.37	0.1482	0.14593	Trapezoid	30	45
910R	Automatic Fixed Interval	4541.102	0.143	0.36493	Trapezoid	30	45
911R	Automatic Fixed Interval	17658.37	0.1679	0.0129075	Trapezoid	30	45
912R	Automatic Fixed Interval	41044.55	0.1868	0.0583198	Trapezoid	30	45
913R	Automatic Fixed Interval	58307.61	0.01834	0.0257314	Trapezoid	30	45
914R	Automatic Fixed Interval	3678.926	0.5475	0.16116	Trapezoid	30	45
915R	Automatic Fixed Interval	3085.722	0.5393	0.0964029	Trapezoid	30	45
916R	Automatic Fixed Interval	27502.19	0.2057	0.032599	Trapezoid	30	45
917R	Automatic Fixed Interval	26217.71	0.2116	0.16228	Trapezoid	30	45
918R	Automatic Fixed Interval	1225.716	0.062	0.012923	Trapezoid	30	45
919R	Automatic Fixed Interval	3361.405	0.1541	0.16218	Trapezoid	30	45
920R	Automatic Fixed Interval	3604.334	0.2008	0.0622848	Trapezoid	30	45
921R	Automatic Fixed Interval	2648.707	0.0996	0.40264	Trapezoid	30	45
922R	Automatic Fixed Interval	32126.11	0.0484	1	Trapezoid	30	45
923R	Automatic Fixed Interval	27656.05	0.1403	0.0331806	Trapezoid	30	45
924R	Automatic Fixed Interval	2026.455	0.1915	0.12201	Trapezoid	30	45
925R	Automatic Fixed Interval	3268.213	0.1626	0.089933	Trapezoid	30	45
926R	Automatic Fixed Interval	1201.095	0.8	0.10165	Trapezoid	30	45
927R	Automatic Fixed Interval	2377.086	0.4985	0.0445988	Trapezoid	30	45
928R	Automatic Fixed Interval	21346.58	0.1359	0.10106	Trapezoid	30	45
929R	Automatic Fixed Interval	3618.808	0.2258	0.0141271	Trapezoid	30	45
930R	Automatic Fixed Interval	8337.668	0.1351	0.14252	Trapezoid	30	45
931R	Automatic Fixed Interval	9937.166	0.4501	0.0711747	Trapezoid	30	45
932R	Automatic Fixed Interval	6606.517	0.2801	0.24419	Trapezoid	30	45
933R	Automatic Fixed Interval	3962.694	0.461	0.10584	Trapezoid	30	45
934R	Automatic Fixed Interval	4472.585	0.0173	0.10824	Trapezoid	30	45
935R	Automatic Fixed Interval	8494.313	0.2412	0.0666753	Trapezoid	30	45
936R	Automatic Fixed Interval	2569.065	0.2613	0.0427846	Trapezoid	30	45
937R	Automatic Fixed Interval	3958.792	0.0745	0.0724078	Trapezoid	30	45
938R	Automatic Fixed Interval	2129.473	0.1806	0.0708996	Trapezoid	30	45
939R	Automatic Fixed Interval	1515.696	0.1863	0.0715752	Trapezoid	30	45
940R	Automatic Fixed Interval	8446.354	0.0001	0.11028	Trapezoid	30	45
941R	Automatic Fixed Interval	71352.06	0.2146	0.11463	Trapezoid	30	45
942R	Automatic Fixed Interval	18306.43	0.1506	0.0224857	Trapezoid	30	45
943R	Automatic Fixed Interval	40479.43	0.2375	0.0858422	Trapezoid	30	45
944R	Automatic Fixed Interval	1389.935	0.8	0.31426	Trapezoid	30	45



Appendix

Reach Number	Muskingum Cunge Channel Routing						
	Time Step Method	Length (m)	Slope	Manning's n	Shape	Width	Side
945R	Automatic Fixed Interval	10605.6	0.0965	0.24046	Trapezoid	30	45
946R	Automatic Fixed Interval	12120.06	0.3439	0.0686921	Trapezoid	30	45
947R	Automatic Fixed Interval	46779.03	0.1718	0.36279	Trapezoid	30	45
948R	Automatic Fixed Interval	865.2062	0.2133	0.11192	Trapezoid	30	45
949R	Automatic Fixed Interval	9059.753	0.2077	0.0001	Trapezoid	30	45
950R	Automatic Fixed Interval	27419.59	0.2081	0.0450158	Trapezoid	30	45
951R	Automatic Fixed Interval	22693.72	0.0363	0.0468937	Trapezoid	30	45
952R	Automatic Fixed Interval	21166.23	0.0924	0.13579	Trapezoid	30	45
953R	Automatic Fixed Interval	11966.26	0.1394	0.12071	Trapezoid	30	45
954R	Automatic Fixed Interval	5333.186	0.0016	0.3156	Trapezoid	30	45
955R	Automatic Fixed Interval	15459.52	0.1227	0.0561444	Trapezoid	30	45



Appendix

Appendix G. Abad Santos Bridge Model Reach Parameters

Reach Number	Muskingum Cunge Channel Routing						
	Time Step Method	Length (m)	Slope	Manning's n	Shape	Width	Side Slope
169R	Automatic Fixed Interval	188194.142	0.008350	0.075	Trapezoid	30	45
170R	Automatic Fixed Interval	50050.972	0.006630	0.030	Trapezoid	30	45
171R	Automatic Fixed Interval	39926.009	0.006090	0.080	Trapezoid	30	45
172R	Automatic Fixed Interval	118717.284	0.000890	0.062	Trapezoid	30	45
173R	Automatic Fixed Interval	31090.867	0.021940	0.050	Trapezoid	30	45
177R	Automatic Fixed Interval	116501.288	0.004790	0.050	Trapezoid	30	45
178R	Automatic Fixed Interval	93115.577	0.001390	0.090	Trapezoid	30	45
179R	Automatic Fixed Interval	91242.846	0.002140	0.050	Trapezoid	30	45
180R	Automatic Fixed Interval	58578.462	0.000220	0.050	Trapezoid	30	45
182R	Automatic Fixed Interval	35666.865	0.010370	0.040	Trapezoid	30	45



Appendix

Appendix H. Alejo Santos Model Reach Parameters

Reach Number	Muskingum Cunge Channel Routing						
	Time Step Method	Length (m)	Slope	Manning's n	Shape	Width	Side Slope
38R	Automatic Fixed Interval	32757.906	0.000200	0.020142	Trapezoid	30	45
39R	Automatic Fixed Interval	43965.735	0.000810	0.020142	Trapezoid	30	45
40R	Automatic Fixed Interval	64087.298	0.001130	0.0196492	Trapezoid	30	45
41R	Automatic Fixed Interval	34552.197	0.005650	0.0200512	Trapezoid	30	45
42R	Automatic Fixed Interval	98720.232	0.001520	0.020142	Trapezoid	30	45
43R	Automatic Fixed Interval	97311.319	0.001540	0.020142	Trapezoid	30	45
44R	Automatic Fixed Interval	76911.542	0.005780	0.020142	Trapezoid	30	45
45R	Automatic Fixed Interval	60839.674	0.002470	0.020142	Trapezoid	30	45
46R	Automatic Fixed Interval	60243.694	0.002050	0.020142	Trapezoid	30	45
47R	Automatic Fixed Interval	69490.620	0.012010	0.0687502	Trapezoid	30	45
48R	Automatic Fixed Interval	46294.567	0.004150	0.0200408	Trapezoid	30	45
49R	Automatic Fixed Interval	43032.218	0.001980	0.020142	Trapezoid	30	45
50R	Automatic Fixed Interval	26184.539	0.001510	0.020142	Trapezoid	30	45
51R	Automatic Fixed Interval	28151.984	0.013820	0.020142	Trapezoid	30	45
52R	Automatic Fixed Interval	30445.321	0.016960	0.020142	Trapezoid	30	45

Appendix

Appendix I. Sto. Nino Model Reach Parameters

Reach Number	Muskingum Cunge Channel Routing						
	Time Step Method	Length (m)	Slope	Manning's n	Shape	Width	Side Slope
100R	Automatic Fixed Interval	101470.2	0.00533	0.0020916	Trapezoid	30	45
101R	Automatic Fixed Interval	110474.6	0.00876	0.0050454	Trapezoid	30	45
102R	Automatic Fixed Interval	26410.85	0.01935	0.0021342	Trapezoid	30	45
103R	Automatic Fixed Interval	70743.73	0.00361	0.0021342	Trapezoid	30	45
104R	Automatic Fixed Interval	81595.9	0.00006	0.0009679	Trapezoid	30	45
105R	Automatic Fixed Interval	88922.96	0.00024	0.005049	Trapezoid	30	45
106R	Automatic Fixed Interval	130474.6	0.00055	0.0050884	Trapezoid	30	45
107R	Automatic Fixed Interval	140828.6	0.00018	0.0045643	Trapezoid	30	45
108R	Automatic Fixed Interval	50981.31	0.00019	0.0050679	Trapezoid	30	45
109R	Automatic Fixed Interval	41496.72	0.00414	0.0076076	Trapezoid	30	45
110R	Automatic Fixed Interval	185701.7	0.00045	0.0022222	Trapezoid	30	45
111R	Automatic Fixed Interval	58403.27	0.00166	0.005097	Trapezoid	30	45
112R	Automatic Fixed Interval	69038.59	0.00297	0.005095	Trapezoid	30	45
113R	Automatic Fixed Interval	76106.65	0.00051	0.016839	Trapezoid	30	45
114R	Automatic Fixed Interval	22253.63	0.00072	0.0021342	Trapezoid	30	45
115R	Automatic Fixed Interval	23434.09	0.0002	0.00098765	Trapezoid	30	45
116R	Automatic Fixed Interval	23085.33	0.00018	0.0014518	Trapezoid	30	45
117R	Automatic Fixed Interval	39393.16	0.00018	0.0049212	Trapezoid	30	45
118R	Automatic Fixed Interval	144533.6	0.00059	0.0050955	Trapezoid	30	45
119R	Automatic Fixed Interval	28606.19	0.00107	0.0014518	Trapezoid	30	45
120R	Automatic Fixed Interval	97885.92	0.00191	0.00098765	Trapezoid	30	45
121R	Automatic Fixed Interval	102358.3	0.00084	0.00098765	Trapezoid	30	45
122R	Automatic Fixed Interval	33751.06	0.00156	0.0014518	Trapezoid	30	45
123R	Automatic Fixed Interval	193624.2	0.00094	0.0050944	Trapezoid	30	45
124R	Automatic Fixed Interval	68319.75	0.0005	0.0050942	Trapezoid	30	45
125R	Automatic Fixed Interval	70270.41	0.00061	0.0050924	Trapezoid	30	45
126R	Automatic Fixed Interval	110924.2	0.00101	0.0022222	Trapezoid	30	45
127R	Automatic Fixed Interval	35115.5	0.00034	0.0009679	Trapezoid	30	45
128R	Automatic Fixed Interval	82915.19	0.00028	0.0050699	Trapezoid	30	45
129R	Automatic Fixed Interval	22837.16	0.00534	0.011125	Trapezoid	30	45
130R	Automatic Fixed Interval	138552	0.00279	0.00098765	Trapezoid	30	45
131R	Automatic Fixed Interval	24375.41	0.00185	0.00509	Trapezoid	30	45
132R	Automatic Fixed Interval	55589.14	0.0034	0.00441	Trapezoid	30	45
133R	Automatic Fixed Interval	39397.54	0.00046	0.00098765	Trapezoid	30	45
134R	Automatic Fixed Interval	48523.06	0.00088	0.0014518	Trapezoid	30	45
135R	Automatic Fixed Interval	58000.71	0.00111	0.0050904	Trapezoid	30	45
136R	Automatic Fixed Interval	64556.54	0.00117	0.0014518	Trapezoid	30	45



Appendix

Reach Number	Muskingum Cunge Channel Routing						
	Time Step Method	Length (m)	Slope	Manning's n	Shape	Width	Side Slope
137R	Automatic Fixed Interval	39098.65	0.00424	0.0025	Trapezoid	30	45
138R	Automatic Fixed Interval	82031.8	0.00124	0.0014518	Trapezoid	30	45
139R	Automatic Fixed Interval	110573.6	0.00143	0.0050908	Trapezoid	30	45
140R	Automatic Fixed Interval	105993.1	0.00092	0.0021342	Trapezoid	30	45
141R	Automatic Fixed Interval	51293.42	0.00675	0.003503	Trapezoid	30	45
142R	Automatic Fixed Interval	30235.71	0.00087	0.0014518	Trapezoid	30	45
143R	Automatic Fixed Interval	31043.93	0.0022	0.0021342	Trapezoid	30	45
144R	Automatic Fixed Interval	75603.23	0.0077	0.0021342	Trapezoid	30	45
145R	Automatic Fixed Interval	147433.9	0.00101	0.0014888	Trapezoid	30	45
146R	Automatic Fixed Interval	52837.85	0.00249	0.0058214	Trapezoid	30	45
147R	Automatic Fixed Interval	76652.02	0.00994	0.0033167	Trapezoid	30	45
148R	Automatic Fixed Interval	165091	0.00125	0.0022222	Trapezoid	30	45
149R	Automatic Fixed Interval	64304.7	0.00459	0.00098765	Trapezoid	30	45
150R	Automatic Fixed Interval	39959.89	0.00385	0.0074118	Trapezoid	30	45
151R	Automatic Fixed Interval	104773	0.00169	0.0022222	Trapezoid	30	45
152R	Automatic Fixed Interval	106923.3	0.00913	0.00098765	Trapezoid	30	45
153R	Automatic Fixed Interval	122093.1	0.00433	0.0032667	Trapezoid	30	45
154R	Automatic Fixed Interval	28212.47	0.01982	0.0032136	Trapezoid	30	45
155R	Automatic Fixed Interval	26565.51	0.0257	0.0032667	Trapezoid	30	45
156R	Automatic Fixed Interval	25727.62	0.00219	0.0014518	Trapezoid	30	45
157R	Automatic Fixed Interval	49005.51	0.00555	0.0032667	Trapezoid	30	45
158R	Automatic Fixed Interval	72895.13	0.00744	0.0046311	Trapezoid	30	45
159R	Automatic Fixed Interval	26951.43	0.00213	0.0031373	Trapezoid	30	45
160R	Automatic Fixed Interval	27860.51	0.00226	0.0031373	Trapezoid	30	45
161R	Automatic Fixed Interval	29238.82	0.00234	0.0014518	Trapezoid	30	45
162R	Automatic Fixed Interval	45533.3	0.01794	0.0014518	Trapezoid	30	45
163R	Automatic Fixed Interval	28835.22	0.013	0.0021342	Trapezoid	30	45
164R	Automatic Fixed Interval	41686.78	0.00243	0.0021342	Trapezoid	30	45
167R	Automatic Fixed Interval	33619.33	0.00753	0.00098765	Trapezoid	30	45
168R	Automatic Fixed Interval	195454.4	0.00083	0.0006453	Trapezoid	30	45
175R	Automatic Fixed Interval	38857.99	0.00002	0.0033818	Trapezoid	30	45
176R	Automatic Fixed Interval	127944.8	0.00018	0.0040851	Trapezoid	30	45



Appendix

Appendix M. Pampanga River Discharge from HEC-HMS Simulation

DIRECT FLOW (cms)							
Time (hr)	100-yr	25-yr	5-year	Time (hr)	100-yr	25-yr	5-year
0	0	0	0	6	0	0	0
0.1666667	0	0	0	6.1666667	0	0	0
0.3333333	0	0	0	6.3333333	0	0	0
0.5	0	0	0	6.5	0	0	0
0.6666667	0	0	0	6.6666667	0	0	0
0.8333333	0	0	0	6.8333333	0	0	0
1	0	0	0	7	0	0	0
1.1666667	0	0	0	7.1666667	0	0	0
1.3333333	0	0	0	7.3333333	0	0	0
1.5	0	0	0	7.5	0	0	0
1.6666667	0	0	0	7.6666667	0	0.1	0
1.8333333	0	0	0	7.8333333	0	0.1	0
2	0	0	0	8	0	0.2	0
2.1666667	0	0	0	8.1666667	0	0.3	0
2.3333333	0	0	0	8.3333333	0	0.4	0
2.5	0	0	0	8.5	0	0.6	0
2.6666667	0	0	0	8.6666667	0	0.8	0
2.8333333	0	0	0	8.8333333	0	1.1	0
3	0	0	0	9	0	1.4	0
3.1666667	0	0	0	9.1666667	0	2	0
3.3333333	0	0	0	9.3333333	0.1	2.7	0
3.5	0	0	0	9.5	0.1	3.6	0
3.6666667	0	0	0	9.6666667	0.3	4.7	0
3.8333333	0	0	0	9.8333333	0.5	6	0
4	0	0	0	10	0.8	7.7	0
4.1666667	0	0	0	10.1666667	1.2	9.9	0
4.3333333	0	0	0	10.3333333	1.7	12.4	0
4.5	0	0	0	10.5	2.6	15.5	0
4.6666667	0	0	0	10.6666667	4	19.1	0.1
4.8333333	0	0	0	10.8333333	6	23.4	0.2
5	0	0	0	11	9	28.5	0.5
5.1666667	0	0	0	11.1666667	13.1	34.4	0.9
5.3333333	0	0	0	11.3333333	18.7	41.3	1.7
5.5	0	0	0	11.5	26.5	49.6	2.9
5.6666667	0	0	0	11.6666667	37.9	59.7	5.2



Appendix

DIRECT FLOW (cms)							
Time (hr)	100-yr	25-yr	5-year	Time (hr)	100-yr	25-yr	5-year
12	83.5	90.1	18.8	18.333333	5347	2798.7	1930.6
12.166667	113	108.5	27.9	18.5	5508	2891.1	1992.7
12.333333	146.9	129	38.5	18.666667	5662.8	2979.9	2052.7
12.5	186	151.9	50.7	18.833333	5810.5	3066	2110.7
12.666667	234.1	178.1	66.4	19	5949.2	3149.4	2165.6
12.833333	292.5	209.3	86.3	19.166667	6072.5	3229.9	2214.4
13	357.1	243.6	108.7	19.333333	6185.4	3306.8	2259.1
13.166667	426.8	280.4	132.8	19.5	6291.2	3377.1	2301.5
13.333333	501.7	319.9	158.6	19.666667	6389.2	3443.3	2341.3
13.5	581.7	361.8	186.2	19.833333	6479.1	3506	2378.4
13.666667	670	407.1	217	20	6555.6	3564.9	2410.2
13.833333	764.3	455.8	250.1	20.166667	6619.1	3620.1	2436.7
14	863.1	507.3	284.7	20.333333	6674.7	3670.1	2460.1
14.166667	967	561.4	320.8	20.5	6723.4	3713.5	2481.2
14.333333	1076.2	618.3	358.7	20.666667	6765.3	3752.7	2500
14.5	1193.4	678.2	399.6	20.833333	6800.5	3788.4	2516.5
14.666667	1319.5	742.7	444	21	6826	3820.4	2529.3
14.833333	1451.8	811	490.8	21.166667	6844.3	3849.2	2539.5
15	1589.2	882.1	539.2	21.333333	6857	3873.8	2547.9
15.166667	1732.5	955.8	589.6	21.5	6863.3	3894.1	2554.3
15.333333	1883	1032.4	642.5	21.666667	6862.6	3911.3	2558.3
15.5	2046.3	1112.3	700.7	21.833333	6849.3	3925.5	2557.3
15.666667	2218.2	1198	762.6	22	6824.5	3936.3	2551.3
15.833333	2395.7	1287	826.5	22.166667	6792.5	3943.3	2542.4
16	2578.7	1378.4	892.5	22.333333	6754.7	3943.7	2531.4
16.166667	2767	1472.1	960.6	22.5	6711.5	3939.2	2518.3
16.333333	2963.3	1568	1032	22.666667	6662.9	3931.3	2503.4
16.5	3167.2	1666.7	1107.1	22.833333	6607.7	3920.2	2485.9
16.666667	3375.3	1768.9	1184.1	23	6547.6	3906.3	2466.5
16.833333	3585.9	1873	1262.6	23.166667	6483.6	3889.5	2445.8
17	3798	1978.4	1342	23.333333	6415.7	3869.2	2423.8
17.166667	4008.6	2084.7	1421.3	23.5	6344.4	3846.3	2400.6
17.333333	4213.4	2190.9	1498.4	22.5	5718.3	4217	2495.5
17.5	4414.7	2295.7	1574.2		5875.3	4333.9	2565.9
17.666667	4613.6	2398.8	1649.5	22.83333333	6035.7	4453.5	2637.9
17.833333	4809.2	2500.9	1724	23	6203.4	4578.7	2713.6
18	4999.6	2601.9	1797.1		6376.3	4707.9	2791.8
18.166667	5179.1	2701.4	1866.2	23.33333333	6552.1	4839.4	2871.5



Appendix

DIRECT FLOW (cms)							
Time (hr)	100-yr	25-yr	5-year	Time (hr)	100-yr	25-yr	5-year
23.5	6344.4	3846.3	2400.6	29.833333	2526.8	1959.1	1040.2
23.666667	6268.7	3821.2	2375.9	30	2460	1914.1	1014.7
23.833333	6188.9	3793.9	2349.5	30.166667	2396.8	1870.1	990.8
24	6105.9	3764.5	2322.1	30.333333	2335.7	1826.8	967.6
24.166667	6019.6	3732.7	2293.5	30.5	2276	1784.2	944.9
24.333333	5929.8	3698.2	2263.8	30.666667	2217.7	1742.5	922.7
24.5	5835.5	3661.6	2232.4	30.833333	2160.4	1701.8	900.7
24.666667	5734.5	3623.1	2198.3	31	2104.2	1662.9	879
24.833333	5628.9	3582.6	2162.3	31.166667	2049	1624.9	857.7
25	5520.1	3540	2125.2	31.333333	1994.4	1587.5	836.4
25.166667	5407.9	3494.4	2086.7	31.5	1940.8	1550.7	815.4
25.333333	5292.5	3445.8	2047	31.666667	1888.2	1514.4	794.6
25.5	5171.4	3395.5	2004.8	31.833333	1837	1478.6	774.4
25.666667	5045.9	3343.7	1960.5	32	1787.6	1443.3	754.8
25.833333	4917.9	3290.4	1915	32.166667	1739.2	1408.4	735.7
26	4788.2	3235.6	1868.5	32.333333	1691.7	1374	716.8
26.166667	4657.9	3178	1821.6	32.5	1645.1	1340.1	698.2
26.333333	4529	3118.7	1774.9	32.666667	1599.2	1306.9	679.8
26.5	4403.5	3058.3	1729.6	32.833333	1554.2	1274.6	661.6
26.666667	4280.3	2996.9	1685	33	1510	1243.1	643.7
26.833333	4158.4	2935.2	1640.8	33.166667	1466.6	1212.3	626
27	4038.3	2873.6	1597	33.333333	1424.1	1181.9	608.5
27.166667	3921.2	2813.2	1554	33.5	1382.7	1152.1	591.4
27.333333	3810.9	2753.1	1513.7	33.666667	1342.9	1122.7	574.8
27.5	3706.4	2693.3	1475.9	33.833333	1305.4	1093.8	559.3
27.666667	3605	2633.8	1439.1	34	1269.2	1065.4	544.3
27.833333	3506.4	2574.9	1403.3	34.166667	1233.9	1037.4	529.6
28	3410.4	2517.4	1368.3	34.333333	1199.5	1009.7	515.3
28.166667	3317.3	2462.2	1334.2	34.5	1165.9	982.5	501.3
28.333333	3228	2408.1	1301.5	34.666667	1133.2	956.1	487.5
28.5	3141.2	2354.7	1269.7	34.833333	1101.2	930.9	474.1
28.666667	3056.5	2302.3	1238.5	35	1069.9	906.5	460.8
28.833333	2973.9	2250.5	1207.9	35.166667	1039.3	882.5	447.8
29	2893.2	2199.8	1177.8	35.333333	1009.4	859.2	435
29.166667	2815.7	2150.1	1148.9	35.5	980.5	836.3	422.7
29.333333	2740.9	2101.1	1121	35.666667	952.9	813.8	410.9
29.5	2667.7	2053	1093.5	35.833333	926.1	791.8	399.4
29.666667	2596.3	2005.6	1066.6	36	899.8	770.3	388.2



Appendix

DIRECT FLOW (cms)							
Time (hr)	100-yr	25-yr	5-year	Time (hr)	100-yr	25-yr	5-year
36.166667	874.2	749.1	377.2	42.5	281.6	253.3	121.4
36.333333	849.1	728.3	366.5	42.666667	273.3	246.4	117.8
36.5	824.5	707.9	355.9	42.833333	265.3	239.6	114.4
36.666667	800.4	688.3	345.6	43	257.7	233.1	111.1
36.833333	776.7	669.3	335.3	43.166667	250.4	226.7	107.9
37	753.5	650.8	325.3	43.333333	243.2	220.4	104.8
37.166667	730.8	632.7	315.4	43.5	236.2	214.3	101.8
37.333333	708.9	615	305.9	43.666667	229.4	208.4	98.9
37.5	688.1	597.7	296.9	43.833333	222.7	202.5	96
37.666667	667.9	580.8	288.1	44	216.2	196.8	93.2
37.833333	648.1	564.3	279.6	44.166667	209.8	191.2	90.5
38	628.8	548.2	271.2	44.333333	203.6	185.9	87.8
38.166667	610	532.3	263.1	44.5	197.5	180.8	85.2
38.333333	591.6	516.9	255.2	44.666667	191.7	175.8	82.6
38.5	573.7	502	247.4	44.833333	186.1	170.9	80.2
38.666667	556.3	487.7	239.9	45	180.7	166.2	77.9
38.833333	539.3	473.9	232.5	45.166667	175.5	161.6	75.6
39	522.8	460.5	225.4	45.333333	170.3	157.1	73.4
39.166667	507.1	447.5	218.5	45.5	165.3	152.7	71.3
39.333333	492.2	434.8	212.1	45.666667	160.4	148.4	69.1
39.5	478	422.5	206	45.833333	155.6	144.2	67.1
39.666667	464.2	410.5	200	46	150.9	140.1	65.1
39.833333	450.8	398.8	194.3	46.166667	146.4	136.1	63.1
40	437.8	387.4	188.7	46.333333	142	132.3	61.2
40.166667	425.1	376.3	183.2	46.5	137.8	128.7	59.4
40.333333	412.7	365.5	177.9	46.666667	133.8	125.1	57.7
40.5	400.7	355.2	172.7	46.833333	130	121.7	56
40.666667	388.9	345.4	167.6	47	126.3	118.3	54.4
40.833333	377.4	335.8	162.6	47.166667	122.7	115	52.9
41	366.4	326.6	157.9	47.333333	119.2	111.7	51.4
41.166667	355.9	317.5	153.3	47.5	115.8	108.6	49.9
41.333333	345.8	308.7	149	47.666667	112.6	105.5	48.5
41.5	335.9	300.2	144.8	47.833333	109.4	102.5	47.1
41.666667	326.3	291.8	140.6	48	106.3	99.6	45.7
41.833333	316.9	283.7	136.6				
42	307.7	275.8	132.7				
42.166667	298.8	268	128.8				
42.333333	290.1	260.5	125.1				





D R E A M
Disaster Risk and Exposure Assessment for Mitigation

